FUNCTIONALIZATION OF CARBON NANOTUBES USING OXYGEN PLASMA TO PREPARE JUTE NANOCOMPOSITES

A dissertation submitted to the Department of Physics, Bangladesh University of Engineering and Technology, Dhaka in partial fulfillment of the requirements for the degree of Master of Science (M.Sc.) in Physics

by

Md. Johurul Islam

Roll No. 1017142504F

Session: October-2017

Department of Physics

BANGLADESH UNIVERSITY OF ENGINEERING AND TECHNOLOGY

Dhaka–1000

December, 2019

BANGLADESH UNIVERSITY OF ENGINEERING & TECHNOLOGY (BUET), DHAKA

DEPARTMENT OF PHYSICS

Certification of Thesis

The thesis titled **"FUNCTIONALIZATION OF CARBON NANOTUBES USING OXYGEN PLASMA TO PREPARE JUTE NANOCOMPOSITES"** submitted by **Md. Johurul Islam,** Roll No. 1017142504F, Session: October/2017, has been accepted as satisfactory in partial fulfillment of the requirement for the degree of **Masters of Science** (M.Sc.) in Physics on 17 December, 2019.

BOARD OF EXAMINERS

Dr. Mohammad Jellur Rahman — Chairman
(Supervisor)
Associate Professor
Department of Physics, BUET, Dhaka

Dr. Md. Forhad Mina — Member (Ex-Officio)
Professor and Head
Department of Physics, BUET, Dhaka-1000

Dr. Mohammad Abu Sayem Karal — Member
Associate Professor
Department of Physics, BUET, Dhaka-1000

Dr. Mohammad Rakibul Islam — Member
Associate Professor
Department of Physics, BUET, Dhaka-1000

Dr. Golam Mohammed Bhuiyan — Member (External)
Professor
Department of Theoretical Physics
University of Dhaka, Dhaka-1000

CANDIDATE'S DECLARATION

It is hereby declared that this thesis or any part of it has not been submitted elsewhere for the award of any degree or diploma.

Signature of the candidate

(Md. Johurul Islam)

Roll No. 1017142504F

Session: October-2017

Dedicated
to
My Dear Parents
Who Have Made Immeasurable Sacrifices
for Me

Contents Page No.

LIST OF FIGURES

LIST OF TABLES

LIST OF ABBREVIATIONS

CNTs	Carbon nanotubes
MWCNTs	Multi-walled carbon nanotubes
p-CNTs	Pristine carbon nanotubes
f-CNTs	Functionalize carbon nanotubes
T.jute	Treated jute
λ	Wavelength
θ	Bragg angle
k_B	Boltzmann constant
ΔE	Activation energy
σ	Electrical conductivity
J	Current density
ρ	Resistivity
D	Crystallite size
β	Full width half maximum
R	Electrical resistance
T	Temperature
λ	Wavelength
θ	Bragg angle

ACKNOWLEDGEMENTS

First of all I am very much grateful to Almighty Allah who has given me the strength and opportunity to complete this research work.

I would like to express my sincere appreciation to my supervisor Dr. Mohammad Jellur Rahman, Associate Professor, Department of Physics, Bangladesh University of Engineering and Technology (BUET), for his wonderful guidance and tremendous support during my M.Sc. study and research. I especially wish to thank him for the generosity he showed during this time. He is a wonderful advisor who helped me go through all the difficulties that I encountered in my study, research and even in my personal life. It is my great honor to be his student. What I learned from him will benefit my whole life.

I am thankful to Professor Dr. Md. Forhad Mina, Head, Department of Physics, BUET, for providing me necessary facilities to carry out this research work. I am very much grateful to Dr. Md. Abu Hashan Bhuiyan, Professor, Department of Physics, BUET for his best wishes and supports to carry out this work. I am very much obligated to Dr. Muhammad Rakibul Islam, Dr. Parvin Sultana as well as all of my respected teachers of the Department of Physics, BUET for their numerous suggestions and inspirations. I would like to especially recognize Professor Dr. Tetsu Mieno, GSST, Shizuoka University, Japan for providing the carbon nanotubes. I would also like to thank Ahaduzzaman Deeraz, Mr. Tanveer Ahmmed, Md. Forhad Hossain, Mahmud Hasan, Md. Mehedi Hasan Sohag, and all my senior and junior for their inspiration during my study.
I am also thankful to all staffs of the Department of Physics, BUET for their sincere help during my research work. I acknowledge with thanks to the Bangladesh University of Engineering and Technology for giving me necessary permission and providing financial support to this thesis work.

Finally, I would like to express my gratitude and love from my heart to my parents and other family members for their constant support and encouragement during this research work.

Md. Johurul Islam
December, 2019

ABSTRACT

Low cost, biodegradable, thin and flexible carbon nanotube (CNT)/jute nanocomposites have been prepared by varying the concentration of multi-walled carbon nanotubes (MWCNTs). To attain effective CNT/jute composites uniform CNT dispersion is made by the oxidative treatment using acetic acid on the CNT surface. The allegations of incorporating CNTs in jute and electrical, structural, mechanical and thermal properties of the composites are investigated in this work. The field emission scanning electron microscope micrographs of the CNT/jute composites display the uniform attachment of CNTs on the surfaces of all the jute fibers of jute fiber. The Fourier- transform infrared spectroscopy spectrum of the CNT/jute composites do not show any significant changes in the band position but the band intensities of –OH and $-CH_2$ groups increase. Thermal studies show that the dominant weight loss of all the samples is observed between 280 and 380 °C. Tensile strength of the composites is observed to be slightly increased of the jute < CNT/jute < CNT/T. jute nanocomposites due to the stronger interaction of the order as CNTs. A gradual decrease of resistance of the composites was observed due to the formation of electrically conducting CNT on the surfaces of all the jute fiber and the nanocomposites exhibit remarkably low resistance varying from 2.30 kΩ/m to 0.02 kΩ/m. The conductivity of the nanocomposites increases with the increase of incorporating wt% of MWCNTs and becomes 5.02 S/m. The conductivity of the nanocomposites also increases with the increase in temperature indicating the semiconducting nature of the composites. The activation energy of all the samples decrease in high temperature region (358 K) compared to the room temperature region (298 K). The jute nanocomposites will find applications in different types of electronic devices as well as in engineering fields such as super capacitor, multifunctional sensors, and conductive fiber textiles.

CHAPTER 1
INTRODUCTION

1.1 Introduction

The search for textiles and fibrous structures with the capacity of conducting electricity is in full growth because of the wide variety of potential applications of these fibrous structures, resulting from their flexibility, lightweight, and capability of adapting different shapes [1–3]. Conductive fibrous systems can transport electrical signals as well as electrical current in order to be used as sensors for monitoring vital biological signs [4]. Their sensing functionalities make them suitable for several other application areas, such as the military sector, sports, engineering, therapeutics, and the automotive or aerospace industries [5, 6]. Nowadays, synthetic fibers are still the most used type of fibers in industry. However, natural fibers, because of their low cost, abundance, biocompatibility, and biodegradability, are very promising materials for replacing the syntheticones [7]. Hence, a wide variety of different natural fibers including jute fibers are being used as reinforcements of composite fabrication [8–11]. Jute and natural fibers are in general electrical insulators or present very limited conductivity. Therefore, it is a huge challenge to use natural fibers for smart conductive fibrous systems. One of the strategies that can be used to decrease the resistivity of natural fibers is to incorporate conductive elements [12–14]. For these nanoparticles (NPs) such as carbon nanotubes (CNTs) are very promising. Because of their size they exhibit a high surface area and excellent surface activity, which make them promising materials with exclusive optical, electrical, and catalytic properties [15–17]. However, these applications are compromised by their poor dispersibility in water, because substantial van der Waals attractive forces between the CNTs aggregate them in solvents [18].The most common method of improving their dispersibility in water is to functionalize their surfaces using hydrophilic oxygen-containing groups, which requires a long processing time and produces a large amount of waste. In these respects, plasma processing is an advantageous technique when it is used in conjunction with conventional wet chemical methods. Plasma surface modification is particularly interesting because the method is flexible, rapid, contaminant-free, and relatively nondestructive [19, 20]. In this study, CNTs will be modified by three-step

processing [21].CNTs will be at first supersonically mixed into ethanol to be deaggregated temporarily. Then, the mixture is dried and pretreated using citric acid solution. Finally, the MWCNTs in the solution will be treated by the oxygen plasma including citric acid and water. This method is safer than the methods mentioned in literature as no hazardous reagents are used [22]. The surfaces of the MWCNTs will be chemically functionalized with carboxyl (–COOH) groups, and they can be easily dispersed in water.

The research work relies on a good and cheap fabrication of the CNTs nanocomposites and characterization of nanocomposites reinforced with CNTs. Jute fiber will be modified by using some chemical treatment the existence of CNTs in the surface of jute fiber the improvement of electrical conductivity, mechanical strength, structural and thermal properties will be analyzed. The functionalized jute fiber with CNTs incorporated in it will be found applications in different types of electronic devices as well as in engineering fields such as multifunctional sensors [4], Super capacitors [5], high speed field effect transistors, gas and pH sensors [23], or simply as high current-carrying components in electronic circuits. CNTs also use in field of actuators, paper battery [10], electric heater, power generators and EMI shielding materials.

1.2 Objectives of the Present Study

The aim of the research is to prepare cost-effective, flexible, conductive CNT/Jute nanocomposites by incorporating CNTs uniformly dispersed into jute fibers, to identify the effects of the addition of CNTs in the jute fibers and to study the variation of properties of the nanocomposites. The main purpose of this research work is to enhance the properties of typical fiber so that it finds new applications as advanced products for the next generation. The objectives of this work are as follows:

i. To establish the citric-acid-assisted radio frequency (RF) oxygen plasma method to functionalize CNTs.
ii. The addition of functionalized CNTs efficiently to the jute fiber to obtain the nanocomposites.

iii. Addition of different amount of CNTs on to the jute fibers to obtain conducting jute fibers of desired conductivity.
iv. Investigation of surface morphology, thermal and electrical conductivity of the jute nanocomposites.
v. Thermal stability and mechanical strength of the jute nanocomposites will also be studied.

1.3 Outline of the Thesis

This thesis paper has been represented by five chapters as follows:

In chapter 1, a general introduction has been presented and it contains objectives of the research work.

Chapter 2 describes about natural polymer, properties and functionalization of CNTs and the basic principles of the characterization techniques. This chapter also provides literature review.

Chapter 3 discusses about the sample preparation procedure and the composite characterization.

Chapter 4 covers the results and discussion part of this research work.

Chapter 5 includes conclusions of this work along with scope for future studies.

CHAPTER 2
THEORETICAL BACKGROUND

2.1 Introduction

Nano composites are widely used in a great number of applications because of their many advantageous general properties such as low density, low cost and process ability. They are being developed in such diverse areas such as: conduction and storage of electricity. In the 1960s, especially during the early development of the microelectronics research and industry, rapid growth of plasma system starts, that was inspired by the hope to use as plasma processing technical jute nanocomposite. Jute and natural fibers are in general electrical insulators or present very limited conductivity. Therefore, it is a huge challenge to use these natural fibers for smart conductive fibrous systems. One of the strategies that can be used to decrease the resistivity of natural fibers is to incorporate conductive elements [24–26]. For these nanoparticles (NPs) such as carbon nanotubes (CNTs) are very promising because, they exhibit a high surface area and excellent surface activity [27–30].This chapter presents a detail of nanocomposite and their general properties. The details of plasma, functionalization of CNTs by oxygen plasma, treatment of jute in oxygen plasma, preparation of jute nanocomposite etc. are illustrated in this chapter. Applications of jute nanocomposite are focused at the end of the chapter.

2.2 Introduction to Carbon Nanotubes

After the discovery of CNTs in 1991 by Iijima [31], these fascinating materials have inspired the global research tremendously and opened up novel possibilities in nanotechnology, electronics, optics, material science, biotechnology and space science. CNTs are allotropes of sp^2 hybridized carbon with a hollow cylindrical nanostructure. These nanotubes can be visualized as rolled sheets of graphene with constant radius comprising of hexagonal network of carbon atoms, often capped by a fullerene-like hemisphere at each ends. CNTs are one-dimensional nanomaterials with large specific area and high aspect ratio. CNTs possess unique and remarkable properties which are varied with the structure, morphology, diameter and length of the tubes. The structure of CNTs depends on the chirality (the degree of twist of graphene sheet) of each nanotube,

2.3.1 Cultivation and production

The plain alluvial soil and standing water are good for jute plant. During the monsoon season growing jute is perfect. 20˚C to 40˚C temperatures and relative humidity of 70%–80% are favorable for successful cultivation. There are two types of Jute: a) white jute (Corchorus Capsularis) and b) Tossa jute (Corchorus Olitorius) [35, 36].

The jute fiber comes from the stem and ribbon (outer skin) of the jute plant. The fibers are first extracted by decomposing. The decomposing process consists of bundling jute stems together and immersing them in slow running water. There are two types of decomposing: stem and ribbon. After the retting process, stripping begins. In the stripping process, non-fibrous matter is scraped off, then the workers dig in and grab the fibers from within the jute stem [29].

Fig. 2.4: Jute stems being decomposing in water to separate the fibers [36].

2.3.2 Feature and uses

Natural fiber jute has promising feature that while it use as of purpose. Some of features are mentioned below:

- Jute fiber is 100% bio-degradable and recyclable and thus eco-friendly.
- Jute can grow without the use of any fertilizers.
- It is a natural fiber with golden and silky shine and hence called the golden fiber.
- The bast or skin of the plant's stem is produced the cheapest fiber.

- It is the second most growing fiber after cotton, in terms of usage, global consumption, production, and availability.
- It has low extensibility, high tensile strength, and ensures better breathability of fabrics.
- As industrial raw materials it has enormous use. The best source of jute in the world is the Bengal Delta Plain in the Ganges Delta, most of which is occupied by Bangladesh.
- Jute has the ability to be blended with other fibers, both synthetic and natural.

Uses:

This process is used for bright and fast coloured value-added diversified products made from jute. Jute is in great market due to its cheapness, softness, length, luster and uniformity of its fiber. It can be uses multipurpose as like fiber, culinary uses, cosmetics, medicine, paints, sonali bag, electronics wire, sensors and others produces.

Fig. 2.5: Fiber of jute [36].

2.4 Nanocomposites

Nanocomposite is a multiphase solid material where one of the phases has one, two or three dimensions of less than 100 nm, or structures having nano-scale repeat distances between the different phases that make up the material. The idea behind nanocomposite is to use building blocks with dimensions in nanometer range to design and create new materials with unprecedented flexibility and improvement in their physical properties. In the broadest sense this definition can include porous media, colloids, gels and

copolymers, but is more usually taken to mean the solid combination of a bulk matrix and nano-dimensional phase(s) differing in properties due to dissimilarities in structure and chemistry. The mechanical, electrical, thermal, optical, electrochemical, catalytic properties of the nanocomposite will differ markedly from that of the component materials. Size limits for these effects have been proposed. The properties of nanocomposites can display synergistic improvements over those of the component phases individually. The addition of nanofillers has drastic improvements in the surface to volume ratio, mechanical strength, electrical or thermal conductivities, flame retardancy, optical clarity etc. This rapidly expanding field is generating many exciting new materials with novel properties [37, 38]. Based on matrix, there are generally three classes of nanocomposites: (a) metal matrix nanocomposites, (b) ceramic matrix nanocomposites, (c) polymer matrix nanocomposites. Also, there are two modes of classification for nanocomposites [39]. They are the organic and inorganic nanocomposites. Nanocomposites offer new technology and opportunities for several sectors. It has very high impact in developing a new generation of composites with enhanced functionality and a wide range of applications. Nanocomposites are currently being used in numerous fields and new applications are being continuously developed.

Applications for nanocomposites include:

- Electronics
- Films
- Aerospace industries
- Automobile sectors
- Food packaging
- Environmental protection
- Biotechnology industries
- Gas barriers

2.5 Jute Based nanocomposite

The natural fibers used to reinforce thermoplastics mainly include wood, cotton, flax, hemp, jute, sisal and sugarcane fibers [40]. Jute appears to be a promising material in tropical countries, among all natural fibers due to it being relatively inexpensive,

nonabrasive, low density, higher strength and modulus than plastic and commercially available, [41]. It has three principal constituents, namely, a-cellulose, hemicellulose, and lignin. In addition, it contains minor constituents such as fats and waxes, inorganic and nitrogenous matters, and traces of pigments like b–carotene and xanthophyll‘s. One of the most focuses of bio-based composites is natural fibers and jute is the unique material that extends the uses of natural composites. Jute is cheap, biodegradable, environmental friendly, and has a low density and good specific mechanical properties. Additionally, it can be woven into different forms and shapes [42, 43]. Jute nanocomposites based electronics provides possibilities for next generation devices with flexible, biodegradable, biocompatible, ecofriendly, lightweight and wearable electronics. High performance flexible jute based nanocomposites are researched extensively, which can be used for the transistor, sensor, actuator, antistatic package, electric heater, electromagnetic interference shielding materials, foldable energy storage device etc.

2.6 Literature Review

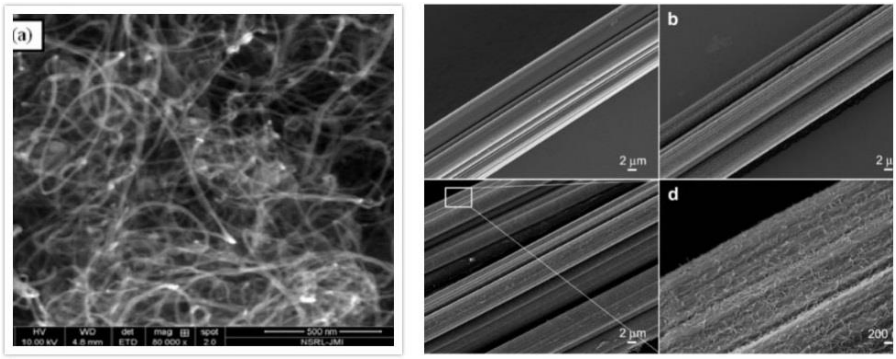

(A) **(B)**

Fig. 2.6: SEM images for surface of (A) MWCNTs [6] and (B) Commercial viscose fiber with MWCNTs [28].

Rahman & Mieno [29] studied the functionalization of MWCNTs and Qi et al. [15] the MWCNTs/ viscose fiber manufactured by dip coating process and observed their performance in electric heating and electromagnetic interference (EMI) shielding materials. The SEM images revealed that MWCNTs/viscose fiber were homogeneously coated with interconnected MWCNTs. For CNT/Cellulose fiber, the current increased linearly with the applied voltage and the slopes of the I-V curves increased significantly with the increase of the dip coating cycle.

Shahnawaz et al. [44] have demonstrated the FTIR spectra of MWCNTs where A peak around 1714- 1726 cm^{-1} appears in the spectra of MWCNTs-COOH that can attributed to the C=O stretching of carboxylic acid group. Peaks at 1034 and 3435 cm^{-1} were observed that can be assigned to CO and OH stretching vibrations of carboxylic acid group, respectively.

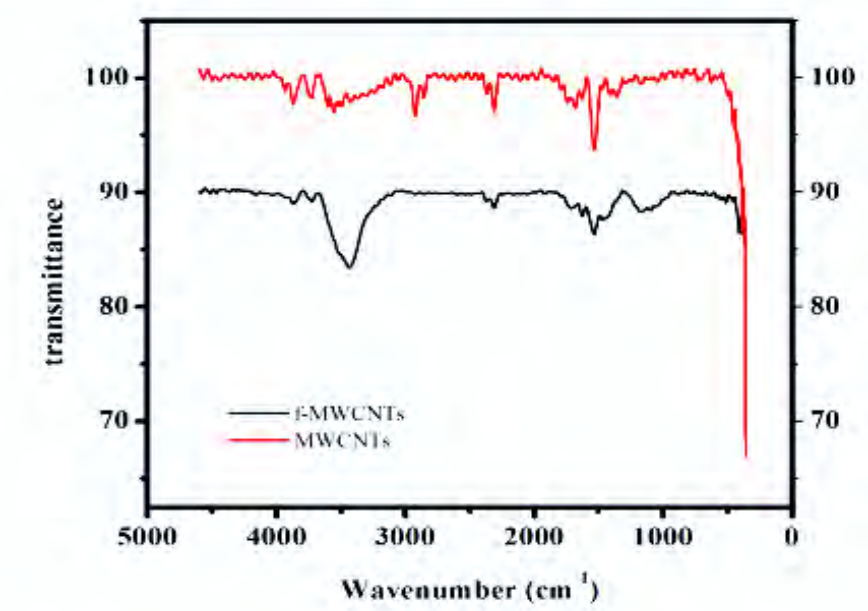

Fig. 2.7: FT-IR spectra of MWCNTs and f-MWCNTs [44].

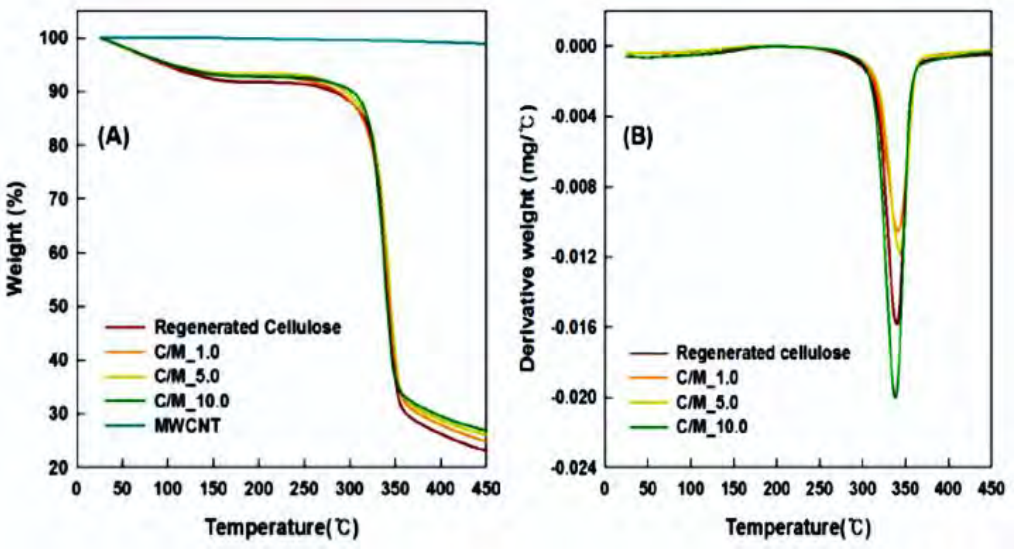

Fig. 2.8: (A) TGA and (B) DTG curves of neat regenerated cellulose and its composite films with different MWCNT contents [45].

Lee et al. [45] investigated the regenerated cellulose/MWCNTs composite films manufactured by a simple solution-casting method and their application as electric heating materials. The composite were found to be thermally stable up to ~ 275 °C.

The composite films with MWCNT contents above 5 wt% the electric current increased noticeably with the applied voltage and the slopes of the I-V curves became steeper with increasing the MWCNT content in the composite films (Fig 2.11). The electrical resistivity of the regenerated cellulose/MWCNT composite films decreased significantly from ~10^{9} Ω cm to ~10^{12} Ω cm with increasing the MWCNT loading. The composite films with 5 10 wt% MWCNT contents possessed low electrical resistivity of ~10^{2} 10^{1} Ω cm.

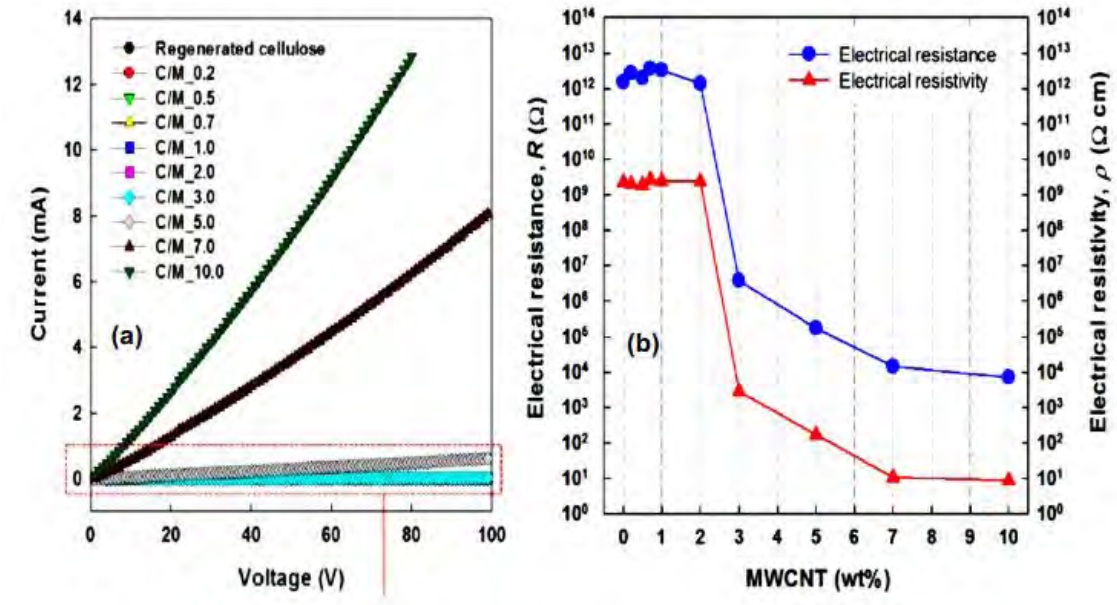

Fig. 2.9: (a) Current-voltage curves and (b) electrical resistance and resistivity of neat regenerated cellulose and its composite films with different MWCNT contents [45].

Salajkova et al. [46] studied the electrically conductive nanofibrillated cellulose (NFC)/CNT nanopapers prepared by a papermaking process. The FE-SEM image of pure NFC nanopaper showed weblike network structure of cellulose nanofibrils. The width of MWCNTs was estimated to be 3–4 times higher than the NFC nanofibrils. The NFC/CNT nanopaper with 9.1 wt% MWCNTs indicated homogenous incorporation of

MWCNTs in the cellulose nanofibril network. The percolation composition (pc) clearly occurs between 6 and 9 wt% and the conductivity changes significantly.

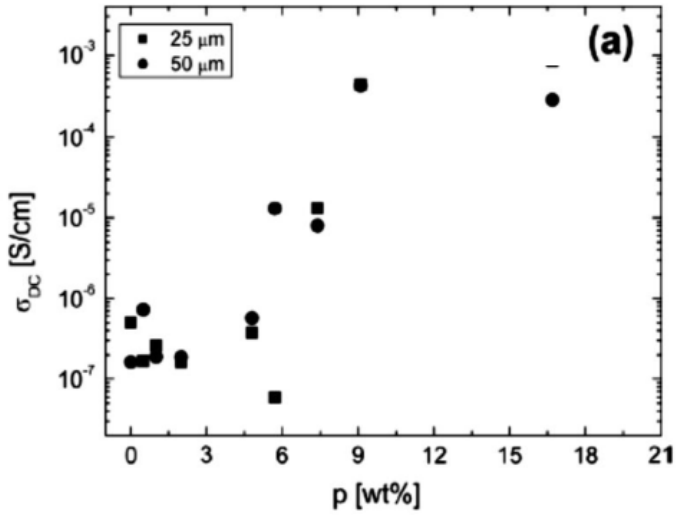

Fig. 2.10: DC conductivity σ versus MWCNT concentration, p (wt%) for the prepared samples [46].

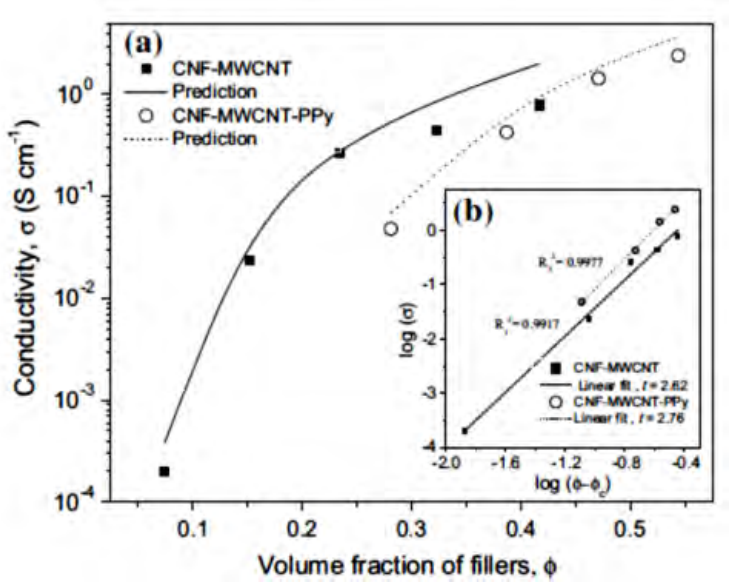

Fig. 2.11: (a) Experimental and predicted electrical conductivities of CNFMWCNT and CNF MWCNT-PPy nanopapers (b) Linear correlation between log σ and log Φ-Φc [47].

Lay et al. [47] stated the effect of MWCNTs and polypyrrole (PPy) on the electrical properties of cellulose Nano papers were 2, 2, 6, 6,-tetramethylpiperidine-1-oxyl

(TEMPO)-oxidized cellulose nanofibers (CNFs) were combined with MWCNTs and PPy polymer to produce binary and ternary formulations of conductive nanopapers.

High mechanical properties and good conductive response was found for these binary and ternary formulations. They reported that the ternary formulation produced nanopapers showed improved electrical conductivity of 2.41 S/cm [1] (Fig 2.11) which was higher than those for the binary formulation with 50 wt% of MWCNTs (0.78 S/cm [1]).

Agarwal et al. [43] have developed conductive paper by layer-by-layer (LbL) nanoassembly technique where lignocellulose wood microfibers coated with anionic composite nanocoating of poly (3,4-ethylenedioxythiophene)-poly (styrenesulfonate) (PEDOT-PSS) and aqueous dispersion of carbon nanotubes (CNT-PSS) and cationic poly (ethyleneimine) (PEI) as shown in Fig. 2.11

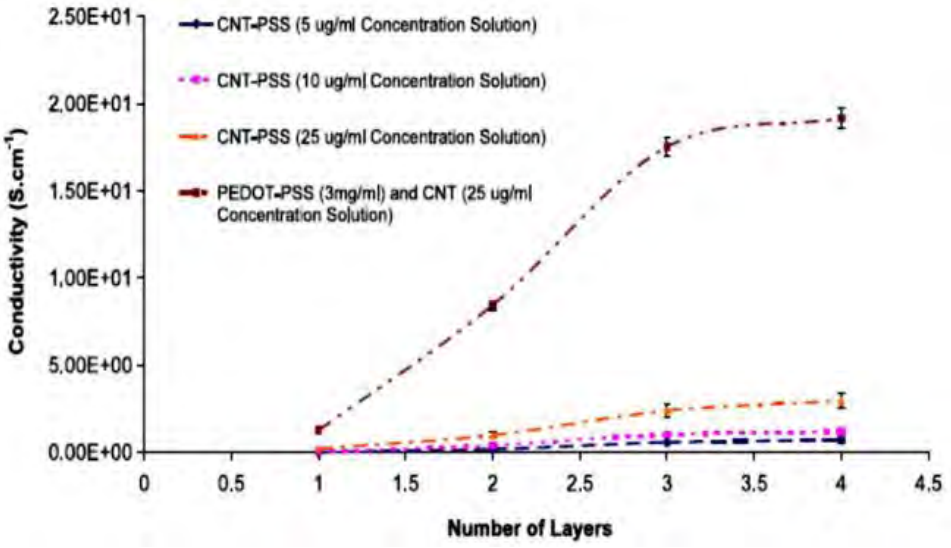

Fig. 2.12: Conductivity of wood microfibers coated with four-bilayers of carbon nanotubes of different concentration [43].

Hai et al. (48) observed that the average tensile modulus of untreated jute composites is 4.2 GPa, while the average tensile modulus of 2% NaOH treated jute is 4.7 GPa, an improvement of about 8% compared with untreated jute fiber. For coir/PP composites, the average tensile modulus is 0.55 GPa with 2% NaOH treatment, and untreated composites have a value of 0.47 GPa. After the NaOH treatment, the tensile modulus was therefore increased by about 14% as shown in Fig. 2.13.

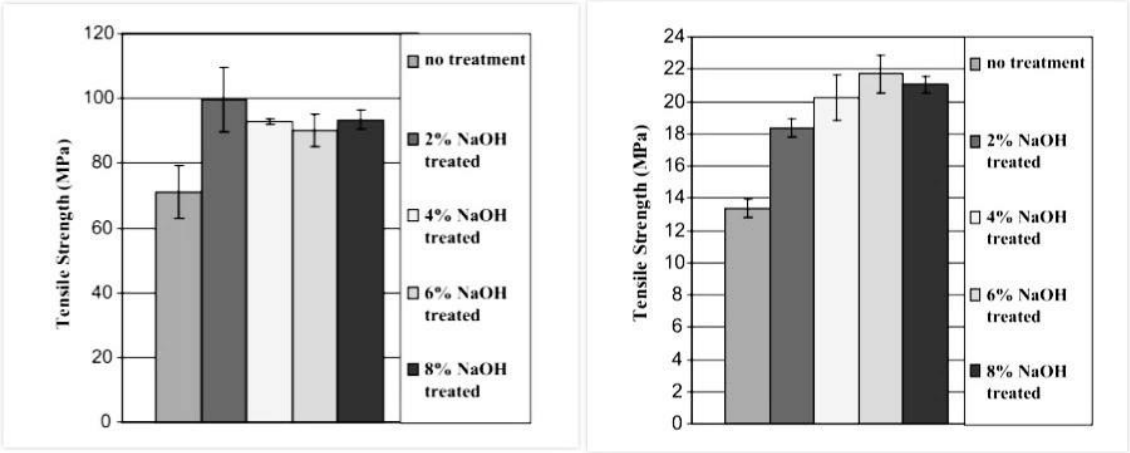

(A): Tensile strength of jute/PP composites (B): Tensile strength of coir/PP composites

Fig. 2.13: The tensile modulus of jute/PP and coir/PP composites, respectively [48].

2.7 Polymers

The simplest definition of a polymer is a useful chemical made of many repeating units. The word ‗polymer' is referred from two Greek words, poly means ‗many' and mer means ‗unit' or ‗part'. Each repeating unit is the "mer" or basic unit with "poly-mer" meaning many repeating units. Repeating units are often made of carbon and hydrogen and sometimes oxygen, nitrogen, sulfur, chlorine, fluorine, phosphorous, and silicon. To make the chain, many links or "mers" are chemically hooked or polymerized together. There are three different types of polymers based on the source.

i. **Natural polymers**

These polymers are found in plants and animals. Examples are proteins, cellulose, starch, some resins and rubber.

ii. Semi-synthetic polymers

These polymers are mostly derived from naturally occurring polymers by chemical modifications. Cellulose derivatives as cellulose acetate (rayon) and cellulose nitrate, etc. are the usual examples of this category.

iii. Synthetic polymers

A variety of synthetic polymers as plastic (polythene), synthetic polymers (nylon 6, 6) and synthetic rubbers (Buna – S), are examples of man-made polymers.

2.7.1 Natural polymers

Recently we are facing different environmental issues which are pushing away from synthetic or petro-chemically derived products, while economic factors are pulling back from often more expensive green options. At present low cost biodegradable polymer should be used to avoid the critical crisis of environmental effects in Bangladesh. We need to focus on applications of any natural polymers available in our country such as jute, cotton, cellulose, coconut coir, etc. to be used in different engineering and technological product. Natural polymers are available in large quantities from renewable sources, generally non-toxic and biodegradable. These polymers are formed in nature during the growth cycles of all organisms. Natural biodegradable polymers are called biopolymers. Polysaccharides such as cellulose, starch, chitosan, represent the most attribute family of these natural polymers. Polynucleotides such as DNA, RNA, polypeptides such as gelatin, proteins, polyisoprene such as rubber etc. are other types of biopolymers. Natural polymers generally occur as fibers or grains. All plant fibers are composed of hemicellulose while animal fibers consist of proteins (hair, silk and wool). Jute fibers are collected from different parts of the jute. The purest fibers, like cotton and kapok, come from the threads that cover the skin of seeds. Fibers are divided based on their origins.

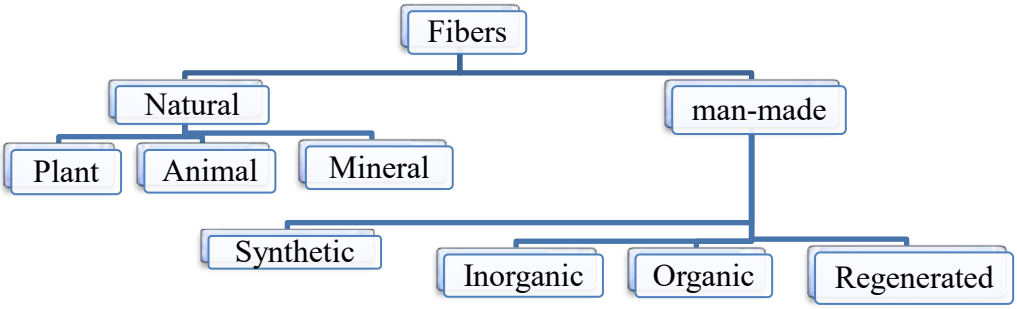

Fig. 2.14: Classification of fibers.

The natural fibers in polymer nanocomposites can be used in fabricating highly efficient engineering and technological products at a low cost. Natural fibers as jute used as a component of modern technology, which increase our wealth because of cheapest price. It‘s also replacing the nondegradable polymer products by degradable biopolymers. The jute fibrils are aligned in the longitudinal direction of the fiber, which render maximum tensile and flexural strengths, in addition to provide rigidity. The reinforcing efficiency of natural fiber is related to the nature of cellulose and its crystallinity. The main components of jute fibers are cellulose (α-cellulose), hemicelluloses, lignin, pectins and waxes [49].

Advantages of Natural Fibers

I. Low specific weight of fibers which results in a higher specific strength and stiffness. This is a benefit especially in parts designed for bending stiffness.
II. It is a renewable resource, the production requires little energy, and CO_2 is used
while oxygen is given back to the environment.
III. Producible with low investment at low cost, which makes the material an interesting product for low-wage countries.
IV. Eco-Friendly processing.
V. Good thermal properties.

2.7.2 Structure of jute

The fibers that are known as bast fiber are come from the inner bark of the plants. Jute is a bast fiber. Different types of natural and man-made fibers are available in the world. So it is necessary to know the properties of fibers. Without that it is impossible to separate one fiber from others. Every fiber has its own properties. Commercial jute changes from yellow to brown to greyish in color. The bundle of fibers held together by gummy material; lignin which plays an important role in structure of plant and it also outer side of jute which show in fig. (2.15)**.**

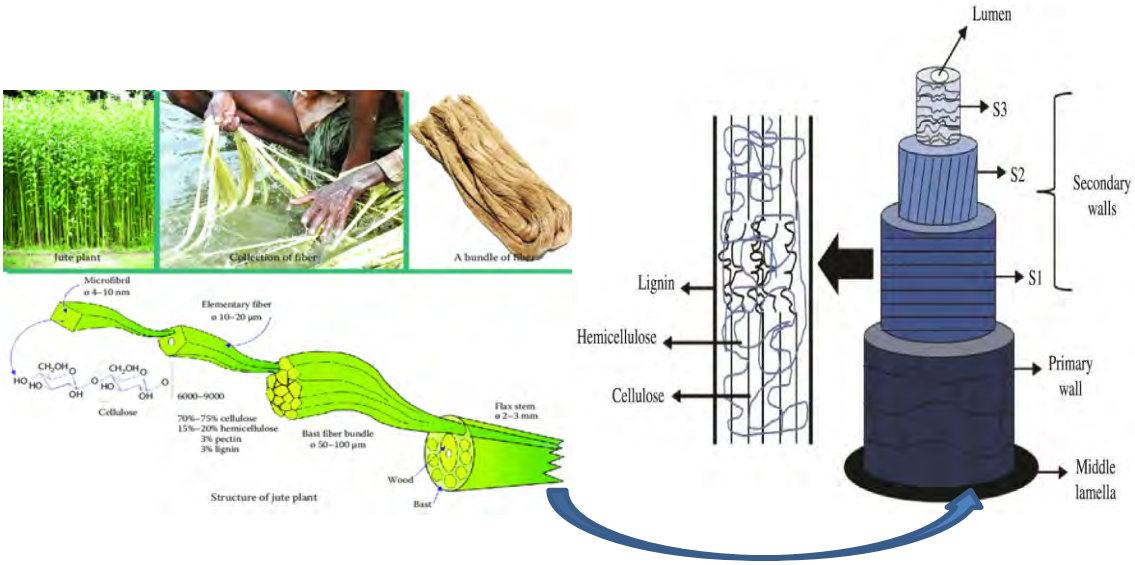

Fig. 2.15: The structure of jute showing their external and internal bond [50].

Physical Properties:

1. Ultimate length: 1.5 – 4 mm
2. Ultimate diameter: 0.015 – 0.020 mm
3. No. of ultimate in cross-section: 6 – 10
4. Fibers length: 5 – 12
5. Color: White, off white, yellow, brown, grey, golden
6. Strength (Tenacity): 3 – 4 gm/den
7. Elongation: 1.7% at the break
8. Specific Gravity: 1.5
9. Moisture Regain (MR %): 13.75%
10. Resiliency: Bad
11. Dimensional Stability: Good
12. Abrasion Resistance: Average

Chemical Properties:

1. Effect of Acids: Easily damaged by hot dilute acids and conc. cold acid.

2. Effect of Alkalis: Fibers are damaged by strong alkali. Fibers losses weight when heated with caustic soda.
3. Effect of Bleaches: Resistant to bleaching agents (Bleaching agent, H_2O_2, NaOCl, $NaClO_2$, Na_2O_2, CH_3COOH, $KMnO_4$, etc.)
4. Effect of Light: Color changes slightly in presence of light sun. It happens due to presence of lignin in fiber.
5. Effect of Mildew: Prevention ability is better than Cotton and Linen.
6. Dyeing ability: Easy to dyeing. Basic dye can be used to color jute fiber.

Mainly jute fibers are made of cellulose, hemi-cellulose and lignin. It is harder than cotton or other fibers. It is for the presence of lignin in its structure. The physical and chemical properties of jute can vary depending on of cultivation. Atmospheric condition and temperature has a great effect on the properties of jute. Different types of machineries and chemicals are used to assess properties of jute. So, now it will be easy to find out jute from other fibers [51].

2.8 Applications of Plasma in Nanocomposites

Plasma is considered as the fourth state of matter. Solid, liquid, and gas are the other three. Plasma is a cloud of protons, neutrons and electrons, where all the electrons become loosely bound from their respective molecules and atoms. Plasma is giving the ability to act as a whole rather than as a bunch of atoms. Plasma is more like a gas than any of the other states of matter because the atoms are not in constant contact with each other, but it behaves differently from a gas. Scientists call it has collective behavior. This means that the plasma can flow like a liquid or it can contain areas that are like clumps of atoms sticking together. Plasma can be created by heating a gas or subjecting it to a strong electromagnetic field applied with a laser or microwave generator.
There are different types of plasma those are:

1. Ultra cold plasma
2. Non-neutral plasma
3. Dusty plasma and grain plasma

4. Artificial plasma

Artificial plasma

Most artificial plasmas are produced by the application of electric and/or magnetic fields through a gas. Plasma produced in a laboratory can be generally categorized by:

- The type of power source used to produce the plasma—DC, AC (typically with radio frequency (RF) and microwave
- The pressure they operate at—vacuum pressure (< 10 mTorr or 1 Pa), moderate pressure (≈1 Torr or 100 Pa), atmospheric pressure (760 Torr or 100 kPa)
- The degree of ionisation within the plasma—fully ionized, partially ionized, or weakly ionized
- The temperature relationships within the plasma—thermal plasma ($T_e = T_i = T_{gas}$), non-thermal or "cold" plasma ($T_e >> T_i = T_{gas}$)
- The electrode configuration used to generate the plasma
- The magnetization of the particles within the plasma—magnetized (both ion and electrons are trapped in Larmor orbits by the magnetic field), partially magnetized (the electrons but not the ions are trapped by the magnetic field), non-magnetized (the magnetic field is too weak to trap the particles in orbits but may produce Lorentz forces).

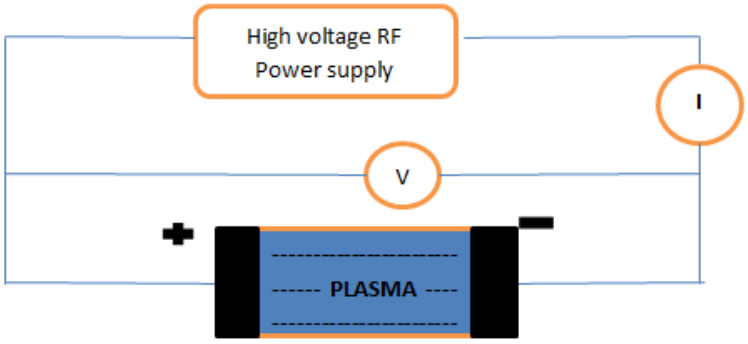

Fig 2.16: Artificial plasma generation.

Applications of plasma

1. Cleaning of metal parts before printing, lacquering, sticking together.

2. Activation of plastics and elastomers before sticking together, printing, painting, pouring.
3. Etching of components.
4. Reducing of metals.
5. Synthesizing and coating components.
6. Pretreatment before soldering / soldering without fluxing agents.
7. Treatment of nanoparticles.
8. Bond pretreatment.
9. Cleaning of metal powder.

2.8.1 CNTs in nanocomposites

Carbon nanotubes (CNT) have lots of unique properties. The atomic arrangement of carbon atoms is responsible for the exceptional electrical, thermal and mechanical properties of CNTs. These properties of CNTs are mentioned below:

Electrical Conductivity

There has been considerable practical interest in the conductivity of CNTs. CNTs with particular combinations of N and M (structural parameters indicating how much the nanotube is twisted) can be highly conducting, and hence can be said to be metallic. Their conductivity has been shown to be a function of their chirality (degree of twist), as well as their diameter. CNTs can be either metallic or semi-conducting in their electrical behavior.

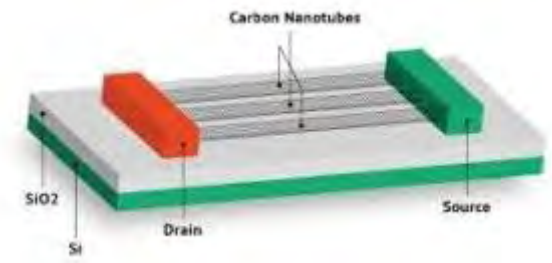

Fig 2.17: Carbon nanotube electronics [52].

Conductivity in MWNTs is quite complex. Some types of ―armchair"-structured CNTs appear to conduct better than other metallic CNTs. Furthermore, interwall reactions within MWNTs have been found to redistribute the current over individual tubes non-uniformly. However, there is no change in current across different parts of metallic single-walled CNTs. However, the behavior of ropes of semi-conducting SWNTs is different, in that the transport current changes abruptly at various positions on the CNTs [52].

Strength and Elasticity

The carbon atoms of a single (graphene) sheet of graphite form a planar honeycomb lattice, in which each atom is connected via a strong chemical bond to three neighboring atoms. Because of these strong bonds, the basal-plane elastic modulus of graphite is one of the largest of any known material.

For this reason, CNTs are expected to be the ultimate high-strength fibers. MWNTs are stiffer than steel, and are very resistant to damage from physical forces. Pressing on the tip of a nanotube will cause it to bend, but without damage to the tip. When the force is removed, the tip returns to its original state. This property makes CNTs very useful as probe tips for very high-resolution scanning probe microscopy.

Quantifying these effects has been rather difficult, and an exact numerical value has not been agreed upon. Using an atomic force microscope (AFM), the unanchored ends of a freestanding nanotube can be pushed out of their equilibrium position and the force required to push the nanotube can be measured. The current Young's modulus value of MWNTs is about 270-950GPa [53].

Thermal Conductivity and Expansion

New research from the University of Pennsylvania indicates that CNTs may be the best heat-conducting material man has ever known. Ultra-small MWNTs have even been shown to exhibit superconductivity below 20 K. Research suggests that these exotic

strands, already heralded for their unparalleled strength and unique ability to adopt the electrical properties of either semiconductors or perfect metals, may someday also find applications as miniature heat conduits in a host of devices and materials.

The strong in-plane graphitic C-C bonds make them exceptionally strong and stiff against axial strains. Reports of several recent experiments on the preparation and mechanical characterization of CNT-polymer composites have also appeared. These measurements suggest modest enhancements in strength characteristics of CNT-embedded matrixes as compared to bare polymer matrixes. Preliminary experiments and simulation studies on the thermal properties of CNTs show very high thermal conductivity. It is expected, therefore, that nanotube reinforcements in polymeric materials may also significantly improve the thermal and thermo-mechanical properties of the composites.

Electron Emission

Field emission results from the tunneling of electrons from a metal tip into vacuum, under application of a strong electric field. The small diameter and high aspect ratio of CNTs is very favorable for field emission. Even for moderate voltages, a strong electric field develops at the free end of supported CNTs because of their sharpness.

This was observed by de Heer and co-workers at EPFL in 1995. He also immediately realized that these field emitters must be superior to conventional electron sources and might find their way into all kind of applications, most importantly flat-panel displays. It is remarkable that after only five years Samsung actually realized a very bright color display, which will be shortly commercialized using this technology.

Fig. 2.18: Carbon Nanotubes Field Emission Display.

Studying the field emission properties of MWNTs, Bonard and co-workers at EPFL observed that together with electrons light is emitted, as well. This luminescence is induced by the electron field emission, since it is not detected without applied potential. This light emission occurs in the visible part of the spectrum, and can sometimes be seen with the naked eye.

High Aspect Ratio

CNTs represent a very small, high aspect ratio conductive additive for plastics of all types. Their high aspect ratio means that a lower loading (concentration) of CNTs is needed compared to other conductive additives to achieve the same electrical conductivity. This low loading preserves more of the polymer resins‘ toughness, especially at low temperatures, as well as maintaining other key performance properties of the matrix resin. CNTs have proven to be an excellent additive to impart electrical conductivity in plastics. Their high aspect ratio (about 1000:1) imparts electrical conductivity at lower loadings, compared to conventional additive materials such as carbon black, chopped carbon fiber, or stainless steel fiber.

2.8.2 Functionalization of CNTs by oxygen plasma

Nanoparticles (NPs) such as carbon nanotubes (CNTs) are very promising filler composite in NCs. Because of their size they exhibit a high surface area and excellent

surface activity, which make them promising materials with exclusive optical, electrical, and catalytic properties [25-27]. However, these applications are compromised by their poor dispersibility in water, because substantial van der Waals attractive forces between the CNTs aggregate them in solvents [28]. Unfunctionalized CNTs have less mechanical or electrical properties that are different from those of the functionalized CNTs, and thus may be utilized for fine-tuning the chemistry and physics of CNTs.

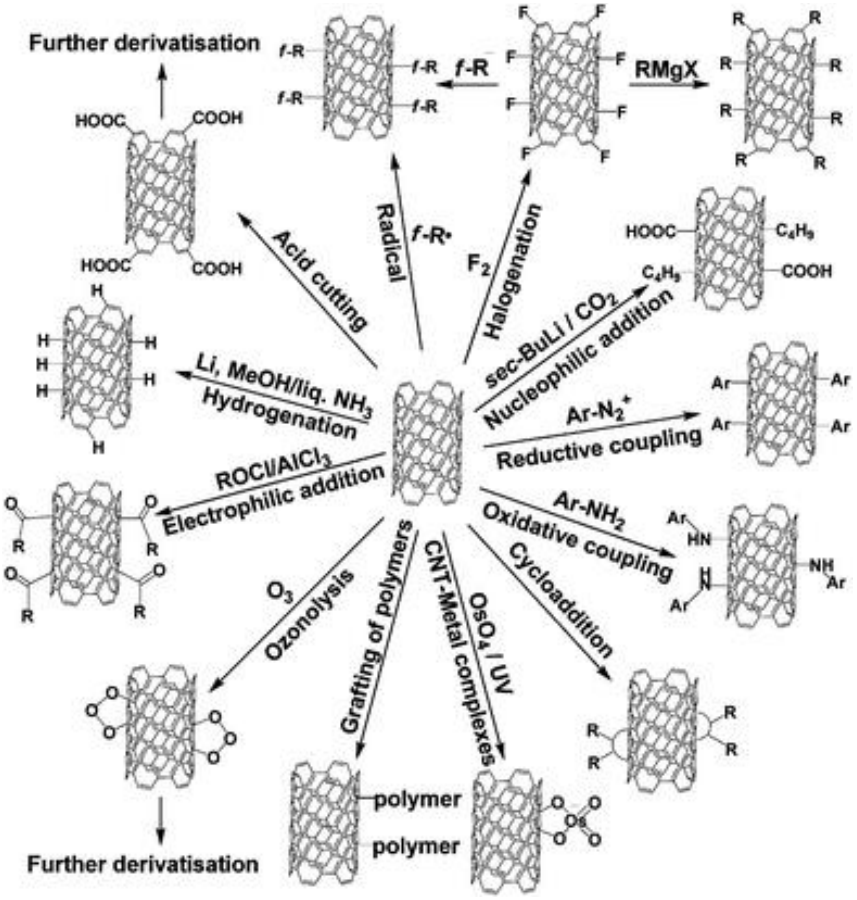

Fig. 2.19**:** Different types of possibilities of the functionalization of CNTs [28].

The most common method of improving their dispersibility in water is to functionalize their surfaces using hydrophilic oxygen-containing groups, which requires a long processing time and produces a large amount of waste. In these respects, plasma processing is an advantageous technique when it is used in conjunction with conventional wet chemical methods. Plasma surface modification is particularly interesting because the

method is flexible, rapid, contaminant-free, and relatively nondestructive [29].In this study, multiwalled CNTs (MWCNTs) is modified by three-step processing as described in Ref. [30].

Functionalization to increase water dispensability

Functionalization techniques are the oxidative treatment of CNTs by liquid-phase or gas-phase oxidation. One of the most common way is the introduced of carboxylic (-COOH) groups and some other oxygen-bearing functionalities such as hydroxyl, carbonyl, ester, and nitro groups into the tubes. In this process, CNTs are treated by strong acids, such as refluxing in a mixture of sulfuric acid and nitric acid, ‗piranha' solution (sulfuric acid-hydrogen peroxide), boiling in nitric acid, or treating with oxidative gases, such as ozone. At first MWCNTs supersonically mixed into ethanol to be deaggregated temporarily. Then, the mixture is dried and pretreated using citric acid solution. Upon oxidative treatment the introduction of -COOH groups and other oxygen-bearing groups at the end of the tubes and at defect sites is promoted, decorating the tubes with a somewhat indeterminate number of oxygenated functionalities. However, mainly because of the large aspect ratio of CNTs, considerable sidewall functionalization takes place (Fig. 2.20).

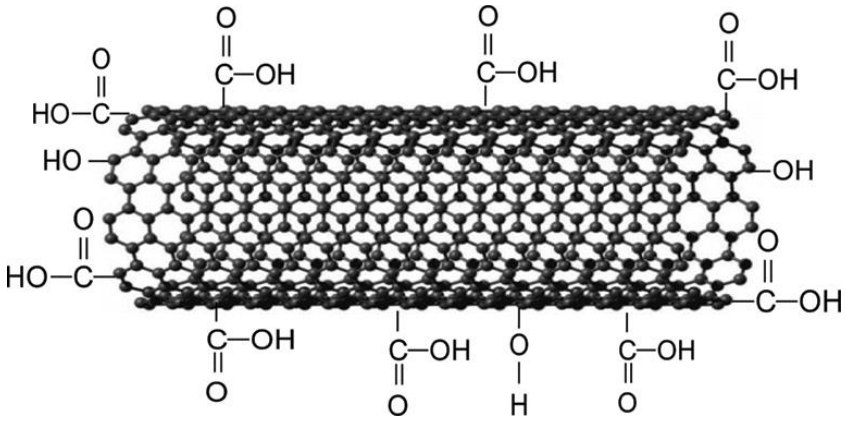

Fig 2.20**:** Section of an oxidized CNT, reflecting terminal and sidewall oxidation [29].

Finally, the MWCNTs in the solution will be treated by the oxygen plasma including citric acid and water. This method is safer than the methods mentioned in literature as no hazardous reagents are used [49]. The surfaces of the MWCNTs will be chemically functionalized with carboxyl (–COOH) groups, and they can be easily dispersed in water. Here, an environmentally friendly approach to functionalizing CNTs has been described, which is developed to attach -COOH groups onto their surfaces, and carried out under a wet condition using citric acid solution in RF (13.56 MHz) oxygen plasma.

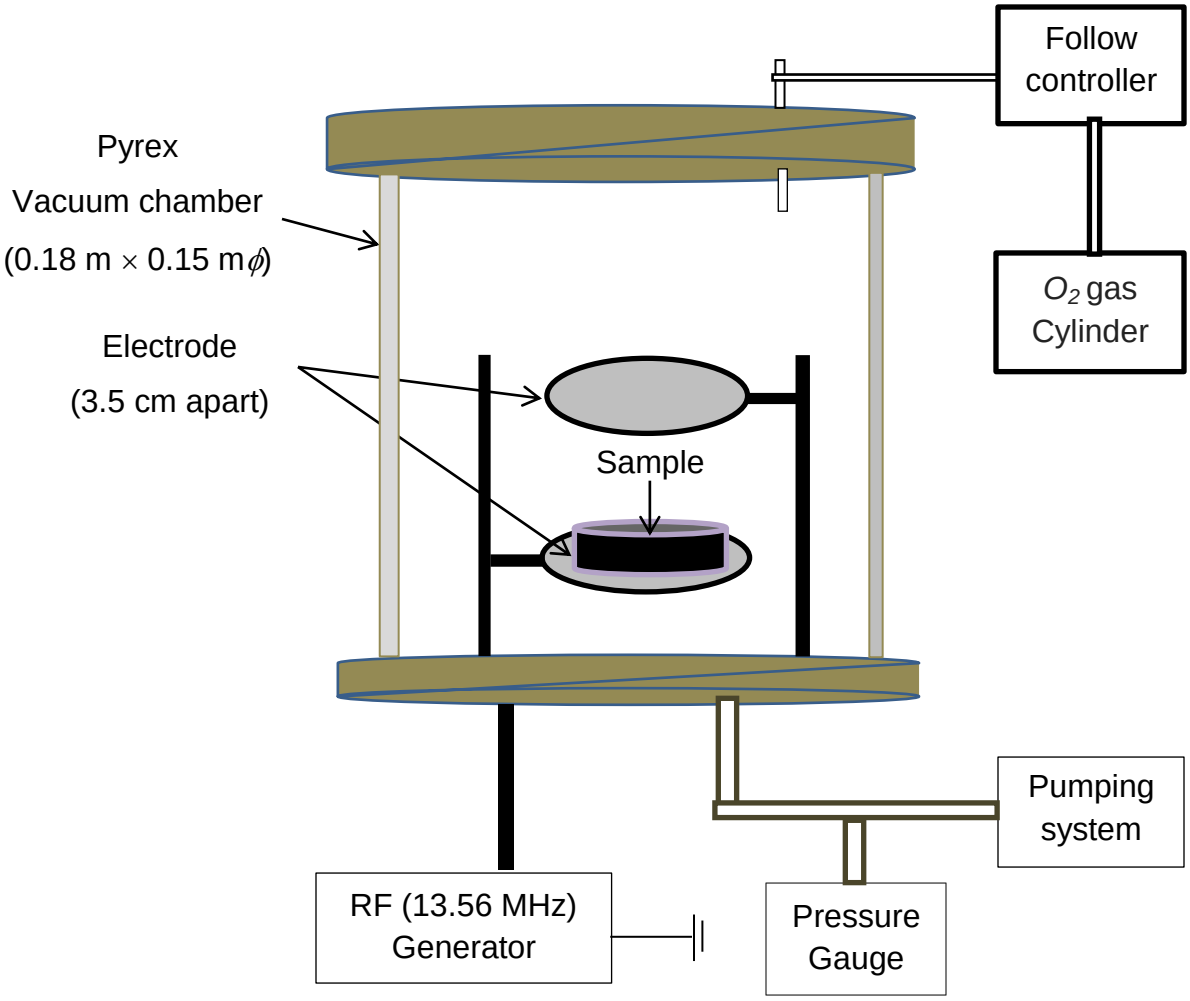

Fig. 2.21: Schematic diagram of the plasma reactor.

2.8.3 Treatment of jute using oxygen plasma

The search for textiles and fibrous structures with the capacity of conducting electricity is in full growth because of the wide variety of potential applications of these fibrous structures, resulting from their flexibility, lightweight, and capability of adapting to different shapes [54, 55]

However, jute consists of 71% cellulose, 13% hemi-cellulose, 11% lignin, 2.3% water soluble, 0.5% fats and waxes and 0.2% pectin. Most of the pectin, hemi-cellulose, and lignin need to be removed to give jute as a high tensile strength and to making it useful in production of reinforced composites [56, 57]. There are three steps to removing that element from the raw jute

Alkali treatment is one of the processes to improve mechanical property of jute fibers. The process removes chemicals such as lignin, hemi-cellulose and pectin from the raw fiber to change the state of the materials from hydrophilic to hydrophobic. The large loss of hemi-cellulose makes the fibers lose their cementing capacity and they consequently separate out from each other, making them finer [58]

The second step is an acidic treatment to removing alkaline elements to make jute as neutralize and wash out by distilled water. So that jute goes to ready to makes jute composite.

The third one is the most important are in treating the jute in which jute is putted on plasma chamber and oxygen plasma is produced by a RF frequency generator. The entire step is shown below:

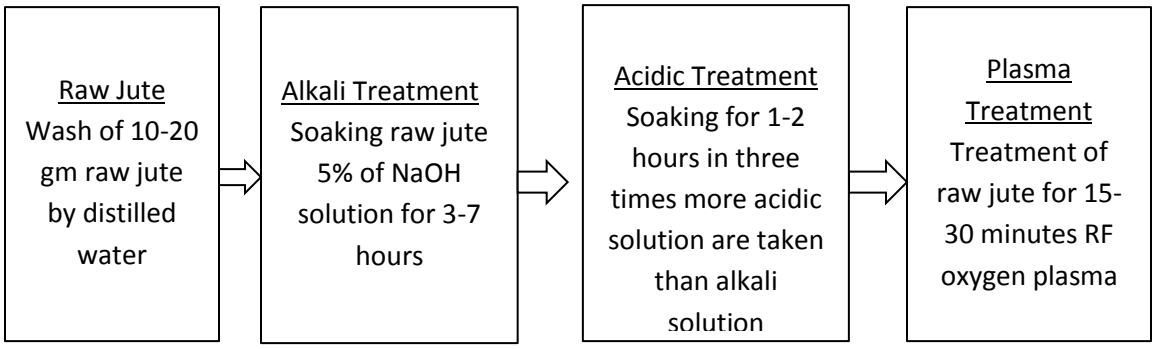

Fig. 2.22: Flow chart of the jute treatment.

2.8.4 Preparation of jute nanocomposite

Jute is environmental friendly, cheap, has a low density, biodegradable, and good specific mechanical properties. It can be woven into different forms and shapes [59, 60]. Natural jute is generally electrical insulators or has very limited conductivity. Therefore, it is a big challenge to use natural fibers in conductive fibrous systems. One of the ways that can be used to decrease the resistivity of natural fibers is their functionalization with conductive material [61]. Because of size, metal nanoparticles (NPs) exhibit a high surface area and excellent surface activity, which make them promising materials with exclusive optical, electrical, and catalytic properties. One of the mostly used NPs to improve the conductivity and mechanical properties of coatings and jute composites is CNTs.

2.9 Characterization Techniques of the Nanocomposite

Jute based nanocomposite have received great attention in recent years for their electrical response. The basic principles of the characterization techniques of the nanocomposite setup used will be introduced in this chapter. A brief view on such techniques are important to identify the properties on nanocomposite are started below.

2.9.1 Surface morphology

For materials surface Characterization scanning electron microscopy (SEM) has been a powerful and popular tool. A scanning electron microscope (SEM) is a type of electron microscope that generates images of a sample by scanning the surface with a focused beam of electrons. The electrons interlude with atoms in the sample, producing various signals that contain information about the surface topography and composition of the sample. A high-speed electron beam instead of light waves to generate the image of the sample and magnification is obtained by ‗electromagnetic fields'. Very high magnification and incredibly high resolution gives by electron microscope. Magnified and more detailed highly resolved images of small sample produce by electron microscope. The electronic beam passes through the specimen, then through a series of lenses that magnify the image. The image results from a scattering of electrons by atoms in the specimen. SEM generates various types of signals and can include characteristic X-

ray, secondary electrons and back scattered electrons. The sample excited by the incident electron beam are emitted light is detected by the most popular SEM of secondary electrons. An electron gun is fitted with a tungsten filament cathode from which an electron beam is emitted by SEM. Thermionic electron gum is used because of having highest melting point and lower vapor pressure of all metals. The electron beam energy rang is 0.2 KeV to 40 KeV, is focused by one or two condenser lenses to a spot about 0.4 nm to 5 nm in diameter. The beam passes through scanning coils in the electron column direct and position the focused beam onto the sample surface which deflects the bean in the x and y axes so that it scans in a raster pattern over a rectangular area of the surface for imaging. The electron loss energy by repeated random scattering and absorption which sample extends volume less than 100 nm to approximately 5μm into the surface. Vacuum prior is used to avoid interference with the electron beam. Brightness on a display monitor and/or in a digital image file is displayed the intensity of the emitted electron signal. The morphology of the sample surface area is displayed by synchronizing the position in the image scan to that of the incident electron beam. The ratio of the image display size to the sample area magnified by the electron beam. SEM analysis is considered to be non-destructive; that is, x-rays generated by electron interactions do not lead to volume loss of the sample, so it is possible to analyze the same materials repeatedly. A schematic diagram of SEM is illustrated in Fig 2.23.

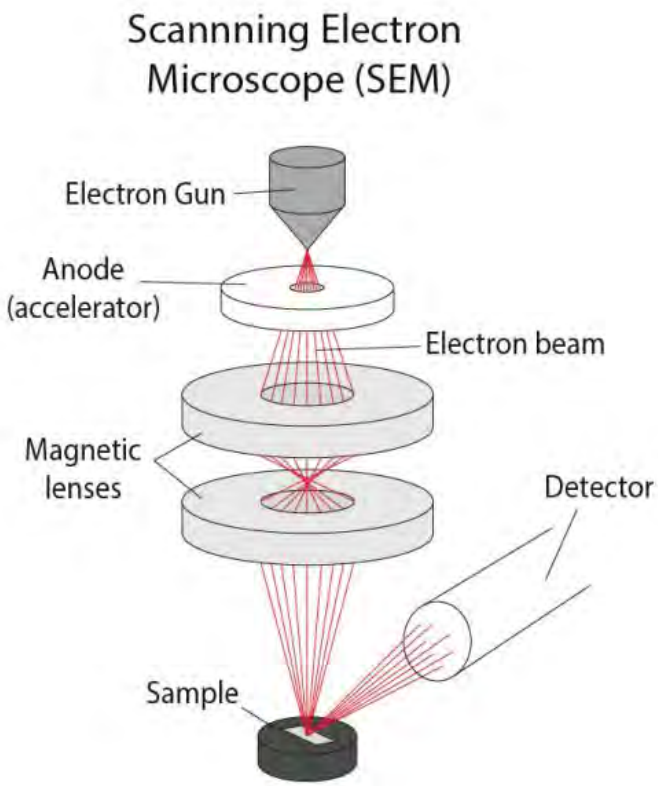

Fig 2.23: Schematic diagram of a scanning electron microscope (SEM).

2.9.2 Structural characterization

To describe a material uniquely, information like detailed structural properties are very important. Generally the answer of these types of questions: how are they arranged or what their functional groups are and other structural properties are obtained by various types of structural analysis such as X-ray diffraction, infrared spectroscopy, Raman spectroscopy, etc.

2.9.2.1 Fourier Transform Infrared Spectroscopy

General principle IR spectroscopy is an extremely effective method for determining the presence or absence of a wide variety of functional groups in a molecule. It measures the different IR frequencies by a sample positioned in the path of an IR beam and it reveals information about the vibrational state of molecule. The main goal of IR spectroscopic analysis is to determine the chemical functional groups in the sample. Different functional group absorbs characteristic frequencies of IR

radiation and its absorption results due to the changes in vibrational and rotational status of the molecules. Actually a molecule when exposed to radiation to produce by the thermal emission of a hot source (a source of IR energy), absorbs only at frequencies corresponding to its molecular modes of vibration in the region of the electromagnetic spectrum between visible (red) and short wave (micro waves). These changes in vibrational motion give rise to bands in the vertical spectrum; each spectral band is characterized by its frequency and amplitude. The absorption frequency depends on the vibrational frequency of the molecules, whereas the absorption intensity depends on how effectively the infrared photon energy can transferred to the molecule, and this depends on the change in dipole moment that occurs as a result of molecular vibration. As a consequence, a molecule will absorb infrared light only if the absorption causes a change in the dipole moment. Thus all compounds except for clement diatomic such as N_2, H_2, and O_2 have infrared spectra and most components present in a flue gas can be analyzed by their characteristic infrared absorption. Furthermore, using various sampling accessories, IR spectrometers can accept a wide range of sample types such as gases, liquids and solids. Thus, IR spectroscopy is an important and popular tool for structural elucidation and compound identification.

Infrared Frequency Range

Infrared radiation spans a section of the electromagnetic Spectrum having numbers from roughly 3000 to 10 cm^{1} or wavelength from 0.78 to 1000μm. IR absorption positions are generally presented as either wavenumbers (V̄) or wavelengths λ. Thus, wavenumbers are directly proportional to frequency, as well as energy of the of the infrared (IR) absorption. In the contrast, wave lengths are inversely 'proportional to frequencies and their associated energy. Wavenumbers and wavelengths can be inter-converted using the following equation: cm^{1}

$$\bar{V}\ (cm^{1}) = \frac{1}{\lambda(\mu m)} \times 10^{4} \quad \text{..... (2.1)}$$

$$A = \log_{10}\left(\frac{1}{T}\right) = \log_{10}\left(\frac{I}{I_{\circ}}\right) \quad \text{..... (2.2)}$$

Where, A=Absorbance, T=Transmittance, I_0 = Intensity of incident light and I= Intensity of emerged light.

The IR region is commonly divided into three smaller areas: near IR, Mid IR and far IR. The region of most interest for chemical analysis is the mid-infrared region ($4000cm^{-1}$ to $10cm^{-1}$) which corresponds to changes in vibrational energies within molecules. The far infrared region ($400cm^{-1}$ to $10cm^{-1}$) is useful for molecules containing heavy atoms such as inorganic compounds but requires rather specialized experimental techniques. The far and near IR are no frequently employed because only skeletal and secondary vibrations (overtones) occur in these regions producing spectra that are difficult to interpret.

Infrared Absorption

At temperatures above zero, all the atoms in molecules are in continuous vibration with respect to each other. When the frequency of a specific vibration is equal to the frequency of the IR radiation directed on the molecule, the molecule absorbs the radiation. For a molecule to absorb IR, the vibrations or rotations within a molecule must case a net change in the dipole moment of the molecule. The alternating electrical field of the electromagnetic radiation interacts with fluctuations in the dipole moment of the molecule. If the frequency of the radiation matches the vibrational frequency of molecule then radiation will be absorbed, causing a change in the amplitude of molecular vibration. The energy of the molecule consists of transational, rotational vibrational and electronic energy

$$E=E_{electronic}+E_{vibrational}+E_{rotational}+E_{translatinal} \quad \text{(2.3)}$$

Translation energy of a molecule is associated with the movement of the molecule as a whole, for example in a gas. Rotational energy is related to the rotation of the molecule, whereas vibrational energy is associated with the vibration of atoms within the molecule. Finally, electronic energy is related to the energy of the molecule.

Like radiant energy, the energy of a molecule is quantized too and a molecule can exist only in certain discrete energy levels. Within an electronic energy level a

molecule has many possible vibrations energy levels. The vibration energy of a molecule is not determined by the orbit of an electron but by the shape of the molecule, the masses of the atoms and eventually by the associated vibrational coupling. For example, simple diatomic molecules have only one bond allowing only stretching vibrations. More complex molecules may have many bonds, and vibrations can be conjugated.

The major types of molecular vibrations are stretching and bending. Infrared radiation is absorbed and the associated energy is converted into these types of motions. The absorption involves discrete, quantized energy levels. However, the individual vibrational motion is usually accompanied by other rotational motions. These combinations lead to the absorption bands, not the discrete lines, commonly observed in the mid IR region.

The atoms in a CH_2 group, commonly found in organic compounds, can vibrate in six different ways:

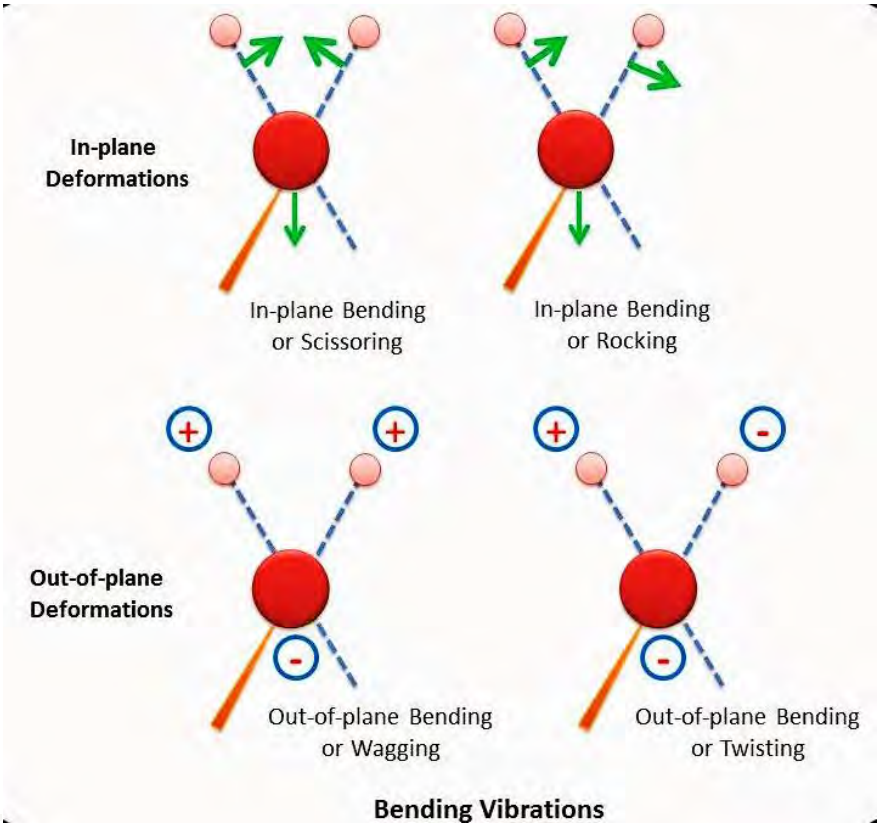

Fig. 2.24: Different types of molecular vibrations [62].

The IR Spectrum of a clay mineral is sensitive to its chemical composition, isomorphous substitution and layer stacking order. This makes Fourier Transform Infrared (FTIR) spectroscopy, the most informative single technique for assessing the mineralogy and crystal-chemistry of a clay mineral sample. The absorption of IR radiation by clay minerals depends critically on atomic mass, and the length, strength and force constants of interatomic bonds in the structures of these minerals. Absorption is also influenced by the Overall symmetry or the unit cell, and the local site symmetry of each atom within the unit Cell. Since theory alone give only limited Crystallo-chemical information. The interpretation of IR spectra is generally done by empirically assigning the observed signals to vibrational modes. Structural investigations of well-characterized families or natural and Synthetic clay minerals played an essential role in relating spectral features to mineral Structures. The monograph by Farmer [45] provides one of the most useful texts on the IR spectra of clay minerals.

A block diagram of an FTIR spectrometer show in bellow [62]:

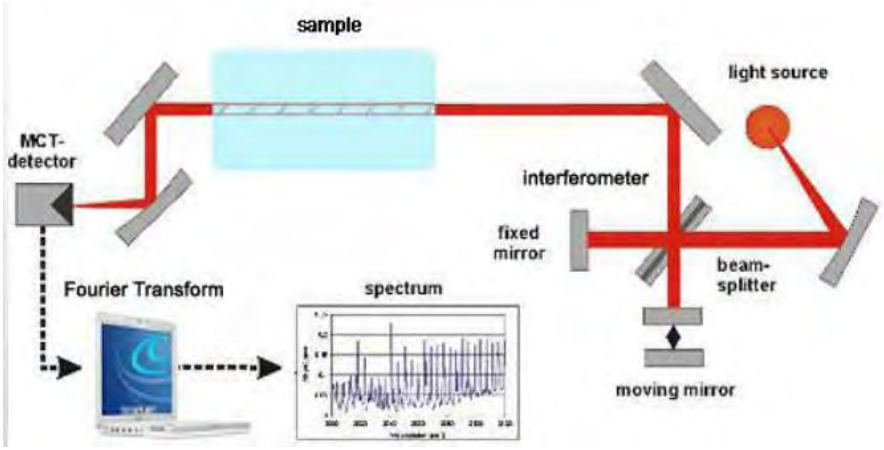

Fig. 2.25: Block diagram of an FTIR spectrometer [62].

2.9.3 Thermal analyses

Thermal analysis deals with the theories of thermal analysis (thermodynamics, irreversible thermodynamics, and kinetics) as well as instrumentation and techniques

(thermometry, differential thermal analysis, calorimetry, thermomechanical analysis and dilatometry, and thermogravimetry). Thermal analysis is used to establish the physical or chemical properties of a substance as it is heated, cooled or held at constant temperature in a controlled atmosphere. In advanced level, simultaneous thermal analysis (STA) refers to the simultaneous application of two different measurements to one and the same sample in a single run. Thermal analysis is a good analytical tool to measure: thermal decomposition of solids and liquids, solid-solid and solid-gas chemical reactions, material specification, purity and identification, inorganic solid material adsorption, phase transitions.

2.9.3.1 Thermogravimetric analysis (TGA):

Thermogravimetry (TG) or thermogravimetric analysis (TGA) is a powerful thermal analysis technique in which the weight or the mass of a substance is monitored as a function of temperature or time as the specimen is subjected to a controlled temperature program in a controlled atmosphere. Inorganic materials, metals, polymers and plastics, ceramics, glasses, and composite materials can be analyzed by TGA

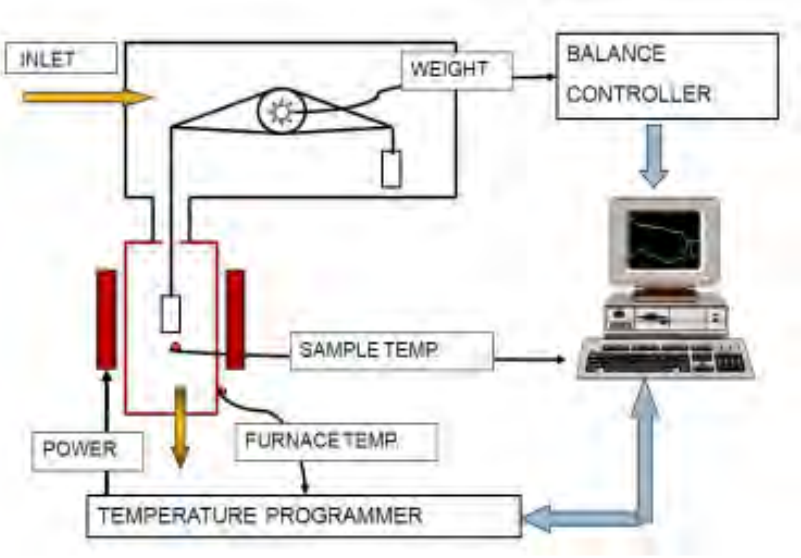

Fig. 2.26: Schematic diagram of thermogravimetric analysis [63].

The thermogravimetric analyzer is an necessary laboratory tool used for material characterization. The basic principle of TGA is that as a sample is heated, it‘s mass changes. This change can be used to recount the composition of a material or its thermal stability. The sample is typically heated at a constant heating rate (so-called dynamic

measurement) or held at a constant temperature (isothermal measurement), but may also be subjected to non-linear temperature programs such as those used in sample controlled TGA (so-called SCTA) experiments. The type of information required about the sample that‘s types of temperature program will be set. Additionally, the atmosphere used in the TGA experiment plays an important role and can be reactive, oxidizing or inert. Changes in the atmosphere during a measurement may also be made. Usually, a sample loses weight as it is heated up due to decomposition, reduction, or evaporation. A sample could also gain weight due to oxidation or absorption. A TGA consists of a sample pan that is supported by a precision balance. That pan resides in a furnace and is heated or cooled during the experiment. The mass of the sample is monitored during the experiment. A sample purge gas controls the sample environment. Purging gas can be provided from both horizontal and vertical directions. This gas may be inert or a reactive gas that flows over the sample and exits through an exhaust. The results of a TGA measurement are usually displayed as a TGA curve in which mass or per cent mass is plotted against temperature and/or time.

2.9.3.2 Differential Scanning Calorimetry (DSC):

Differential scanning calorimetry (DSC) is one of the thermo-analytical techniques which measures the amount of energy absorbed or released by a sample when it is heated or cooled or held isothermally, providing quantitative and qualitative data on endothermic (heat absorption) and exothermic (heat evolution) processes. Both the sample and reference are maintained at nearly the same temperature throughout the experiment. The reference sample should have a well-defined heat capacity over the range of temperatures to be scanned and analyzed. Usually, the reference is an inert material such as alumina or just an empty pan. Pans of Al, Cu, Au, Pt, alumina, and graphite are available and need to be chosen to avoid reactions with samples and with regard to the temperature range of the measurement. The most common purge gas is nitrogen. There are two types of DSC commercially available: heat flux (HF) type and power compensation (PC) type.

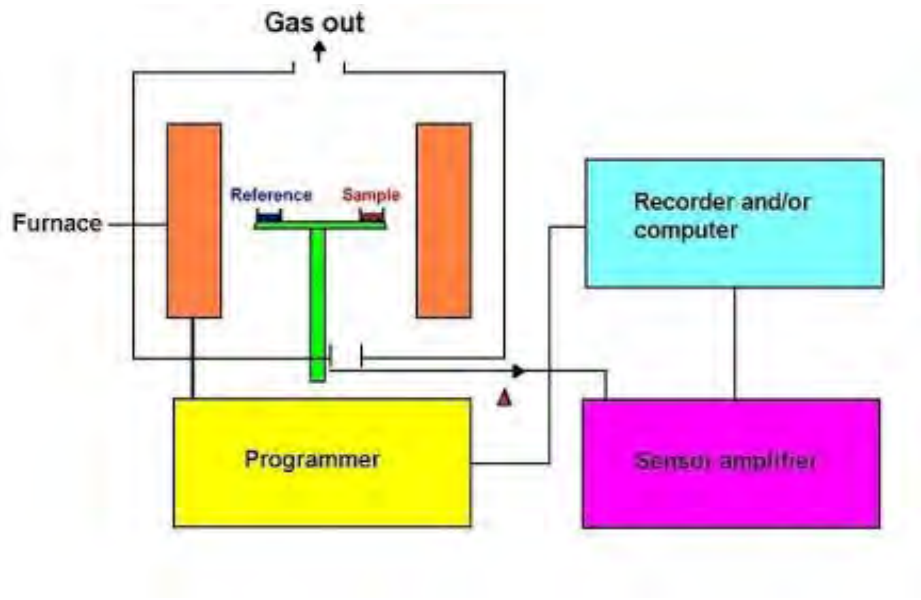

Fig. 2.27: Schematic diagram of heat flux type DSC [63].

In HF type DSC, both sample and reference pans are heated by a single furnace through heat sink and heat resistor. Heat flow is proportional to the heat difference of heat sink and holders. The temperature versus time profile through a phase transition in a heat flux instrument is not linear. At a phase transition, there is a large change in the heat capacity of the sample, which leads to a difference in temperatures between the sample and reference pan. A set of mathematical equations convert the signal into heat flow information. By calibrating the standard material, the unknown sample quantitative measurement is achievable. In heat flux DSC, we can write the total heat flow $^{dH}/_{dt}$ as,

$$\frac{dH}{dt} = C_P \frac{dT}{dt} + f\,(T, t) \quad \text{.....(1)}$$

Where, H = enthalpy in J mol ^{1}

Cp = specific heat capacity in JK ^{1}mol ^{1}

f (T,t) = kinetic response of the sample in J mol ^{1}

Thus, the total heat flow is the sum of the two terms, one related to the heat capacity, and one related to the kinetic response.

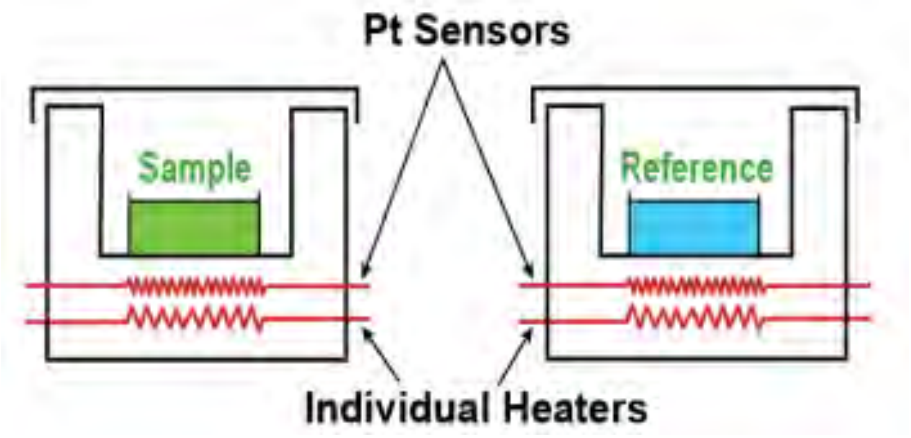

Fig 2.28: Schematic diagram of power compensation type DSC [63].

In PC type DSC, both sample and reference pans are heated by different furnaces. When an event occurs in the sample, sensitive platinum resistance thermometer (PRT) find out the changes in the sample, and power (energy) is applied to or removed from the sample furnace to compensate for the change in heat flow to or from the sample. As a result, the system is maintained at a ~~"t~~hermal null" state at all times. The amount of power required to maintain system equilibrium is directly proportional to the energy changes occurring in the sample. No complex heat flux equations are necessary with a power compensation DSC because the system directly measures energy flow to and from the sample. The heating and cooling rate of PC types DSC can be as high as 500°C/min. DSC analysis is used to analyses melting temperature, heat of fusion, latent heat of melting, reaction energy and temperature, glass transition temperature, crystalline phase transition temperature and energy, precipitation energy and temperature, oxidation induction times, and specific heat or heat capacity.

2.9.4 Mechanical properties

The mechanical properties are physical properties that a material exhibits upon the application of forces. The range of usefulness of a material and establish the service life determined by the mechanical properties. Classification and identification of material are also used mechanical properties. The most common properties considered are strength, ductility, hardness, impact resistance, and fracture toughness. Most structural materials are anisotropic, which means that their material properties vary with orientation. To

directionality in the microstructure (texture) from forming or cold working operation, the controlled alignment of fiber reinforcement and a variety of other causes can be change the properties. Mechanical properties are generally specific to product form such as sheet, plate, extrusion, casting, forging, and etc. The directional grain structure of the material, it is common to see mechanical property. In products such as sheet and plate, the rolling direction is called the longitudinal direction, the width of the product is called the transverse direction, and the thickness is called the short transverse direction. The grain orientations in standard wrought forms of metallic products are shown the image.

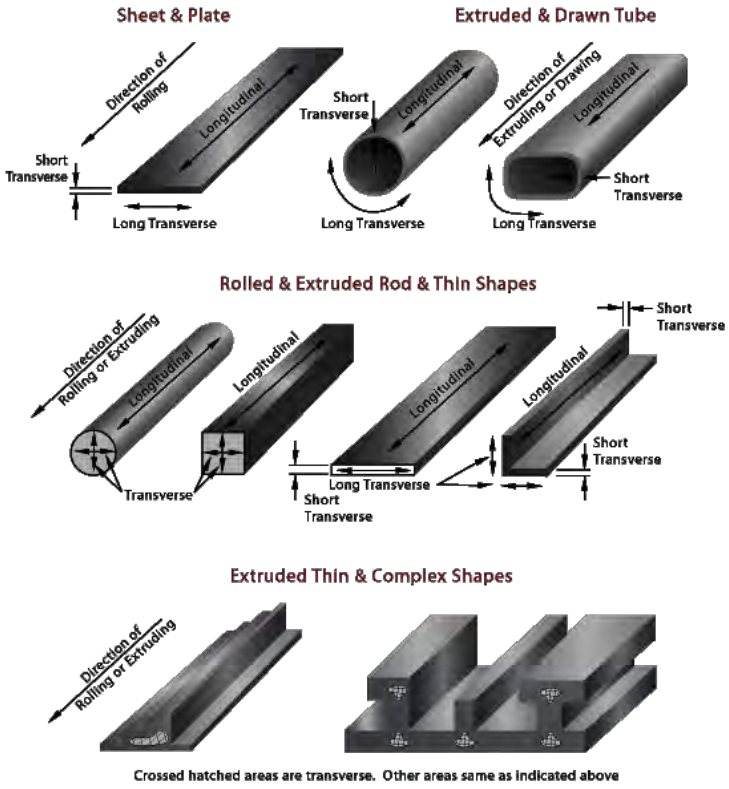

Fig. 2.29: The grain orientations in standard wrought forms of metallic products [46].

The effect of temperature, rate of loading and other conditions, mechanical properties of a material are not constant. For example, temperatures high than room temperature generally cause decrease in strength properties of metallic alloys; while ductility, fracture toughness, and elongation usually increase. Temperatures below room temperature usually cause an increase in the strength properties of metallic alloys. Ductility may

decreases or decrease with increasing temperature depending on the same variables. It should also be noted that there is often significant variability in the values obtained when measuring mechanical properties. The same lot of material will often generate considerable different results seeming identical test specimen. Therefore, multiple tests are commonly conducted to determine mechanical properties and values reported can be an average value or calculated statistical minimum value. Also, a range of values are sometimes reported in order to show variability.

2.9.4.1 Tensile strength:

The force required to push something such as rope, wire, or a structural beam to the point where it breaks is measured by tensile strength. The tensile strength of sample is the maximum content of tensile stress that it can take before failure, for example breaking.

There are three typical of tensile strength:

- Yield strength – Yield stress is the stress level at the point where the material begins to have unchangeable deformation. The stress a material can withstand without permanent deformation of 0.2% of the original dimension.

  $$E = \frac{\sigma}{\varepsilon}$$

  Where:

  E is the Yield strength

  σ is the stress required to cause a certain strain

  ε is the strain caused by a certain amount of stress

- Ultimate strength - The maximum stress a material can withstand.

  $$UTS = \frac{\text{Ultimate Force}}{\text{Original cross-Sectional area}} = \frac{F}{A}$$

- Breaking strength - The stress coordinate on the stress-strain curve at the point of rupture.

Some typical tensile strengths of some materials:

Material	Yield strength (MPa)	Ultimate strength (MPa)	Density (g/cm^3)
Structural steel	250	400	7.8
Steel, Piano wire	2000		7.8
High density polyethylene	26-33	37	0.95
Aluminum Alloy 2014-T6	400	455	2.7
Glass	4400		2.53
Copper 99.9% Cu	70	220	8.92
Bamboo	142	265	0.4
Carbon Fiber	N/A	5650	1.75
Rubber	-	15	
Carbon nanotube	**N/A**	**6200**	**1.34**

Table 2.1: Some typical tensile strengths of some materials.

Multiwalled carbon nanotubes have the highest tensile strength of any material yet measured, with labs producing them at a tensile strength of 63 GPa, still well below their theoretical limit of 300 GPa. However, as of 2004, no macroscopic object constructed of carbon nanotubes has had a tensile strength remotely approaching this figure, or substantially exceeding that of high-strength materials like Kevlar [46, 63].

2.9.5 Electrical conduction in polymer nanocomposites

Electrically conductive composites consist of an insulating matrix material and conductive filler particles of various shape (spheres, flakes, fibers etc.). Most polymers are inherently electrically insulating and conductive nano-fillers are found to impart significant conductivity to polymers and render them insulating to conductive. The electrical properties of nanocomposites are controlled through the material selection, volume fractions of components, conductivity, percolation behavior and anisotropy.

Percolation theory has been a successful tool for describing the transition behavior of insulating polymers filled with conductive inclusions [64-66].

Factors Influencing the Conductivity of CNTs/Jute Nanocomposites

The electrical conductivity of composites mainly depends on the filler, matrix and temperature. From the filler point of view the type, size, volume fraction and orientation of particles in the matrix are crucial here.

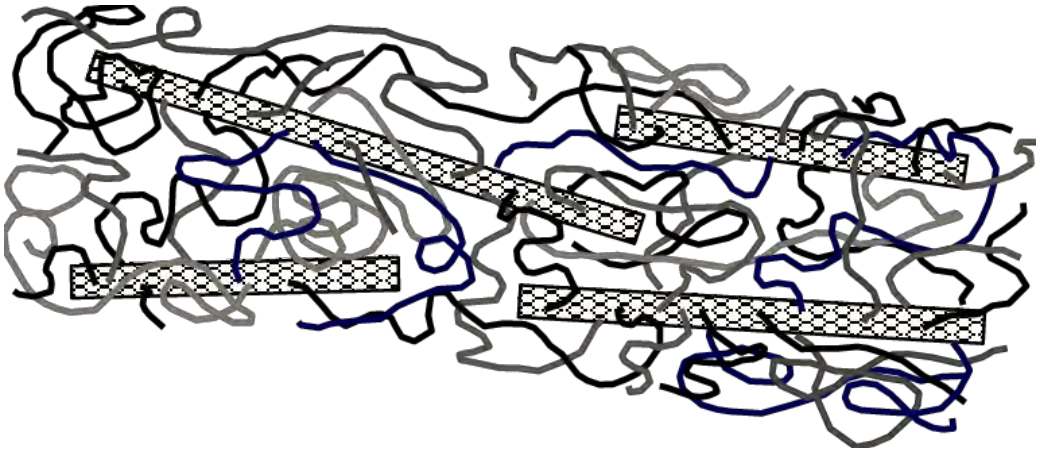

Fig. 2.30: Integration of nanotubes into the polymer cross-linked structure [67].

According to Bigg [68], the fibrous fillers improve conductivity much more significantly than spheres, flakes of irregular particles, i.e. aspect ratio plays important roles here. In the nanocomposites reinforced by CNTs, nanotubes are covalently integrated into the polymer matrix and become part of the cross-linked structure rather than just a separated component [69].

(i) Structure of CNTs

The aspect ratio is a proportion of maximum length, L to minimum diameter, D, according to this classification $L/D \approx 1$ for symmetrical particles (spheres, cubes and ellipsoids), $1 < L/D < 1000$ for short fibers and flakes and $L/D > 1000$ for long fibers [45]. The larger the particle aspect ratio is and the more randomly the particles are oriented, the smaller value of the threshold filler content, vcrit, appears. The larger values of L/D are more effective in enhancing the conductivity of composites. CNTs exhibit the

highest potential for an efficient enhancement of the electrical conductivity, due to the relatively low surface area, chirality and high aspect ratio that enables a good dispersibility. At similar states of CNTs orientation, the higher the aspect ratio, the lower the CNTs concentration necessary to reach the percolation threshold, and to get conductive composites.

(ii) Volume fraction of CNTs

With increasing MWNT loading, the nanocomposites undergo transition from electrically insulated to conductive and then the electrical conductivity was increase with additional weight percent of CNTs in the matrix [70, 71]. The incorporation of a small quantity of CNTs into polymer composites could exhibit higher electrical conductivity due to the formation of an extra effective electrical network. However, higher CNTs loading in polymer composites may cause serious CNTs aggregation, and the bulk electrical conductivity will be leveled off, even decreased [72]. Thus, choosing a suitable CNTs percentage is very important. The CNT/polymer nanocomposites have critical exponent related to the system dimension ranges from 1.6 to 2.0 by theoretical prediction, while experimental values between 0.7 and 3.1 have been reported [73, 74].

(iii) Types of polymer

Due to the different structures and different properties especially electrical conductivity of different kinds of polymers, when reinforced by CNTs, the nanocomposites will show different electrical percolation thresholds. The polymer matrix plays very important roles in a composite material; it acts as a path for stress transfer between fillers and protects the reinforcement from an adverse effect of the environment. The matrix has a major influence on the processing characteristics of composites. Several types of polymers have been used as matrix for reinforcement by CNTs.

(iv) Temperature and activation energy:

The composite conductivity is influenced by temperature in various aspects; activation energy is the most important. The energy required to transfer charge from one initially

neutral island to another is known as activation energy and denoted by ΔE. The temperature dependence of conductivity, σ can be expressed by the Arrhenius equation

$$\sigma = \sigma_0 \exp\left(-\frac{\Delta E}{K_B T}\right) \quad (2.7)$$

Where ΔE is the activation energy of conductivity, k_B stands for the Boltzmann constant, T is the temperature and σ_0 is a pre-exponential factor depending on mobility of charge carriers. Equation (2.7) can be written as

$$\text{Ln } \sigma = -\frac{\Delta E}{K_B T} + \ln\sigma \quad (2.8)$$

Equation (2.8) is equivalent to a straight line equation, y = mx + c. So that ΔE can be determined from the slope of the straight line. From the graph of lnσ versus $\frac{1}{T}$, ΔE can be calculated by using the relation

$$\Delta E = -\left(\frac{\ln\sigma}{\frac{1}{T}}\right) \times k_B(eV) \quad (2.9)$$

The correlation between $\sigma_\circ$ and ΔE can be expressed by Meyer-Neldel rule [61], or according to Turvey as the compensation law [44],

$$\ln\sigma_\circ = a + b\Delta E \quad (2.10)$$

Where a and b (with b > 0) are constants. Several authors [76-78] stated that the compensation law is generally valid not only for inorganic substances but for many semiconducting materials as well.

CHAPTER 3
EXPERIMENTAL DETAILS

3.1 Materials

3.1.1 Raw jute

The jute fiber used in this work collected from by Bangladesh local market (Shailkupa Upazila, Jhenaidah), specific weight of which is ~ 0.95 g/cm^3, diameter = 20–200 μm, melting point = 170°C and molecular weight >10 000g/mol.

3.1.2 Multi-Walled Carbon Nanotubes (MWCNTs)

MWCNTs (CNano Technology L.) of purity >95% were obtained from Shizuoka University, Japan as a gift. The diameter of the tubes is 10 ± 2.1 nm, and the length is between 1-10 μm. To prepare CNTs/jute nanocomposites functionalized MWCNTs (f-MWCNTs) are used as conductive additive.

3.1.3 Ethanol

Ethanol was manufactured by Merck, Germany. Ethanol evaporates quickly, without leaving a residue and is very effective for surface cleaning application. Distilled water and ethanol are used for cleaning purpose throughout the experiments.

3.1.4 Citric acid

Citric acid was manufactured by Merck, Germany. Citric acid is a weak organic acid in materials science, the Citrate-gel method is a process similar to the sol-gel method, which is a method for producing solid materials from small molecules. During the synthetic process, metal salts or alkoxides are introduced into a citric acid solution. The polycondensation of ethylene glycol and citric acid starts above 100 °C, resulting in polymer citrate gel formation.

3.1.5 Acetic acid

Acetic acid was manufactured by Merck KGaA, 64271 Darmstadt, Germany. The hydrogen centre in the carboxyl group (−COOH) in carboxylic acids such as acetic acid can separate from the molecule by ionization:

$$CH_3COOH \rightleftharpoons CH_3CO_2^- + H^+$$

Because of this release of the proton (H^+), acetic acid has acidic character and reaction with alkali produce salts and water.

$$CH_3COOH + NaOH \rightarrow CH_3COONa + H_2O$$

3.1.6 Sodium hydroxide

Sodium hydroxide (NaOH) was manufactured by Merck, Germany. Water and NaOH detergent-based parts washers are considered to be an environmental improvement over the solvent-based cleaning methods. Jute fibers were alkali treated for 4 h with 5% concentrations of NaOH, respectively.

3.1.7 Oxygen gas

Oxygen Gas was manufactured by Linde, 285 Tejgaon Industrial Area, Dhaka, Bangladesh. Oxygen is one of the most abundant elements on this planet. Our atmosphere is 21% free elemental oxygen. Oxygen gas is used to functionalization of CNTs and treatment of jute fibers.

3.2 Apparatus used to fabricate the Nanocomposites

(i) Analytical balance

Fig. 3.1: A photograph of an ALN 220 analytical balance.

Analytical Balances are instruments used for accurate and precise determining weight of balances have built-in calibration weights to maintain accuracy. The balance that is used in this experiment is highly sensitive and can weigh sample to the nearest tenth of a milligram. We use the ALN 220 analytical balance was manufactured by Axis, Poland.

(ii) Ultrasonic homogenizer

Sonication is a process in which sound waves are used to agitate particles in solution. Ultrasonic frequencies (>20 kHz) are usually used in sonication, leading to the process also being known as Ultra-sonication. Sonication processes can be carried out by of probe-type ultrasonic homogenizer. Ultrasonic homogenizer is used in this research work for evenly dispersing CNTs in ethanol was manufactured by BioLogics Inc., USA. The Model 150VT Ultrasonic homogenizer delivers up to 150 watts of ultrasonic disruption with analog controls for superior sample processing. This model offers all the advanced engineering features necessary to create a total system for ultrasonic disruption. A compact footprint and cost effective pricing make the Model 150VT ideal for processing small sample volumes of 250 µl to 300 ml.

Fig. 3.2: A photograph of 150VT ultrasonic homogenizer.

(iii) Hot air oven

A hot air oven is electrical operated equipment which is used widely in research and analysis works. It offers simple operation of heating and drying of the common material. The hot air oven (Cowbell, India) used in this research can be operated from 50 to 250 ^{o}C.

Fig. 3.3: A photograph of a Hot Air Oven.

The temperature is controlled by using a thermostat and PID controller. Controller and automatically control units that helps to maintain the homogeneous temperature in the cabinet. It is constructed with double walled cabinet and inner chamber is made up of anodized aluminum/stainless steel. The double walled insulation keeps the heat in and conserves energy. For keeping samples, there are two trays fitted inside. Fig. 3.3 shows a photograph of a hot air oven that is used to evaporate the solvent from the composite.

(iv) Radio Frequency (RF) generator:

RF (radio frequency) signal generator is used for testing components, producing plasma, receivers and test systems in a wide variety of applications including cellular communications, Wi Fi, WiMAX, GPS, audio and video broadcasting, satellite

communications, radar and electronic warfare. RF signal generator normally has similar features and capabilities, but is differentiated by frequency range. RF signal generators typically range from a few kHz to 6 GHz. RF Generator which is used widely in research works was manufactured by ENI.COM, Piazzale Enrico Mattei, 1 – 00144. In this research work we using 13.56 MHz frequency range RF Generator which output power is 100 W.

Fig. 3.4: A photograph of a RF Generator.

(v) Plasma reaction chamber

The glow discharge plasma system is shown in Fig. 3.5. A cylindrical Pyrex glass bell-jar having 0.15 m in inner diameter and 0.18 m in lengths was used as plasma chamber. The top and bottom edges of the glass are covered with two rubber L-shaped (height and base 0.015 m, thickness 0.001 gaskets.

Fig. 3.5: Plasma reaction chamber.

The cylindrical glass was placed on the lower flange. The lower flange is well fitted with the diffusion pump by an ‗I' joint. The upper flange is placed on the top edge of the bell-jar. The flange is made up of brass having 0.01 m in thickness and 0.25 m in diameter. On the upper flange a lay bold pressure gauge head, Edwards's high vacuum gas inlet valve and an oxygen gas injection valve are fitted. In the lower flange two highly insulated high voltages feed-through are attached using screwed copper connectors of 0.01 m high and 0.004 m in diameter via Teflon insulation.

Electrode system

A capacitive coupled electrode system is used in the system. Two circular stainless steel plates of diameter 0.090 m and thickness of 0.001 m are connected to the high voltage copper connectors.

Pumping unit

For creating laboratory plasma, first step is pumping out the air/gas from the plasma chamber. In this system a rotary pump of Alcatel Vacuum Technology, UK (Model-OME- 25-S) is used.

Input Power Supply

The input power supply for plasma excitation comprises of a 13.56 MHz RF generator. The maximum output voltage is 100 W. The deposition increase with power at first and then becomes independent of power at high power values at constant pressure and flow rate.

Pirani Vacuum Gauge

The Pirani gauge consists of a metal filament (usually platinum) suspended in a tube which is connected to the system whose vacuum is to be measured. Pirani Vacuum Gauge which was used in this work manufactured by ULVAC, Inc., 2500 Hagisono, Chigasaki, Kanagawa, Japan 253-8543.

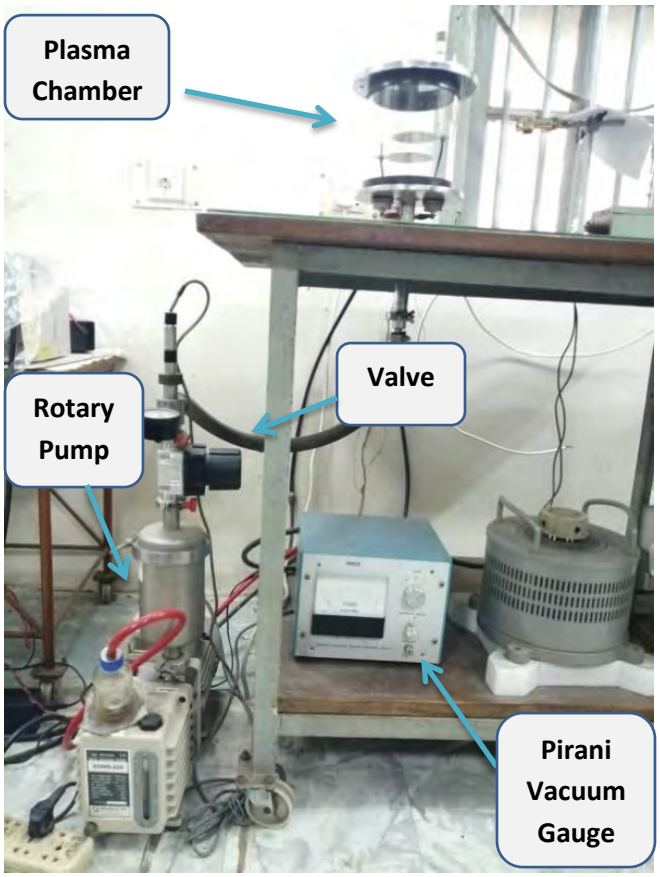

Fig. 3.6: Plasma ionization set-up.

Oxygen injection system

The Oxygen injection system consists of a plastic pipe line with metallic tube of the nozzle of high vacuum needle valve from oxygen cylinder. The pipe is fixed with oxygen cylinder by clamp arrangement.

Supporting frame

A metal frame of dimension 1.15 m × 0.76 m × 0.09 m is fabricated with iron angle rods, which can hold the components described above. The upper and lower bases of the frame are made with polished wooden sheets.

3.3 Composite Fabrication

Total research work is done by three steps: (i) functionalization of MWCNTs (ii) treated the jute (iii) Prepared jute composite. All those steps discuses below:

(i)Functionalization of MWCNTs:

A flow chart of the functionalization process is shown in Fig. 3.7 and the setup of the plasma chamber, indicating the dissociation of oxygen, water, and citric acid molecules. 30 mg of MWCNT powder (Sigma-Aldrich, outer diameter = 10±2.1 nm, inner diameter = 3-10 nm, length = 1-10 μm, purity >95%) is added to 20 mL of pure ethanol (Merck Co., purity >95%) and sonicated at room temperature using an ultra-sonic homogenizer (Model 150VT, BioLogics Inc., USA) at an input f = 20 kHz, power of 20 W for 30 min. The CNTs/ethanol suspension is dried under reduced pressure and soaked in 0.15 mole (5 ml) of citric acid (Merck., assay >98%) solution for more than 48 h. The CNTs in the solution are then placed on the lower electrode of a plasma reactor (0.18 m × 0.15 m) which is evacuated to ca. 0.13 Torr or 17.33 Pa using a rotary pump at a very slow rate. When the wet phase starts to disappear, oxygen gas is introduced into the reactor at a rate of 5 sccm and the background chamber pressure is kept at about 0.13 Torr. Though the water molecules, and part of the citric acid molecules evaporate, it is considered that they remain inside the chamber and in the gas container connected to the chamber, and contribute to the functionalization process. Then the plasma reaction is carried out for about 15 min by an RF input power of P_{rf} = 100 W, f = 13.56 MHz.

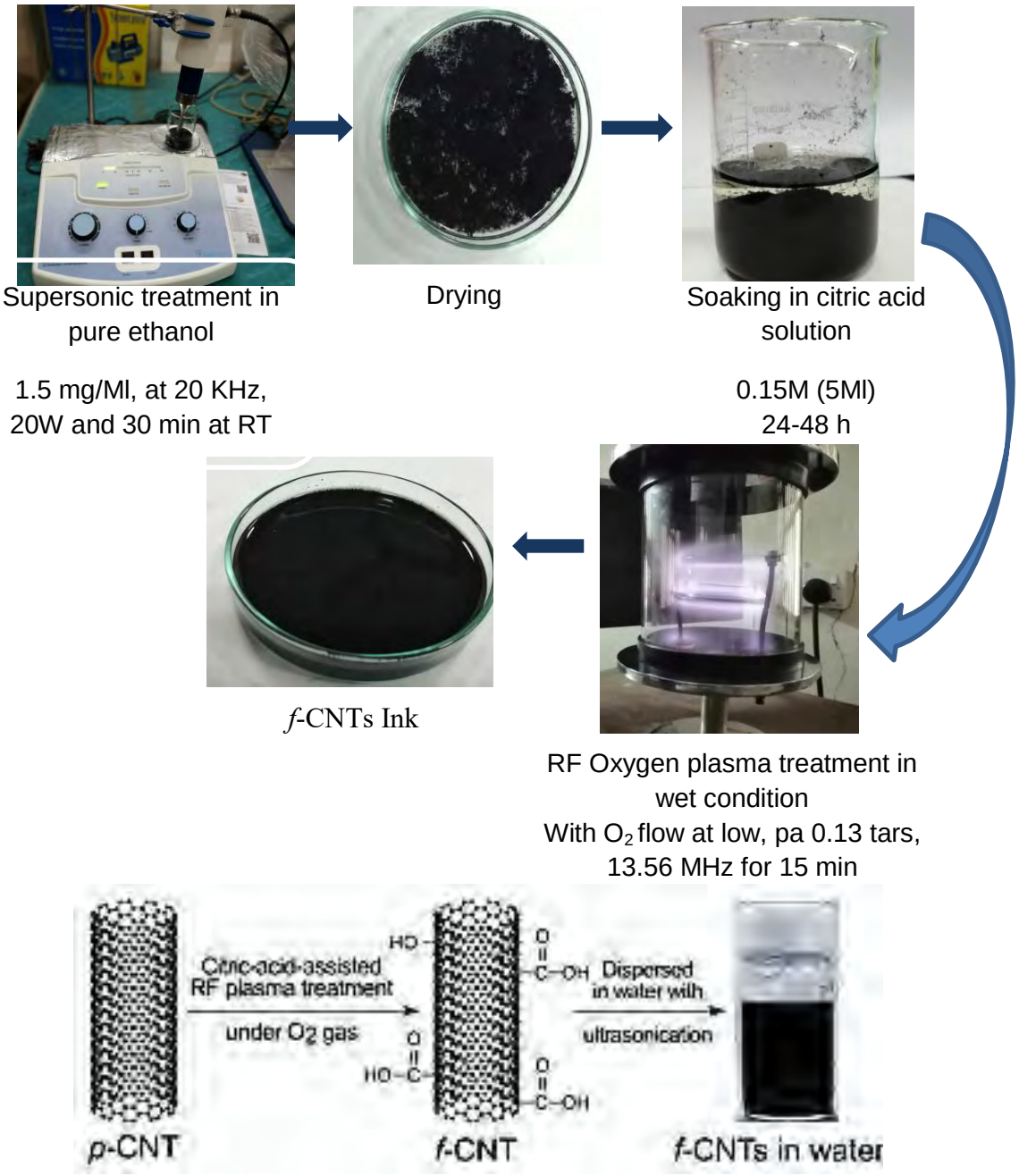

Fig. 3.7: The flow chart of the functionalization process with the optimum treatment conditions and the schematic of the functional group attachment.

It is noted that when the samples become fully dried before starting the plasma reaction, they are less reactive for the oxygen plasma. However, when the plasma started in the wet phase, the water molecules and part of the citric acid molecules evaporate with the processing time, and considered to remain inside the chamber and in the gas container connected to the chamber, contributing to the functionalization process. After the

treatment, the MWCNTs are washed at least three times using distilled water and dried under reduced pressure at room temperature. It is observed that approximately 15% of the CNTs are lost by the oxygen plasma, which is measured from the analytical balance of the samples before placing in the citric acid and after the final washing process.

(ii) Treated the jute

Jute fibers were washed with water at room temperature to make the fibers free from the dust. Wetted jute fibers were dried in air for 24 h at 25 ^{o}C before keeping them in oven so as to remove initial part of water from the fibers surface. The remaining traces of water were removed by keeping them in oven at 80 ^{o}C for 24 h. After that surface treatment of the jute fibers were done by two steps: i) alkali (NaOH) and ii) alkali followed by acid (NaOH + acid) separately.

Alkali Treatment

Jute fibers were soaked in 5 % (w/v) aqueous alkaline (NaOH) solution for 2 h at 25 ^{o}C maintaining fibers: solution ratio 1:30 (w/w). After treatment jute fibers were washed 3-4 times by distilled water to remove any traces of NaOH from surface. Jute fibers were then neutralized by adding acetic acid solution which is three times more than NaOH. NaOH treated jute fibers were treated by oxygen plasma in vacuum dried at 60 W RF power for 10 min. The reaction of alkali with jute fibers is shown in Fig. 3.8.

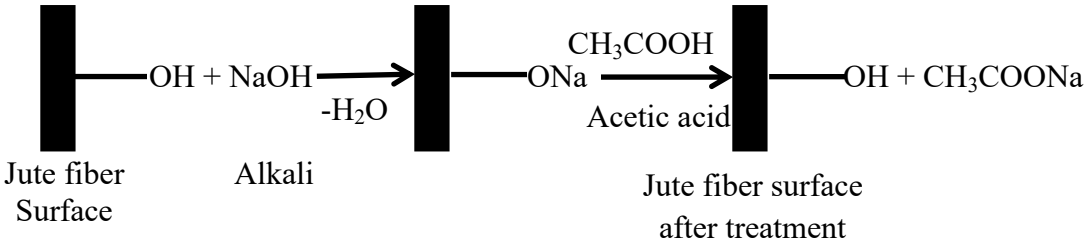

Fig. 3.8: The reaction of alkali with jute fibers.

Reaction mechanisms of alkali and jute fibers consists of: (i) replacement of hydride ion (H+) from the jute fiber surface hydroxyl group by the sodium ion (Na+) of NaOH followed by (ii) replacement of sodium ions (Na+) from the fiber surface by the hydride

ions (H+) of acetic acid. During this reaction process, NaOH soluble impurities such as -hemicellulose, wax and oily substances get removed. After treatment, jute fibers were washed several times by water to remove the chemical residues from the fibers surface and dried in an oven at 80 ^{o}C for 24 h. The hydrolysis process of jute fibers are shown in Fig. 3.9.

Fig. 3.9: Treatment of jute.

(iii) Preparation of jute composite

Samples of plasma-treated jute fabric (10 cm × 10 cm, average weight ~2.425 g) were immersed in 30 mg functionalized CNTs aqueous solutions in 50 ml water for 1.5 h (optimized time), while ultrasound was used to stirring for 20 min. After this, the excess of solution was discarded and the samples were placed under room temperature for several irradiation times on each side (10 cm distance). After irradiation, the samples were washed with distilled water to remove any residue and dried at room temperature. Fig. 3.10 shows the process of CNT/Jute nanocomposite.

Fig. 3.10: CNT/Jute nanocomposite.

3.4 Characterization

In this research work, CNT/Jute nanocomposite was investigated using different experimental techniques. The techniques are below:

- Fourier transforms infrared spectroscopy (FT-IR) for the chemical groups attached onto the CNTs and to investigate the chemical structure of the jute fibers.
- Scanning electron microscopy (SEM) for the surface morphology of the jute and nanocomposite fibers.
- Thermo gravimetric analysis (TG) for the thermal stability and degradation temperature of the sample.
- Electrical measurement for the electrical conductivity of the jute and nanocomposites.
- Mechanical properties of the nanocomposites were examined using a universal testing machine.

3.4.1 Surface morphology

The surface morphology of the produced nanocomposites is observed by using field electron microscopy (FESEM, JEOL JSM-7600F). The electron microscope quipped with a field emission gun and the incorporation of the gentle beam mode, built-in r-filter and ultra-high vacuum for high resolution image acquisition. FESEM images (1,280 x 1,024 pixels) are captured at 5,000 30,000× magnifications, acceleration voltage of 5 kV and a constant working distance of 7.7 mm. Figure 3.11 indicates a

field emission scanning electron microscope set up that is -used in this research work.

Fig. 3.11: Field emission scanning electron microscope.

3.4.2 Structural characterization

Fourier Transform Infrared Spectroscopy group identification is carried out using a spectrometer (SIMADZU, FMR- $4000 spectrophotometer, Japan) in the region of 650-4000 cm^{-1}.

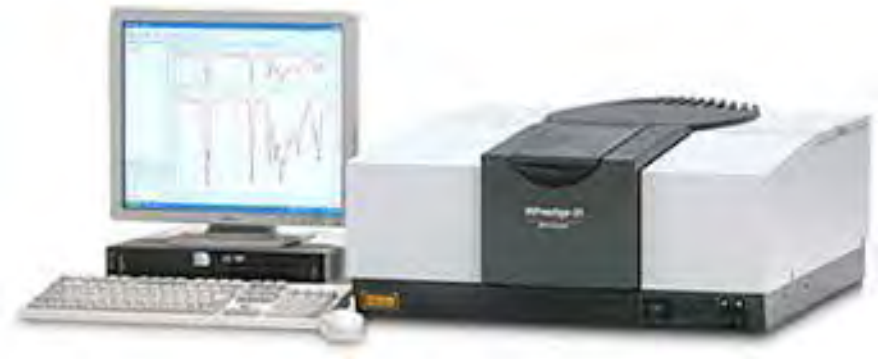

Fig. 3.12: Fourier transforms infrared spectroscopy set up.

3.4.3 Thermal analyses

Thermogravimetric analysis (TGA) and derivative thermo-gravimetric (DTG) behavior of the prepared samples is examined by NETZSCH STA 449 F3 Jupiter. This simultaneous thermal analyzer is used for TGA and differential scanning calorimetric (DSC) analysis. Samples were placed in alumina crucibles and heated from 26 ^{o}C to 600 ^{o}C. A heating rate of 10 ^{o}C/min is used under nitrogen atmosphere and at a flow rate of 40 ml/minute. The sample weight was about 5.5 mg. DTG is obtained by using TGA instrument software.

Fig. 3.13: Simultaneous thermal analyzer.

3.4.4 Mechanical properties

Single Fiber Tensile

Test Single fiber tensile test was done as per ASTM D3379-75 test method using an Instron 5848 micro tester (Shenzhen Wance Testing Machine Co. Ltd., Japan) with 10 N load cell and equipped with special pneumatic grips suitable for fiber type samples. By assuming that fibers have cylindrical shape, diameters of all fibers were measured at 5 different places using a microscope and average values were calculated and used for

calculations. The cross-head speed used was kept 0.5 mm/min and gauge length was taken 10 mm for all fibers samples. 30 replicates for all kinds of fibers samples were tested and average values reported.

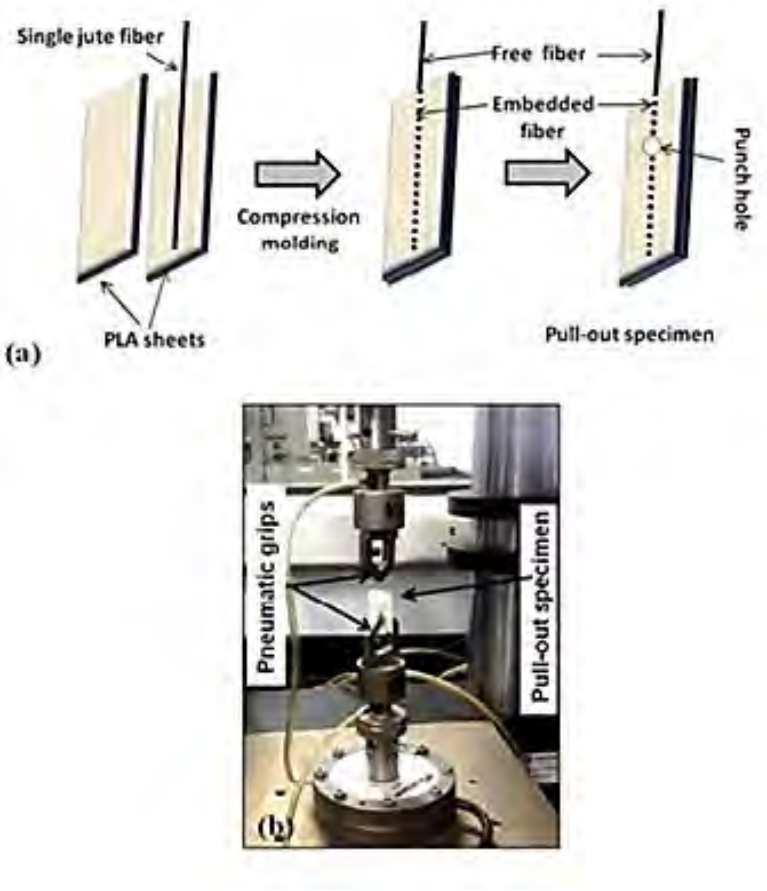

Fig. 3.14: Single fiber pull-out test; (a) schematic of specimen preparation and (b) experimental set up

Characterization of Interfacial Shear Strength (IFSS) and Critical Fiber Length (Lc)

Single fiber pull-out test was performed to evaluate the IFSS of CNT/jute fibers composite systems and critical fiber length of jute fibers inside the CNTs matrix. Fiber was kept straight by fixing it at both the end using glue in such a way that tips of the fiber came out from the sheets. The whole assembly was kept between the mold of a compression molding machine (Carver: 3893. 4011A00). The mold was closed and a pressure of 1089.6 Pascal was applied at 100 ^{o}C for 5 min, the assembly was then cooled

down to room temperature. Finally the compression molded specimen was cut in a rectangular shape (5×3 cm^2) in such a way that the fiber remains embedded along the main axis of the specimen. In order to obtain the desired embedded length, the fiber was cut by making a hole through the sample. For each type of CNT/jute fiber composite, specimens at 2, 4, 6, 8 and 10 mm embedded length with a free fiber length of 4 mm were prepared. A schematic of the preparation of pullout specimen is shown in Fig. 3.13(a).

Pull-out Test

Single fiber pull-out test was carried out using the same instrument as described in section 2.3.7 at a cross head speed of 0.5 mm/min. The samples were fixed between the pneumatic grips of tensile testing machine and load was applied at the free end of fiber to exert stress to pull it out of the matrix. At least ten specimens were tested for each embedded length for each type of CNT/jute fiber composite. The force required to pull-out the fiber from the matrix was recorded. An experimental setup for single fiber pull-out test is given in Fig. 3.13(b).

Interfacial Shear Strength (IFSS) and Critical Fiber Length (L_c)

IFSS was calculated from the maximum debonding force obtained from the force-displacement curve of fiber pull-out test. Equation (3) was applied to calculate the IFSS

$$\tau_c = \frac{Fmax}{\pi \times d\, L \times e} \quad \text{...} \quad (1)$$

where, τ_c is IFSS, F_{max} is the maximum debonding force, d is the diameter of the jute fiber and L_e is the embedded length of the jute fibers.

The minimum length of the fiber at which it can bear the maximum load is called the critical fiber length. For each type of CNT/jute fiber composites L_c was calculated using equation.

$$L_C = \frac{\sigma \times D}{2 \times \tau_c} \quad \text{..} \quad (2)$$

Where σ is the ultimate tensile strength of jute fiber, d is the diameter of the jute fibers.

3.4.5 Electrical Measurements

TWO-point DC Measurement

In order to get the electrical measurements, the single weir nanocomposites of 2 inches, are cut and then the sample is placed inside a vacuum chamber attached with two conductors. A digital multimeter (CD 800a, Sanwa, Japan) is used to measure the current, I, and a dc voltage is supplied by a stabilizer DC power supply (6545A, Agilent, Japan). The current of the CNT/Jute nanocomposite is measured by a digital Keithley 6517B electrometer (USA). A schematic circuit diagram for the DC measurement is shown in fig. 3.15. The temperature-dependent electrical characteristics of the samples are studied for the temperature range of 273—373 K. For these measurements the samples are heated by a heating coil which is wrapped around the specific chamber.

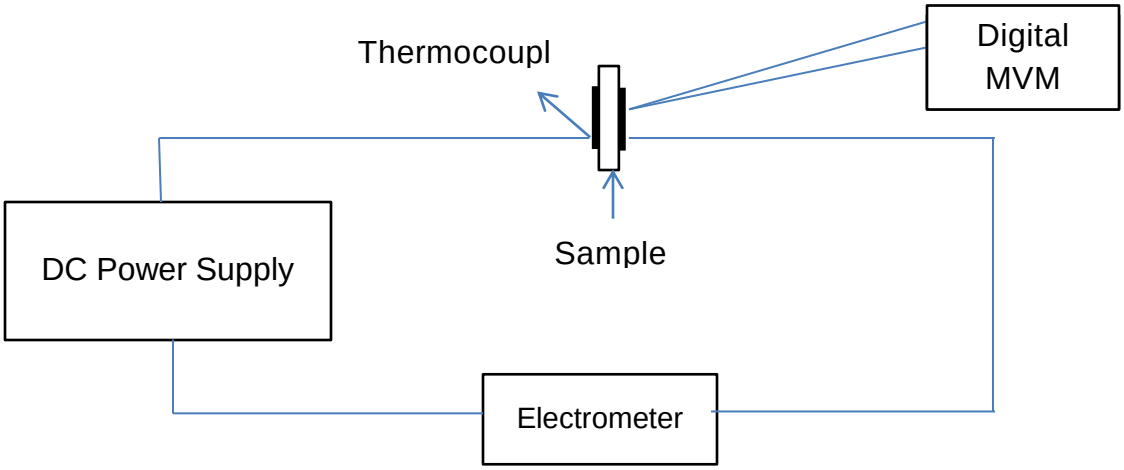

Fig. 3.15: A schematic circuit diagram of DC

The temperature is measured by a Chromel-Alumel (Cr-Al) thermocouple placed very close to the sample. To avoid oxidation, all the measurements are performed in a vacuum of about 10-20 torr. DC measurement setup is shown in Fig 3.16.

Fig. 3.16: DC measurement set up.

To measure the sheet resistance, Rs of the composites, copper of width 1.97 cm are placed on the CNT/Jute composites at a distance L. The sheet resistance of the composites is calculated by using the equation (3.2).

$$R_s = R \times \left(\frac{D}{L}\right) \quad \ldots\ldots\ldots\ldots\ldots\ldots \quad (3.2)$$

Where R, D, and L are the resistance, width of the electrode and the distance between the electrodes, respectively. A digital multimeter (CD 800a, Sanwa, Japan) is used to measure resistance across the sample by varying the distance between the electrodes.

CHAPTER 4
RESULTS AND DISCUSSION

4.1 Introduction

This chapter contains results and discussion on findings using different characterization techniques. The morphological, structural, thermal and electrical properties of the CNT/Jute nanocomposites have been characterized by means of FESEM, FTIR, TGA/DTG and DC electrical measurements.

4.2 Surface Morphology

4.2.1 Surface morphology of f-CNTs

Morphologies and structures of CNTs were observed though SEM micrographs. SEM images of *f*-CNTs are taken at ×100k magnification using FESEM (JEOL JSM-7600F SEM), at an acceleration voltage of 5kV as shown in Fig. 4.1.

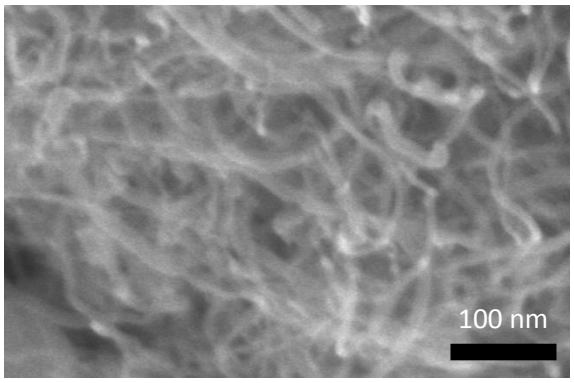

Fig 4.1: SEM images of *f*-CNTs at ×100k magnification.

SEM image display CNTs of high aspect ratio with apparent aggregation and entangled in nature. The length of CNTs range is from 1-10 μm, their outer diameter ranges from 10-30 nm as maintained by the manufacturer.

4.2.2 Surface morphology of the CNT/Jute nanocomposites

FESEM imaging is used to characterize the surface morphology of the jute fiber CNT/untreated jute and CNT/treated jute nanocomposites. The low magnification

FESEM image of the jute fiber presented in Fig. 4.2(a) shows that the jute fiber are entangled together and porous in structure but after treated it is clean and porous less.

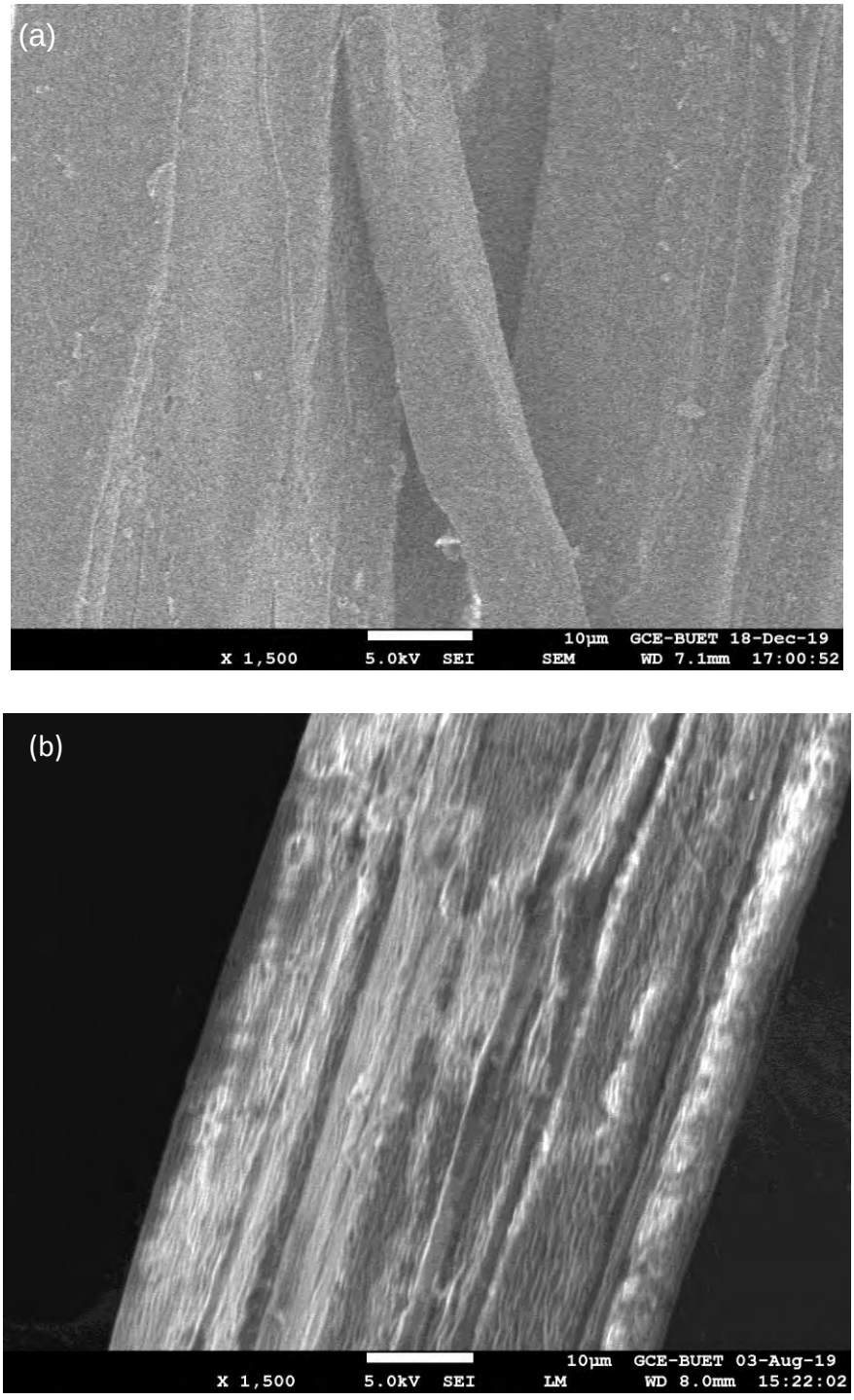

Fig. 4.2: FESEM images of (a) untreated jute fiber, (b) treated jute at ×1.5k magnification.

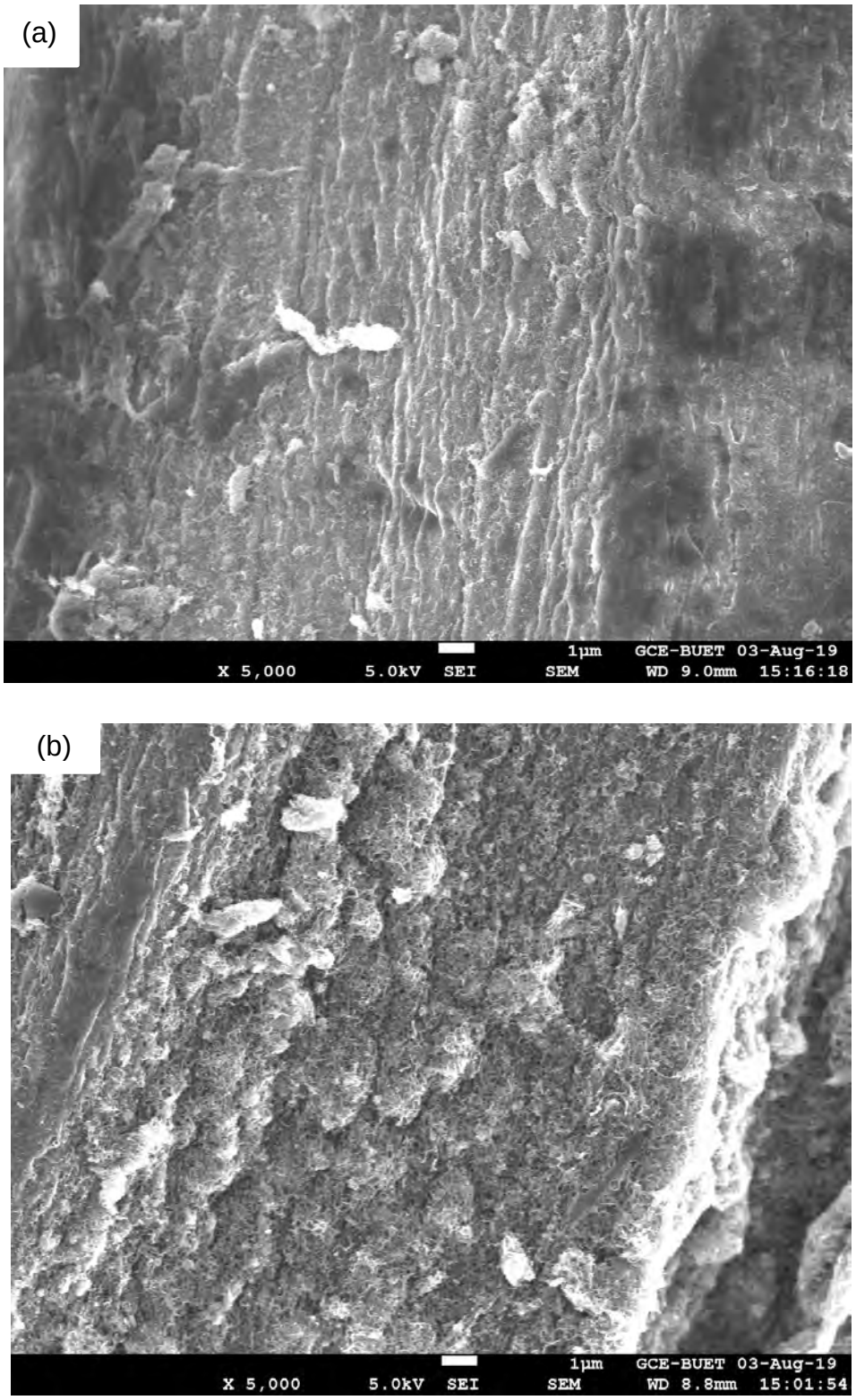

Fig. 4.3: FESEM images of nanocomposites at ×5k magnifications for (a) CNT/untreated jute and (b) CNT/treated jute nanocomposite.

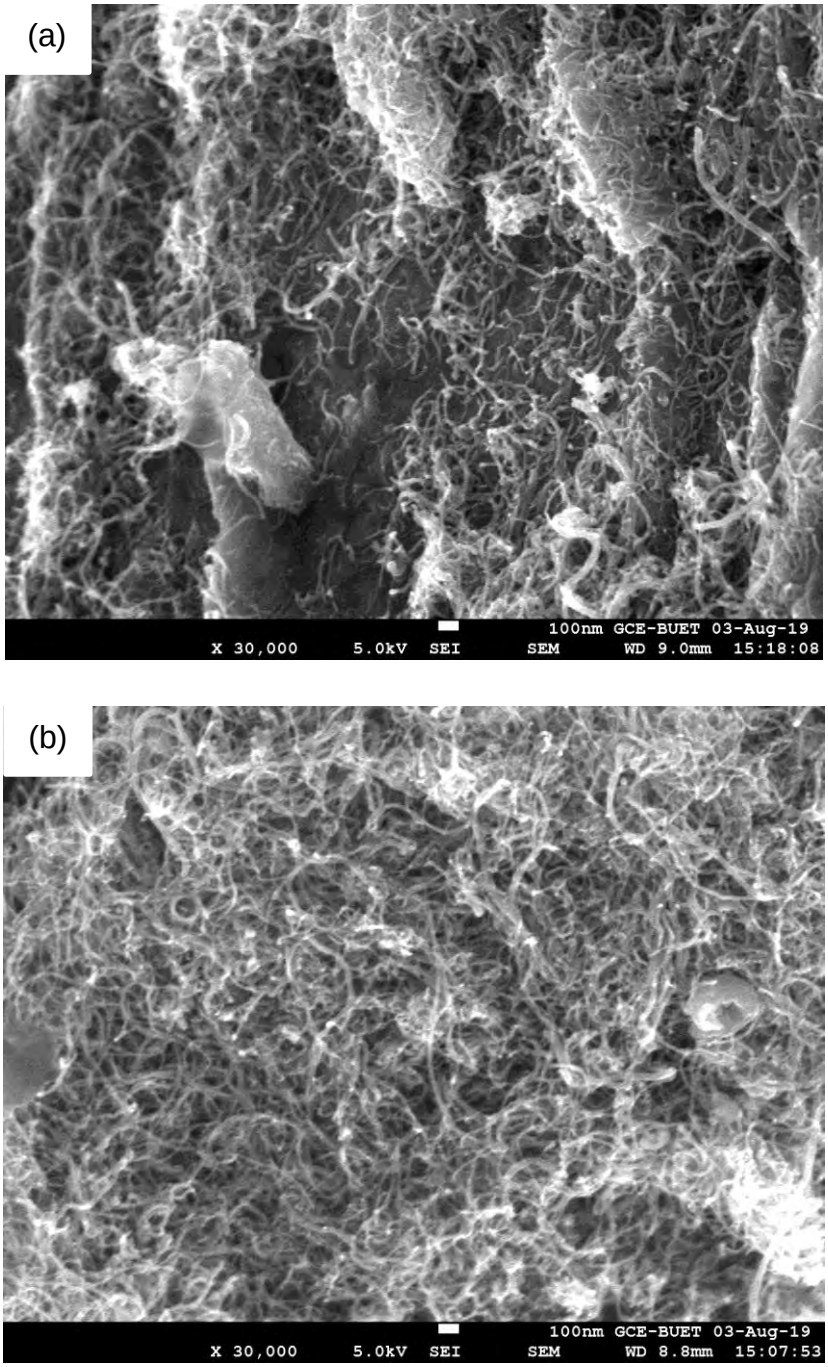

Fig. 4.4: FESEM images of nanocomposites at ×30k magnifications for (a) CNT/untreated Jute and (b) CNT/treated Jute nanocomposite.

High magnification images of the jute fiber as shown in Fig. 4.2(a) represents clean surface of the jute fiber. The FESEM images of the CNT/untreated Jute composite reveal that due to CNTs incorporation the jute fibers are not fully covered as shown in Fig. 4.3

and 4.4 but in CNT/Treated jute composite are covered uniformly with CNTs on the jute fibers as shown in Fig 4.3 and 4.4. Plasma treated jute has extra ability to absorption water than untreated jute that‘s why CNTs ink incorporate promisingly.

4.3 Structural Analysis

4.3.1 Fourier Transform Infrared Spectroscopy (FTIR)

FTIR is used to study the structural properties of the composites. Fig. 4.5 shows the FTIR transmittance spectra of the jute fiber, CNT/jute and CNT/treated jute nanocomposites after baseline correction.

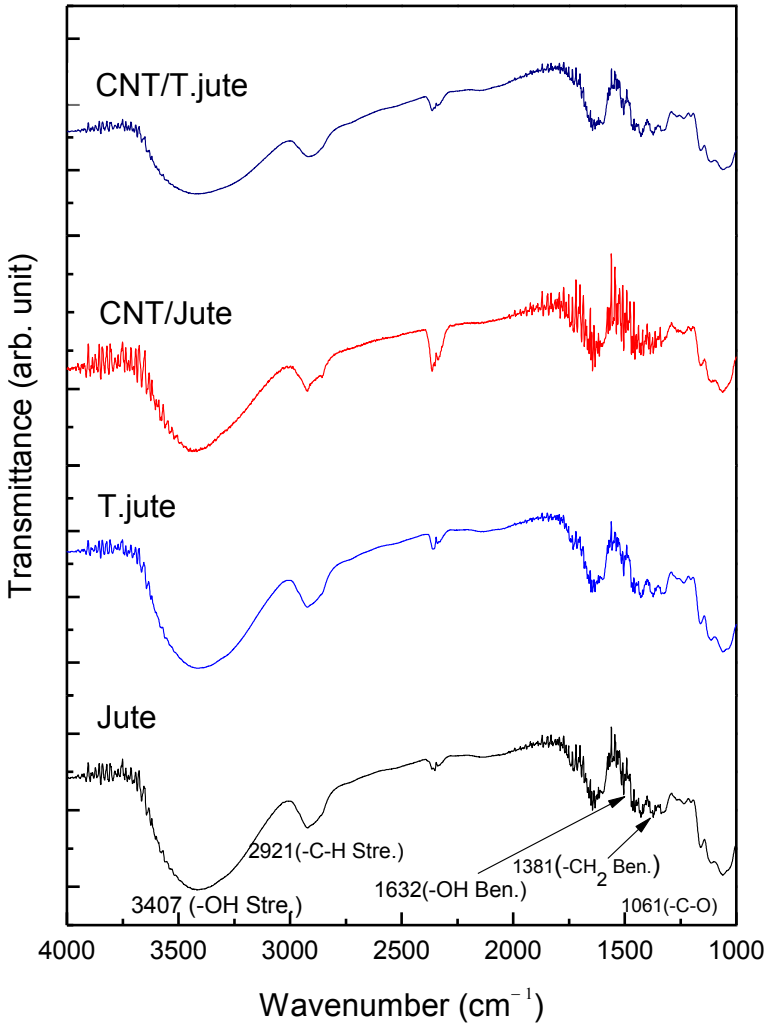

Fig. 4.5: FTIR spectra of the jute, CNT/ jute and CNT/ treated jute nanocomposites.

FTIR spectrum of jute is featureless because there are many varieties of jute, but almost all have the same properties: long, soft and shiny fibers [79-81]. An absorption band around 3407 cm ^{1} for the spectrum of jute represents the presence of O-H stretching bonds and also a small peaks at 2921 cm ^{1} is attributed to C-H bonds [82]. The other spectrum of the jute shows the characteristic peaks of respectively –OH bending, CH_2 bending, C O C pyranose and glycosidic C H at 1632, 1381 and 1061 cm ^{1}. The spectrum of CNT/ jute shows the characteristic peaks of molecules at 3443 cm ^{1}, 2934 cm ^{1}, 1644 cm ^{1}, 1161 and 1053 cm ^{1}. Absorption band around 3443 cm ^{1} can be ascribed to O H stretching. Additionally, the band at 2934 cm ^{1} is attributed to the characteristic C-H stretching of CH_2 group, the peak at 1644 cm ^{1} is related to OH bending of absorbed water. A band at 1161 cm ^{1} represents C O bond vibrations. A peak at 1053 cm ^{1} is associated to C O C pyranose ring skeletal vibration. The absorption peak at 896 cm ^{1} is assigned to the vibration of glycosidic C H deformation. The spectrum of the CNT/treated jute composites do not show any significant changes in the band position, but intensities of the bands at 3418 cm ^{1} is increased and stretching mode at 2934 cm ^{1} is shifted to higher wavenumber at 2903 cm ^{1}. Also, the band at 1644 cm ^{1} and 1161 cm ^{1} are shifted to lower wavenumber at 1632 cm ^{1} and 1159 cm ^{1}, which ar related to OH and C O bending vibration respectively. A new peak in CNT/Treated jute is found at 1427 cm ^{1} which indicates the asymmetric CH_2 bending vibration. The bands at 4000-2995 cm ^{1}, 2900 cm ^{1} and 1430 cm ^{1} are especially sensitive to crystallinity [83]. The bands at 3340 cm ^{1}, 2913 cm ^{1} and 1432 cm ^{1} are increased in absorbance indicating that the crystallinity of the composites might be enhanced by the incorporation of CNTs in the jute matrix.

4.4 Thermal Analyses

4.4.1 TGA and DSC

TGA and DSC curves of jute, treated jute, CNT/jute and CNT/treated jute nanocomposites are shown in Fig. 4.6. Thermal behavior of the jute and jute/CNT composite has been investigated using the techniques of TGA and DSC and the corresponding curves are shown in Fig. 4.6. Initial weight loss of about 15 % at the temperature range of 50-100 $^{\circ}$C is observed due to the evaporation of bound moisture from jute, since the moisture regain of jute is known to be 13.75% [80, 81] or may be

due to the removal of water molecules released in the composites. The second dominant weight loss is observed at 280-380 °C, leading to the formation of volatile chemicals of low molecular weight owing to the pyrolysis of jute. Generally, thermal degradation of jute involves dehydration, depolymerization and decomposition of glycosyl-units and then formation of a chaffed residue. TGA curves for jute, jute/CNT and treated jute/CNT nanocomposite show residue of 29.5%, 38.2% and 57.7% respectively after 700°C. There for it can be said that Thermal stability of the jute composite increased significantly after the incorporation of f-CNT in the treated jute fibers.

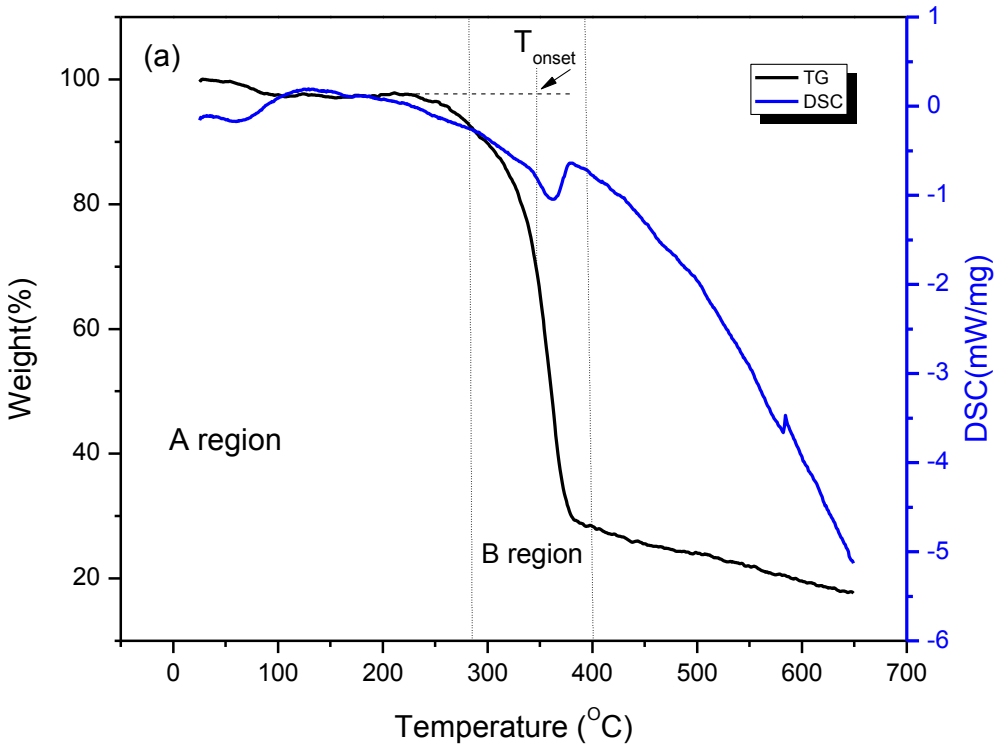

Fig. 4.6: TGA and DSC curve for untreated jute

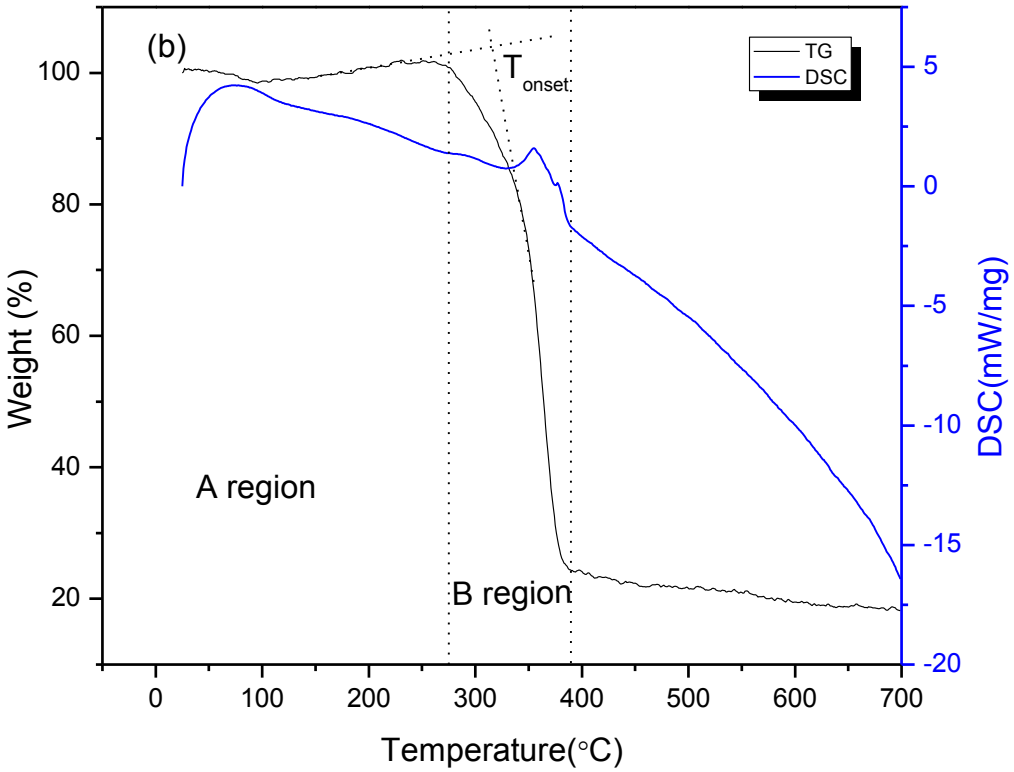
(b)
T onset
TG
DSC
A region
B region
Weight (%)
DSC(mW/mg)
Temperature(◦C)
100
80
60
40
20
5
0
-5
-10
-15
-20
0
100
200
300
400
500
600
700

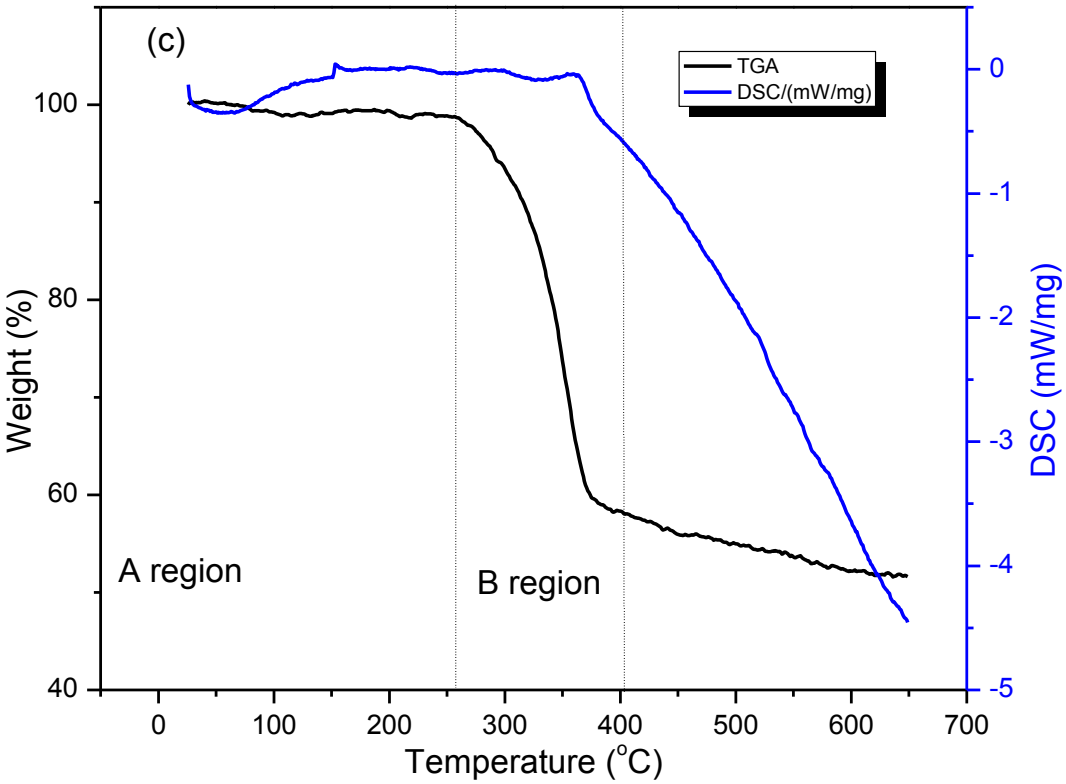
(c)
TGA
DSC/(mW/mg)
A region
B region
Weight (%)
DSC (mW/mg)
Temperature (°C)
100
80
60
40
0
-1
-2
-3
-4
-5
0
100
200
300
400
500
600
700

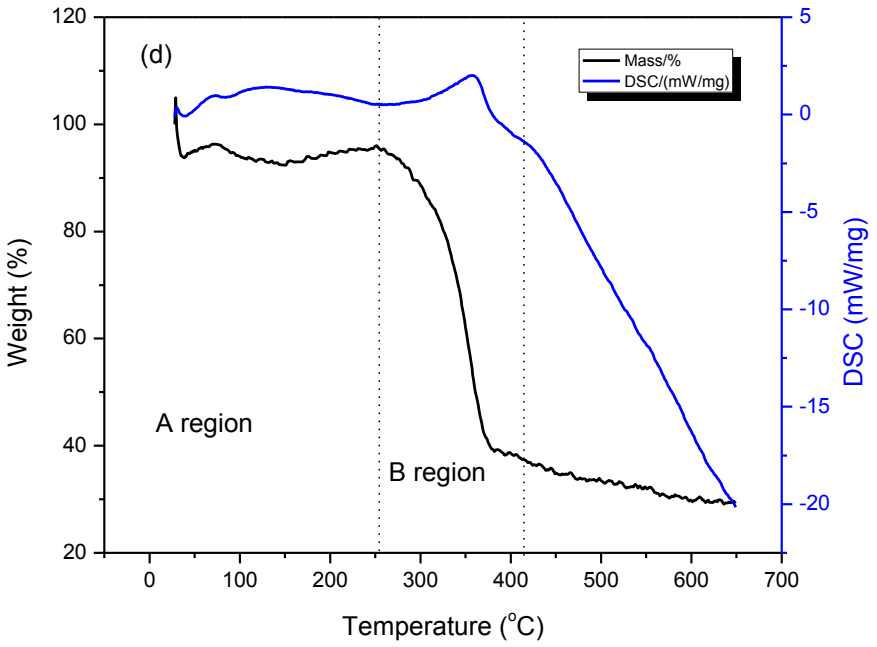

Fig. 4.7: TGA and DSC curve for (b) treated jute, (c) CNT/jute and (d) CNT/treated jute nanocomposite.

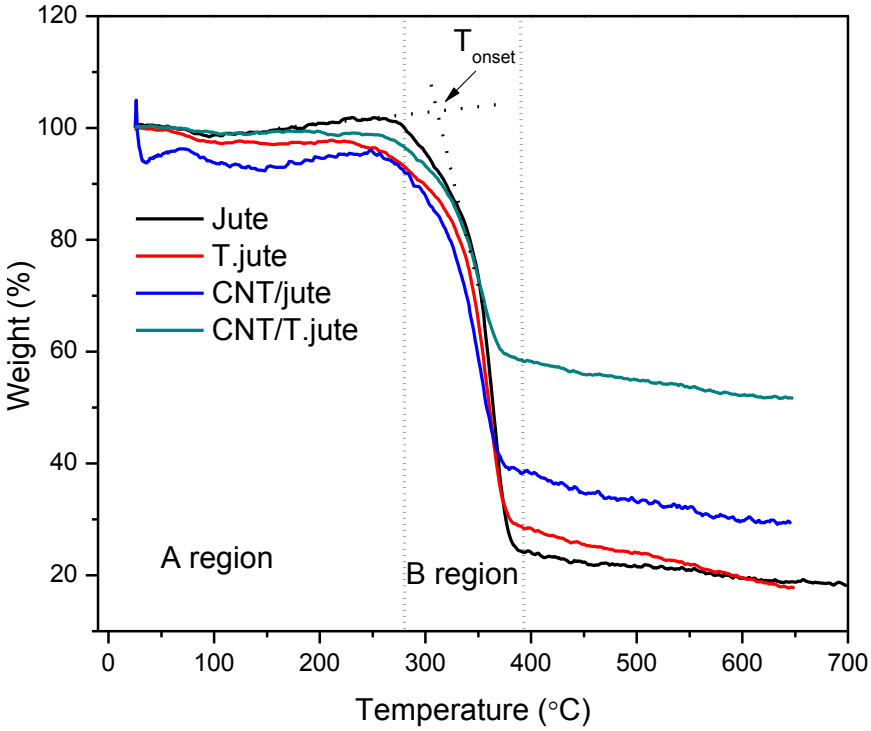

Fig. 4.8: TGA curves of the jute, treated jute, CNT/jute and CNT/t.jute nanocomposite.

Table 4.1: Data of weight loss calculation for jute, treated jute, CNT/ jute and CNT/ t.jute nanocomposites.

Sample	First Stage (A) (50-280 °C) Weight loss (%)		Second Stage(B) (280-380 °C) Weight loss(%)		T_{onset} (°C)	$T_{50\%}$ (°C)	Crystallinity (%)
	Exp.	Ref. [84]	Exp.	Ref. [84]			
Jute	15	10	70	84	330	367	25
T.jute	3	9	65	78	330	367	28
CNT/jute	13	-	62	-	320	360	25
CNT/T.jute	3	-	42	-	340	370	87

4.5 Mechanical Properties

4.5.1 Tensile strength

The tensile strength and elongation at break of the single jute fiber, CNT /jute and CNT /treated jute nanocomposite are measured from mechanical testing. It is observed that tensile strength increase with increasing CNT content in jute. Our study supports the results of Mia. et al. [84] who investigated the tensile strength for jute and treated jute. The maximum tensile strength they got for jute was 16.92 MPa, but in our case we are able to increase the tensile strength to 20 MPa. The values of it are tabulated in Table 4.2. The EB is observed to decrease with increasing CNT wt% in jute.

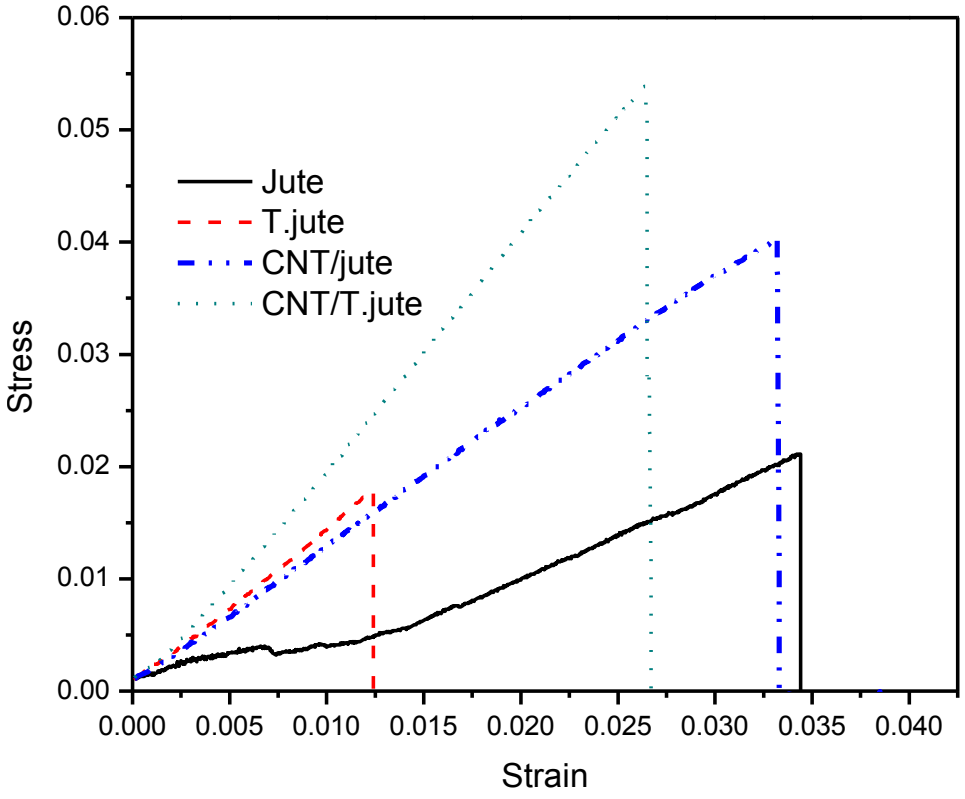

Fig. 4.9: Strain-Stress curve for jute, treated jute, CNT/jute, CNT/t.jute nanocomposite.

Table 4.2 Tensile strength and Elongation at breaking % for jute, T.jute, CNT/jute and CNT/treated jute nanocomposites

Sample Identification	Average Thickness at Gauge (mm)	Ultimate Tensile Strength (MPa)		Elongation at Break %		Young's Modulus (MPa)
		Exp.	Ref. 86]	Exp.	Ref.[86]	Exp.
Jute	15	10±3.80	12±5.56	1.63	1.70	0.80
T.jute		15±3.00	17±5.56	1.25	1.30	1.43
CNT /Jute		40±3.70		3.30		1.25
CNT /treated Jute		55±1.70		2.60		2.00

4.6 Electrical Measurements

4.6.1 Resistance

Pure jute is an insulating material which has high resistance. Fig. 4.9 represents the graph of resistance vs composites with different percentages of CNTs. The resistance is measured across the entire sample and at least 21 measurements are taken for each sample. The resistance of the nanocomposites gradually decreases as the concentration of the CNTs increases in the jute. The nanocomposites exhibit remarkably low resistance varying from 2.30 kΩ to 0.02 kΩ per unit length with 500 pieces for CNTs/treated jute nanocomposite.

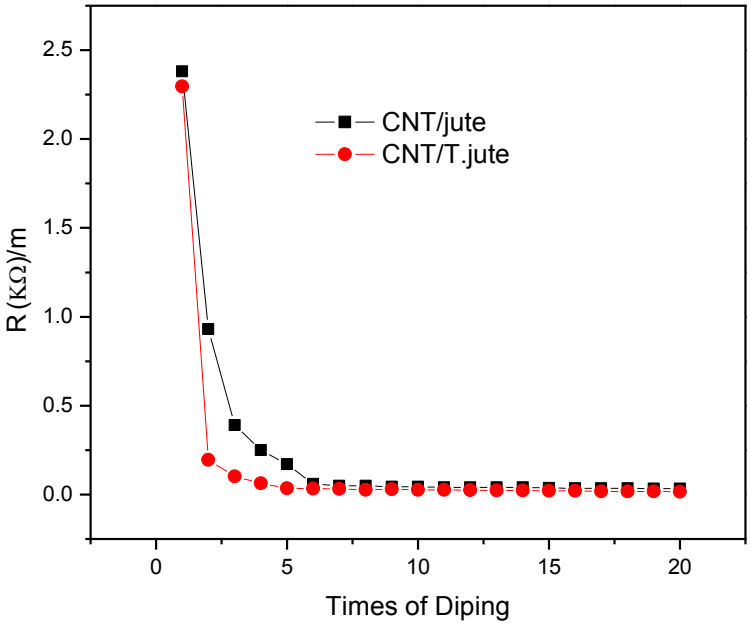

Fig. 4.10: Resistance of the nanocomposites with different percentages of MWCNT loading.

4.6.2 Electrical Conductivity

Jute shows insulating nature which contains a very low concentration of free charge carriers. The incorporation of the little amount of CNTs in the jute matrix exhibits significant improvement in the electrical conductivity of the fiber due to the formation of effective conducting network of CNTs.

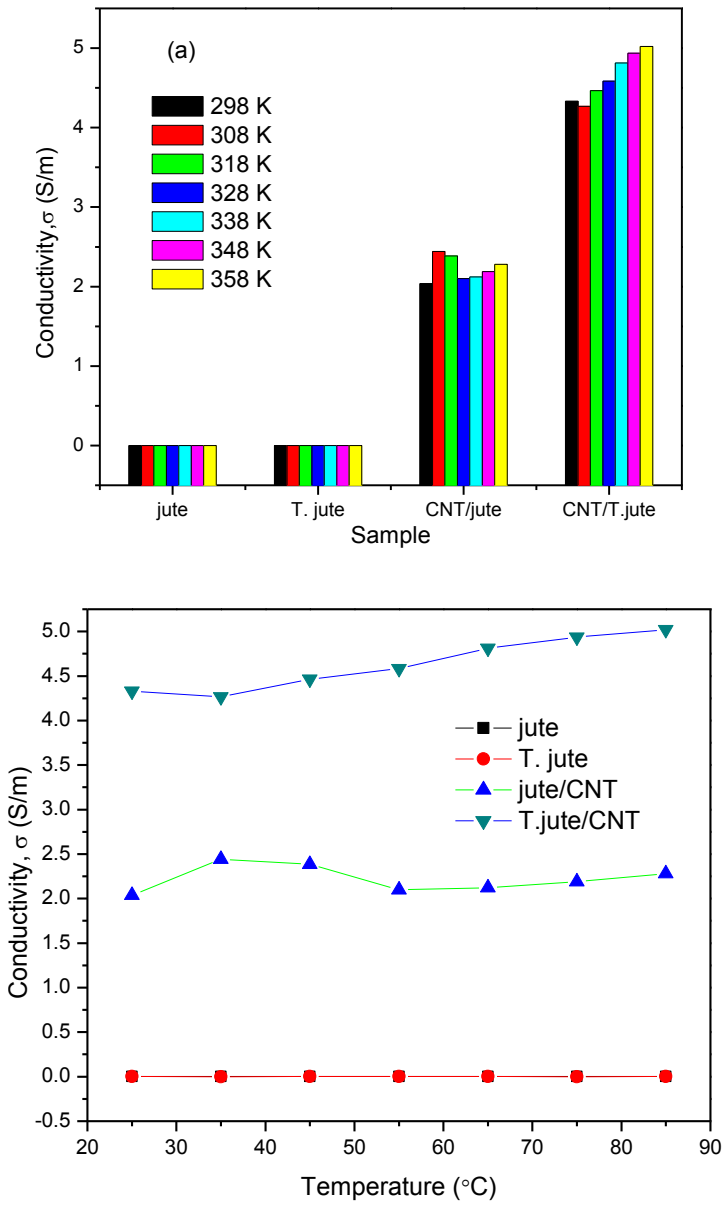

Fig. 4.11: Effect of CNTs loading on conductivity of jute, CNT/jute and CNT/treated jute nanocomposites.

It is observed that the conductivity of the nanocomposites and become 5.02 S/m at an applied voltage (100V) in 85°C for CNT/treated jute nanocomposite increases with the increase of incorporating loading of CNTs in the fiber matrix is shown in Fig. 4.10(a). The temperature dependent electrical conductivity is shown in Figure 4.10(b). The electrical conductivity of the nanocomposites increases with the increase in temperature indicating the semiconducting nature of the composites.

4.6.3 Current Density-Voltage characteristics

The current density-voltage characteristics for jute, CNT/jute and CNT/ treated jute nanocomposites at different temperatures are shown in Figure 4.11 and 4.12.

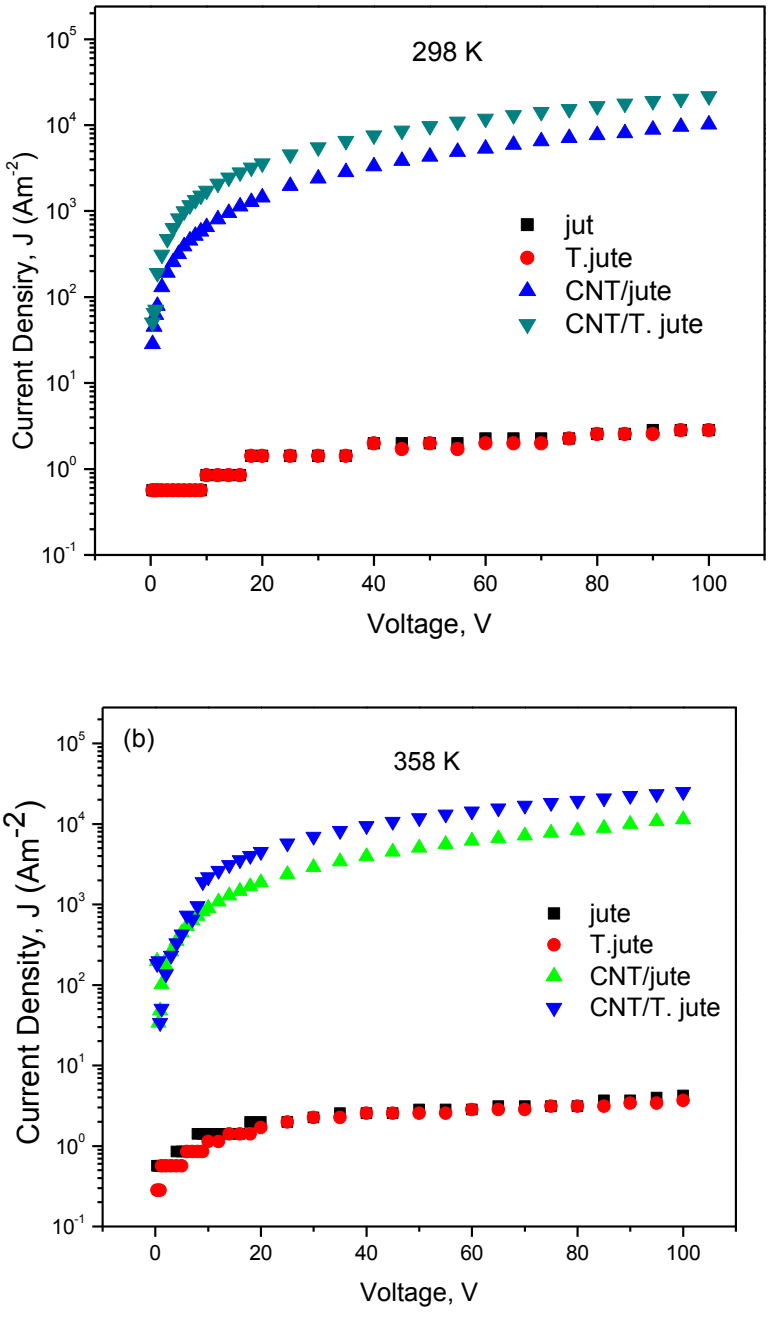

Fig 4.12: J-V characteristics curve for jute, CNT/jute and CNT/treated jute nanocomposites at (a) 298 K and (b) 358 K.

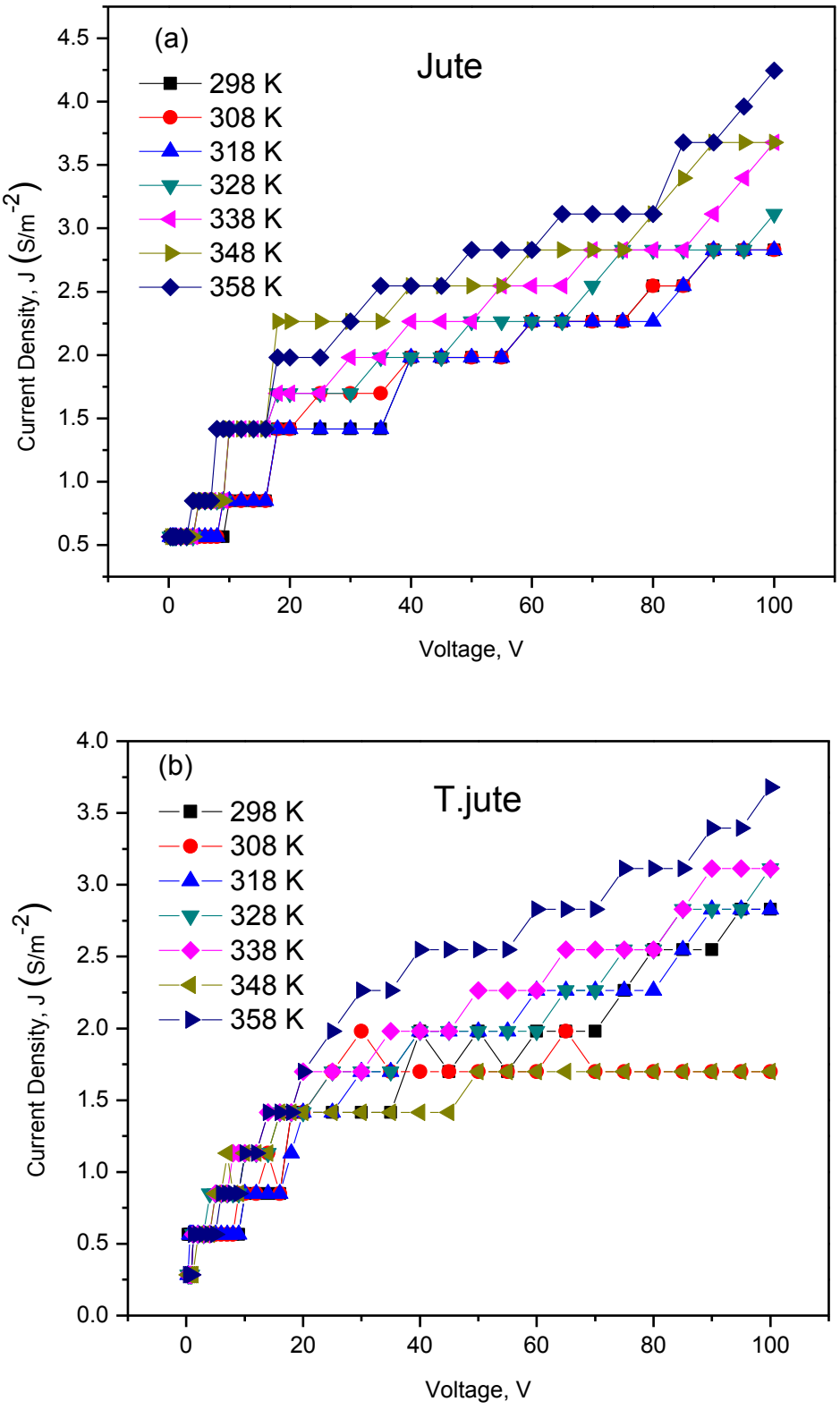

Fig. 4.13: J-V characteristics curve at different temperature for (a) jute, (b) T.jute.

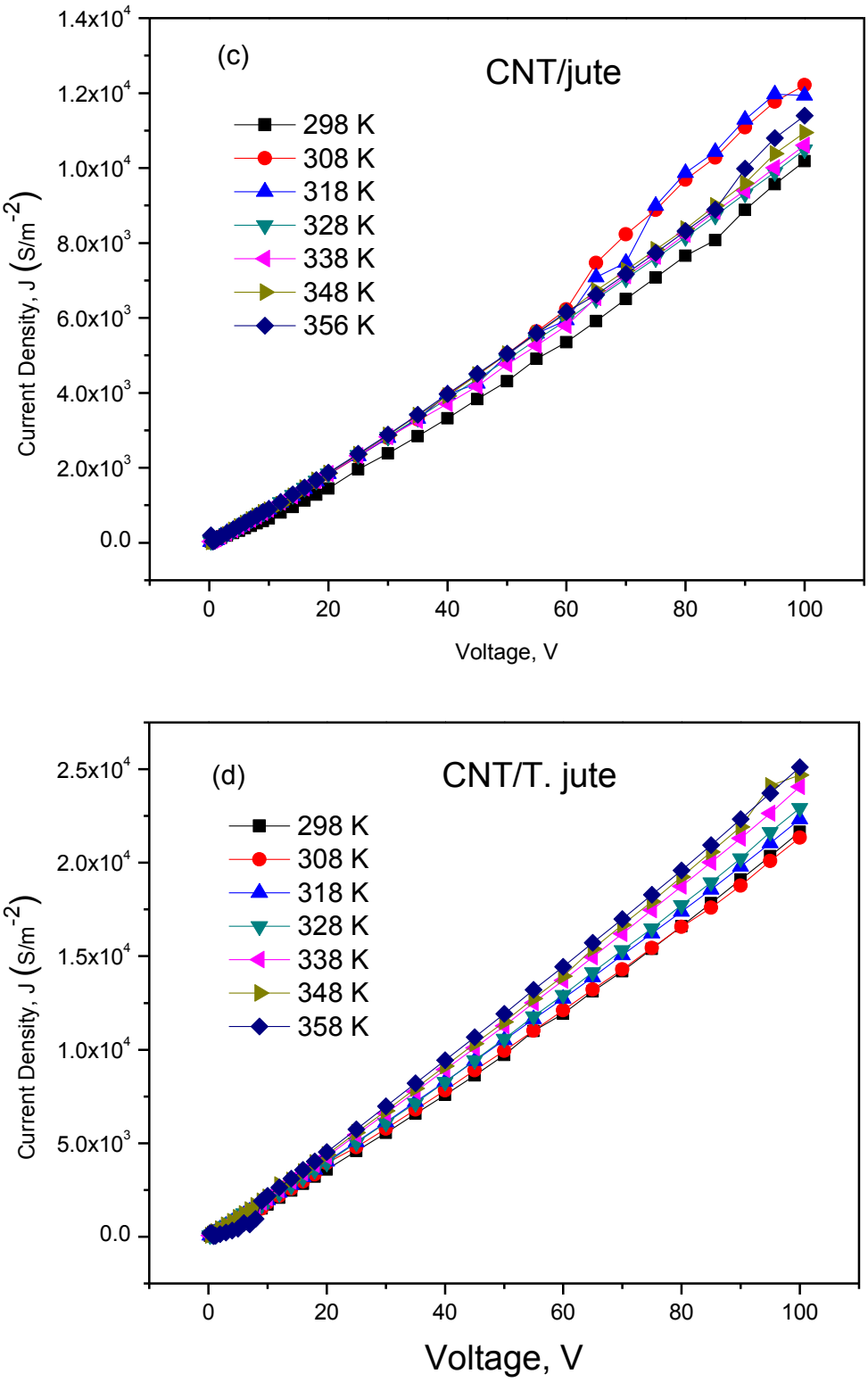

Fig. 4.14: J-V characteristics curve at different temperature for (c) CNT/jute (d) CNT/treated jute nanocomposites.

The J-V curve of the jute fiber represents insulating behavior. All the samples with CNT loading exhibit almost linear relationship between current density and voltage which indicate the Ohmic conduction. The J-V curve of the CNT/jute composite show slight increase in current density which is may be due to the low attachment of CNTs. The slop of the J-V curve of CNT/treated jute nanocomposites are increased with high integration of CNTs. It is also noticed that current density of nanocomposites increases with increasing temperature.

4.6.4 Activation energy:

The activation energy is evaluated from the slopes of the current density versus the inverse temperature curve (J vs 1000/T) by using the equation, $J = J_o e^{-\Delta E/\kappa T}$. Fig. 4.14 illustrates variation of current density with 1000/T with fixed voltage, 100 V of CNTs/jute nanocomposite.

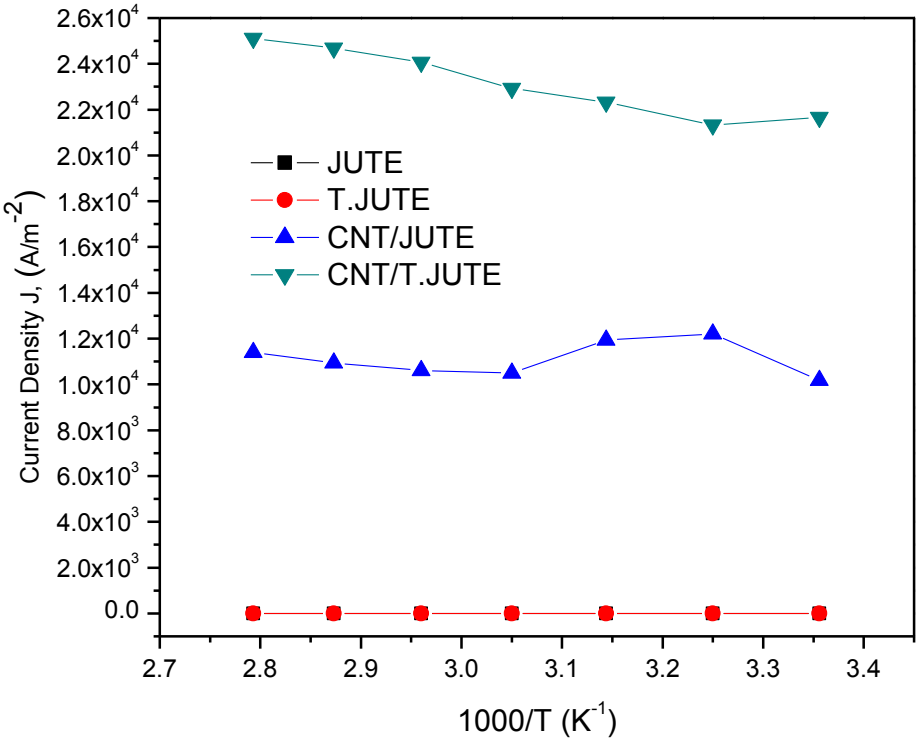

Fig. 4.15: Current density vs 1000/T with fixed voltage, 100 V of CNTs/jute nanocomposite.

Table 4.3 Values of activation energy ΔE (KJ/mol) for jute, CNT/jute and CNT/treated jute nanocomposites.

Sample name	Activation Energies, ΔE (KJ/mol) at 100 V	
Jute	330	
T.jute	331	
CNT/jute	158	160 [86, 87]
CNT/ treated jute	68	

Activation energy was calculated at 100 V voltage and represent in Table 4.3. In the high voltage region (100 V), activation energy decreases with increasing wt% of CNTs in the CNT/treated jute nanocomposite because treated jute active area is more compere to untreated jute [88].

CHAPTER 5
CONCLUSIONS

5.1 Conclusions

The research work relies on a cheap fabrication and characterization of MWCNTs reinforced jute nanocomposites.

MWCNTs are functionalized using a safe method of plasma processing and then used to produce biodegradable jute nanocomposites, which would be used as fiber in the advanced technology as well as in other polymer composites. Thus jute can be used not only in the preparation of household product, but also as technological product.

The FESEM micrographs of Treated jute, CNT/jute and CNT/T. jute composites show clean surfaces of the jute fibers and uniform attachment of MWCNTs on the surfaces of all the fibers of jute.

The FTIR spectrum of the CNT/jute composites do not show any significant changes in the band position but increase of absorption band intensities of OH and – CH_2 groups are observed.

The TGA thermograms show two-stage degradation for all the samples and the dominant weight loss is observed between 280 to 380 ^{o}C. TG-DTA data shows thermal stability of the composites gets improved with the increase in CNTs percentages in the jute fiber, the decomposition of the treated jute is delayed due to the incorporation of more thermally sable CNTs in it.

From the electrical measurements, a gradual decrease of resistance with increasing CNT concentration in the composites are observed and the value of sheet resistance varying from 2.30 kΩ/m to 0.02 kΩ/m per length with 500 pieces of jute fiber. J-V curves of the CNT/jute composites indicate Ohmic conduction. DC conductivity of the nanocomposites increases with the increase in temperature indicating the semiconducting nature of composites. The activation energy of all the samples are decreased in high temperature region (358 K) compared to the low temperature region (298 K).

The conductivity of the nanocomposites also increases with the increase become MWCNTs and becomes 5.02 S/m for CNT/treated jute at an applied voltage 100V. It is seen that the activation energy of all the samples are decreased with the attachment CNTs of in the treated jute.

Tensile strength of the composites is observed to be slightly increased of the order as jute < CNT/jute < CNT/T. jute nanocomposites. This may be due to the stronger interaction of the CNTs with the jute fiber and CNT/treated jute fiber composite tensile strength is more than CNT/untreated jute composite due to incorporation of CNTs.

In summary, low cost, biodegradable, CNT/jute nanocomposite is produce. Due to the incorporation of MWNCTs in jute fiber, the nanocomposites are expected to show improved electrical conductivity, mechanical strength, structural and thermal properties. The jute nanocomposites fiber hopefully may find applications in different types of electronic devices as well as in engineering fields such as super capacitor, multifunctional sensors, and Conductive fiber textiles. Further research is important for more fruitful results and to uncover new uses.

5.2 Scope of Future Study

Further investigations are required to better understand different features and to realize new capabilities of the composites for the development of applications in advanced technological fields. Therefore, the following studies may be carried out to understand the better implications of the composites:

- To perform AC electrical measurements.
- Transmission electron microscopy images analysis.
- It would be useful to measure specific capacitance.
- A comparative study can be done by adding other nanofillers in the jute fiber.
- Application of CNT/jute nanocomposite can be verified in the field of electronic devices

5.3 References

[1] Cui, H.-W., Suganuma, K., Uchida. H., ―Highly stretchable, electrically conductive textiles fabricated from silver nanowires and cupro fabrics using a simple dipping-drying method.” Nano Res. 2015, 8, 1604–1614.

[2] Miao,M., Xin, J.H., ―Engineering of High-Performance Textiles.” Wood head Publishing Ltd.: Cambridge,UK,2018, pp. 305–334.

[3] Guo, L., Bashir, T., Bresky, E.,Persson, N.-K. ―Electroconductive textiles and textile-based electromechanical sensors-Integration in as an approach for smart textiles in Smart Textiles and Their Applications.” Koncar, V., Ed., Woodhead Publishing Series in Textiles, Woodhead Publishing: Oxford, UK, 2016, pp. 657–693.

[4] Kim, Y.K., Wang, H., Mahmud, M.S. ―Wearable body sensor network for health care applications. In Smart Textiles and Their Applications.” Koncar, V., Ed., Woodhead Publishing Series in Textiles, Woodhead Publishing: Oxford, UK, 2016, pp. 161–184.

[5] Stoppa, M., Chiolerio, A. ―Wearable Electronics and Smart Textiles.” A Critical Review. Sensors 2014, 14, 11957–11992.

[6] Yang, T.; Xie, D., Li, Z., Zhu, H. ―Recent advances in wearable tactile sensors: Materials, sensing mechanisms, and device performance.” Mater. Sci. Eng. R Rep. 2017, 115, 1–37.

[7] Fangueiro, R., Rana, S. ―Natural Fibres: Advances in Science and Technology towards Industrial Applications.” Springer: Dordrecht, The Netherlands, 2016, ISBN 978-94-017-7513-7.

[8] Fangueiro, R., Rana, S. ―Advances in Natural Fibre Composites: Raw Materials, Processing and Analysis.” 1st ed., Springer International: Cham, Switzerland, 2018, ISBN 978-3-319-64640-4.

[9] Gopinath, A., Kumar, M.S., Elayaperumal, A. ―Experimental Investigations on Mechanical Properties of Jute Fiber Reinforced Composites with Polyester and Epoxy Resin Matrices.‖ Procedia Eng., 97, 2052–2063, 2014.

[10] Das, S., ―Mechanical properties of waste paper/jute fabric reinforced polyester resin matrix hybrid composites.‖ Carbohydr. Polym., 172, 60–67, 2017.

[11] Ramana, M.V.,Ramprasad, S. ―Experimental Investigation on Jute/Carbon Fibre reinforced Epoxy based Hybrid Composites.‖ Mater. Today Proc. 2017, 4, 8654–8664.

[12] Atwa, Y.,Maheshwari, N.,Goldthorpe, I.A. Silvernano wire coated threads for electrically conductive textiles. J. Mater. Chem. C 2015, 3, 3908–3912.

[13] Dong, B.H., Hinestroza, J.P. ―Metal Nanoparticles on Natural Cellulose Fibers: Electrostatic Assembly and In Situ Synthesis.‖ ACS Appl. Mater. Interfaces, 1, 797–803, 2009.

[14] R.Tian, X. Wang, M. Li., ―An efficient route to functionalize singe-walled carbon Nanotubes using alcohols,‖ Applied Surface Science, vol.255, no.5, pp.3294–3299, 2008.

[15] Popa, M.,Pradell, T., Crespo, D.,Calderón-Moreno, J.M. Stable silver colloidal dispersions using short chain polyethylene glycol. Colloids Surf. A, 303, 184–190, 2007.

[15] Qi, H., Liu, J., & Mäder, E., ―Smart Cellulose Fibers Coated with Carbon Nanotube Networks.‖ Fibers, 2(4), 295–307, 2014.

[17] Müller, H.,Opitz, C.,Skala, L. ―The highly dispersed metal state–Physical and chemical properties.‖ J. Mol. Catal., 54, 389–405, 1989.

[18] D.Tasis, N.Tagmatarchis, A.Bianco, and M.Prato, ―Chemistry of carbon nanotubes,‖ Chemical Reviews, vol. 106, no. 3, pp. 1105–1136, 2006.

[19] A. Felten, C. Bittencourt, J. J. Pireaux, G. Van Lier, and J. C. Charlier,"Radio-frequency plasma functionalization of carbon nanotubes surface O_2, NH_3, and CF_4 treatments," J. of Appl.Phy.,vol.98,no.7, 2005.

[20] C. H. Chiu, C. C. Lin, H. V. Han et al., "High efficiency GaN-based light-emitting diodes with embedded air voids/SiO2 nanomasks,"Nanotechnology,vol.23,no.4, 2012.

[21] M. J. Rahman, and T. Mieno, "Water-Dispersible Multiwalled Carbon Nanotubes Obtained from Citric–Acid-Assisted Oxygen Plasma Functionalization," J. of Nanomater, 508192(9 pages), 2014.

[22] A.Hirsch and O.Vostrowsky, "Functionalization of carbon nanotubes," Top. Curr. Chem., vol. 245, pp.193–237, 2005.

[23] Star, A., Bradley, K., Gabriel, J.C. P., and Gruner, G., "Nano-electronic sensors: Chemical detection using carbon nanotubes", Poly. Mater.: Sci. & Engg., 89, 204 (2003).

[24] Atwa, Y., Maheshwari, N., Goldthorpe, I. A. "Silvernano wire coated threads for electrically conductive textiles." J. Mater. Chem. C 2015, 3, 3908–3912.

[25] Dong, B.H.,Hinestroza, J.P. "Metal Nanoparticles on Natural Cellulose Fibers: Electrostatic Assembly and In Situ Synthesis." ACS Appl. Mater. Interfaces, 1, 797–803, 2009.

[26] R.Tian, X.Wang, M.Lietal., "An efficient route to functionalize singe-walled carbon Nanotubes using alcohols,"Applied Surface Science, vol.255, no.5, pp.3294–3299, 2008.

[27] Popa, M.,Pradell, T., Crespo, D.,Calderón-Moreno, J.M. "Stable silver colloidal dispersions using short chain polyethylene glycol." Colloids Surf. A 2007, 303, 184–190.

[28] Qi, H., Liu, J., & Mäder, E., "Smart Cellulose Fibers Coated with Carbon Nanotube Networks." Fibers, Chapter 2(4), 295–307, 2014.

[29] M. J. Rahman, and T.Mieno., ―Safer Production of Water Dispersible Carbon Nanotubes and Nanotube/Cotton Composite Materials", In: Carbon Nanotubes - Current Progress of their Polymer Composites, Eds. M. R. Berber and I. H. Hafez, InTech Open, Croatia, Chapter 12, 323-343, 2016.

[30] M. J. Rahman, and T.Mieno. ―Water-Dispersible Multiwalled Carbon Nanotubes Obtained from Citric–Acid-Assisted Oxygen Plasma Functionalization." J.Nanomater., 508192, 9 pages, 2014.

[31] Iijima, S., ―Helical microtubules of graphitic carbon", Nature, Vol. 354, pp. 56–58, 1991.

[32] Afzal, R. A., Afrin, R., Manzoor, U., Bhatti, A. S., Islam, M., Amin, M. T., & Alazba, A. A., ―Diameter control of carbon nanotubes using argon–acetylene mixture and their application as IR sensor." Modern Physics Letters B, 29(23), 1550131, 2015.

[33] Baughman, R., H., Zakhidov, A., A., Heer, W., A., ―Carbon Nanotubes—the route toward applications", Science, Vol. 297, pp. 787-792, 2002.

[34] Plants for a Future, retrieved 21 May 2015, https://pfaf.org/user/Default.aspx.

[35] The New Bantam-Megiddo Hebrew & English Dictionary, Sivan and Levenston, Bantam books, NY, 1875

[36] Chiffolo, Anthony F; Rayner W. Hesse, ―Cooking With the Bible: Biblical Food, Feasts, And Lore." Greenwood Publishing Group. p. 237, 2006, Retrieved 13 June 2012.

[37] Kamigaito, O (1991). "What can be improved by nanometer composites?", J. Jpn. Soc. Powder Powder Metall. 38 (3): 315–21. , A, Concise encyclopedia of composites materials, Elsevier Science Ltd, 1994.

[38] Okpala, C., ―Nanocomposites – An Overview", International Journal of Engineering Research and Development, Vol. 8, pp. 17-23, 2013.

[39] Camargo, P., H., Satyanarayana, K., G., Wypych, F., ―Nanocomposites: Synthesis, Structure, Properties and New Application Opportunities", Materials Research, Vol. 12, pp.1-39, 2009.

[40] Hassan Ziaei Tabari, Habibollah Khademieslam. ―A study on nanocomposite properties made of polypropylene/nanoclay and wood flour." World Appl. Sci. J., 16(2):275-9p, 2012.

[41] Khan RA, Khan MA, Zaman H. ―Fabrication and characterization of jute fiber reinforced PVC based composite." Journal of Thermoplastic Composite Materials. 2012; 25: 45–58p

[42] Arfaoui, M.A.,Dolez, P.I.,Dubé, M., David, É. ―Development and characterization of a hydrophobic treatment for jute fibres based on zinc oxide nanoparticles and a fatty acid." Appl. Surf. Sci. 2017, 397, 19–29.

[43] Agarwal, M., Xing, Q., Shim, B. S., Kotov, N., Varahramyan, K., & Lvov, Y., ―Conductive paper from lignocellulose wood microfibers coated with a nanocomposite of carbon nanotubes and conductive polymers." Nanotechnology, 20(21), 215602, 2009.

[44] S. Shahnawaz , B. Sohrabi, a, M. Najafi.; ―The investigation of functionalization role in multi-walled carbon nanotubes dispersion by surfactants". 31 October 2014 by MDPI AG in the 18th International Electronic Conference on Synthetic Organic Chemistry session Ionic Liquids**.**

[45] Wang, H., Memon, H., A. M. Hassan, E., Miah, M. S., & Ali, M. A., ―Effect of Jute Fiber Modification on Mechanical Properties of Jute Fiber Composite." Materials, 12(8), 1226, 2019.

[46] Salajkova, M., Valentini, L., Zhou, Q., & Berglund, L. A., ―Tough nanopaper structures based on cellulose nanofibers and carbon nanotubes." Composites Science and Technology, 87, 103–110, 2013.

[47] Lay, M., Méndez, J. A., Delgado-Aguilar, M., Bun, K. N., & Vilaseca, F., ―Strong and electrically conductive nanopaper from cellulose nanofibers and polypyrrole.‖ Carbohydrate Polymers, 152, 361–369, 2016.

[48] Hai, N. M., Kim, B.-S., & Lee, S. ―Effect of NaOH Treatments on Jute and Coir Fiber PP Composites. Advanced Composite Materials‖,18(3), 197–208, 2009.

[49] John, M., J., ―Biofibers and biocomposites‖, Carbohydrate Polymers, Vol. 71, pp. 343-364, 2008.

[50] Textilefashionstudy.com/physical-chemical-properties-of-jute-identity-of-jute-fiber, February 2012, https://textilefashionstudy.com/tag/structure-of-jute/.

[51] Sahu, U.K.,Mahapatra, S.S., Patel, R.K. ―Synthesis and characterization of an eco-friendly composite of jute fiber and Fe_2O_3 nanoparticles and its application as an adsorbent for removal of As(V) from water.‖ J.Mol.Liq., 237, 313–321, 2017.

[52] Seunghun, H., Myung, S., ―Nanotube electronics: a flexible approach to mobility‖, Nature Nanotechnology, Vol. 2, pp. 207–208, 2007

[53] Yu, M., ―Strength and Breaking Mechanism of Multiwalled Carbon Nanotubes Under Tensile Load.‖ Science 287(5453), 637–640, 2000. .

[54] Cui, H.-W.; Suganuma, K.; Uchida, H. ―Highly stretchable, electrically conductive textiles fabricated from silver nanowires and cupro fabrics using a simple dipping-drying method.‖ Nano Res.**,** 8**,** 1604–1614, 2015.

[55] Miao, M.; Xin, J.H. ―Engineering of High-Performance Textiles.‖ Woodhead Publishing Ltd.: Cambridge, UK, pp. 305–334, 2018.

[56] D. Ray and B. K. Sarkar, ―Characterization of alkali-treated jute fibers for physical and mechanical properties.‖ J. Appl. Polym. Sci. 80, 1013–1020, 2001.

[57] A. K. Mohanty, M. A. Khan and G. Hinrichsen. ―Surface modification of jute and its influence on performance of biodegradable jute-fabric/biopol composites.‖ Compos. Sci. Technol.60, 1115–1124, 2000.

[58] K. W. Sellers, R. W. Zeigler IV and S. L. Morgan. ―Forensic discrimination of selected vegetable fibers by pyrolysis-gas chromatography/mass spectrometry and multivariate statistics.” Anal. Appl. Pyrol. 2005.

[59] Arfaoui, M.A.; Dolez, P.I.; Dubé, M.; David, É. ―Development and characterization of a hydrophobic treatment for jute fibres based on zinc oxide nanoparticles and a fatty acid.” Appl. Surf. Sci. 397, 19–29, 2017.

[60] Sahu, U.K.; Mahapatra, S.S.; Patel, R.K. ―Synthesis and characterization of an eco-friendly composite of jute fiber and Fe_2O_3 nanoparticles and its application as an adsorbent for removal of As(V) from water.” J. Mol. Liq. 2017, 237, 313–321.

[61] Atwa, Y.; Maheshwari, N.; Goldthorpe, I.A. ―Silver nanowire coated threads for electrically conductive textiles.” J. of Materials Science, 2015.

[62] R, Panowicz., D, Miedzińska., N,t Pałka and T, Niezgoda ―The initial results of THz spectroscopy non-destructive investigations of epoxy-glass composite structure”, Computer Methods in Mechanics, 9–12 May 2011, Warsaw, Poland.

[63] Hai, N. M., Kim, B.-S., & Lee, S. ―Effect of NaOH Treatments on Jute and Coir Fiber PP Composites.” Advanced Composite Materials, 18(3), l97-208, 2009. .

[64] Lee, T.-W., & Jeong, Y. G. ―Regenerated cellulose/multiwalled carbon nanotube composite films with efficient electric heating performance.” Carbohydrate Polymers, 133, 456–463, 2015.

[65] Ma, H., M., Gao, X., L., ―A three-dimensional Monte Carlo model for electrically conductive polymer matrix composites filled with curved fibers”, Polymer, Vol. 49, pp. 4230–4238, 2008.

[66] Natsuki, T., Endo, M., Takahashi, T., ―Percolation study of orientated short-fiber composites by a continuum model”, Physica A, Vol. 352, pp. 498–508, 2005.

[67] Chmutin, I., A., Shevchenko, V., G., ―Electroconducting Polymer Composites: Structure, Contact Phenomena, and Anisotropy”, Polymer Science, Vol. 36, pp. 699-713, 1994.

[68] Bigg, D., M., –Conductive polymeric compositions" Polymer Engineering and Science, Vol. 17, pp. 842-847, 1977.

[69] Delozier, D., M., Watson, K., A., Smith, J., G., Clancy, T., C., Connell, J., W., –Investigation of aromatic/aliphatic polyimides as dispersants for single wall carbon nanotubes", Macromolecules, Vol. 39, pp. 1731–1739, 2006.

[70] Taib, M., H., Zainal, N., F., A., Jumali, N., S., Shaameri, Z., Hamzah, A., S., Rusop, M., –Effect of CNTs in the polymer base nano-composite thin films on the structure and electrical properties", Journal of Nanoscience and Nanotechnology, Vol. 1136, pp. 766–769, 2009.

[71] Feng, X., B., Liao, G., X., He, W., Sun, Q.M., Jian, X., G., Du, J., H., –Preparation and characterization of functionalized carbon nanotubes/poly (phthalazinone ether sulfone ketone) composites", Polymer Composites, Vol. 30, pp. 365–373, 2009.

[72] Liao, S., H., Yen, C., Y., Weng, C., C., Lin, Y., F., Ma, C., C., M., Yang, C., H., Tsai, M., C., Yen, M., Y., Hsiao, M., C., Lee, S., J., Xie, X., F., Hsiao, Y., H., –Preparation and properties of carbon nanotube/polypropylene nanocomposite bipolar plates for polymer electrolyte membrane fuel cells", Journal of Power Sources, Vol. 185, pp. 1225–1232, 2008.

[73] Ounaies, Z., Park, C., Wise, K., E., Siochi, E., J., Harrison, J., S., –Electrical properties of single wall carbon nanotube reinforced polyimide composites", Composites Science and Technology, Vol. 63 (11), pp.1637–1646, 2003.

[74] Sandler, J., K., W., Kirk, J., E., Kinloch, I, A., Shaffer, M., S., P., Windle, A., H., –Ultra-low electrical percolation threshold in carbon-nanotube epoxy composites", Polymer, Vol. 44 (19), pp. 5893–5899, 2003.

[75] Li, J., Ma, P.C., Chow, W., S., To, C., K., Tang, B., Z., Kim, J., K., –Correlations between percolation threshold, dispersion state, and aspect ratio of carbon nanotubes", Advanced Functional Materials, Vol. 17, pp. 3207–3215, 2007.

[76] Rosenberg, B., Bhowmikh, B., B., Harder, C., Postow, E., –Pre-exponential Factor in semiconducting organic substances", Journal of Chemical Physics, Vol. 49, pp. 4108, 1968.

[77] Turvey, K., Allan, J., R., –Correlation between the pre-exponential factor and the activation energy for electrical conductivity in monomers and polymers containing the 4-Vinylpyridine molecule" Plastics and Rubber Processing and Applications, Vol. 15, pp. 273, 1991.

[78] Eley, D., D., –Energy gap and pre-exponential factor in dark conduction by organic semiconductors", Journal of Polymer Science Part C., Vol. 17, pp. 73-91, 1967.

[89] Rout, S.K., Tripathy, B.C., Padhi, P., Kar, B.R., Mishra, K.G. –A green approach to produce silver nano particles coated agro waste fibers for special applications." Surf. Interfaces 2017, 7, 87–98.

[80] Cao, X., Ding, B., Yu, J.; Al-Deyab, S.S. –Cellulose nanowhiskers extracted from TEMPO-oxidized jute fibers" .Carbohydr. Polym. 2012, 90, 1075–1080.

[81] Kafi, A.A.; Magniez, K.; Fox, B.L. –A surface-property relationship of atmospheric plasma treated jute composites." Compos. Sci. Technol. 2011, 71, 1692–1698.

[82] Ferreira, D., Ferreira, A., & Fangueiro, R. (2018). Searching for Natural Conductive Fibrous Structures via a Green Sustainable Approach Based on Jute Fibers and Silver Nanoparticles. Polymers, 10(1), 63.

[83] Tian.R., Wang,X., Li. Et al., –An efficient route to functionalize singe-walled carbon nanotubes using alcohols". Applied Surface Science, vol. 255, pp., 3294-3299, 2008.

[84] Ray, D., Sarkar, B. K., Basak, R. K., & Rana, A. K., –Study of the thermal behavior of alkali-treated jute fibers." Journal of Applied Polymer Science, 85(12), 2594–2599, 2002.

[85] Mia.R., Mojumder. J. I. A., Islam M. A., Ahmed. B., Billah. M. S.M., ―Woolenization of jute fibre". European Scientific Journal October 2017 edition Vol.13, No.30.

[86] Du, J.-H., Bai, J., & Cheng, H.-M., ―The present status and key problems of carbon nanotube based polymer composites." Express Polymer Letters, 1(5), 253–273, 2017.

[87] Oza, S., Ning, H., Ferguson, I., & Lu, N., ―Effect of surface treatment on thermal stability of the hemp-PLA composites: Correlation of activation energy with thermal degradation." Composites Part B: Engineering, 67, 227–232, 2014.

[88] Yao, F., Wu, Q., Lei, Y., Guo, W., & Xu, Y., ―Thermal decomposition kinetics of natural fibers: Activation energy with dynamic thermogravimetric analysis." Polymer Degradation and Stability, 93(1), 90–98, 2008.

4th YOUNG SCIENTIST CONGRESS

YOUNG SCIENTISTS FOR ACHIEVING SUSTAINABLE DEVELOPMENT GOALS

13-15 December 2019

Venue

National Museum of Science & Technology Bhaban
Dhaka, Bangladesh

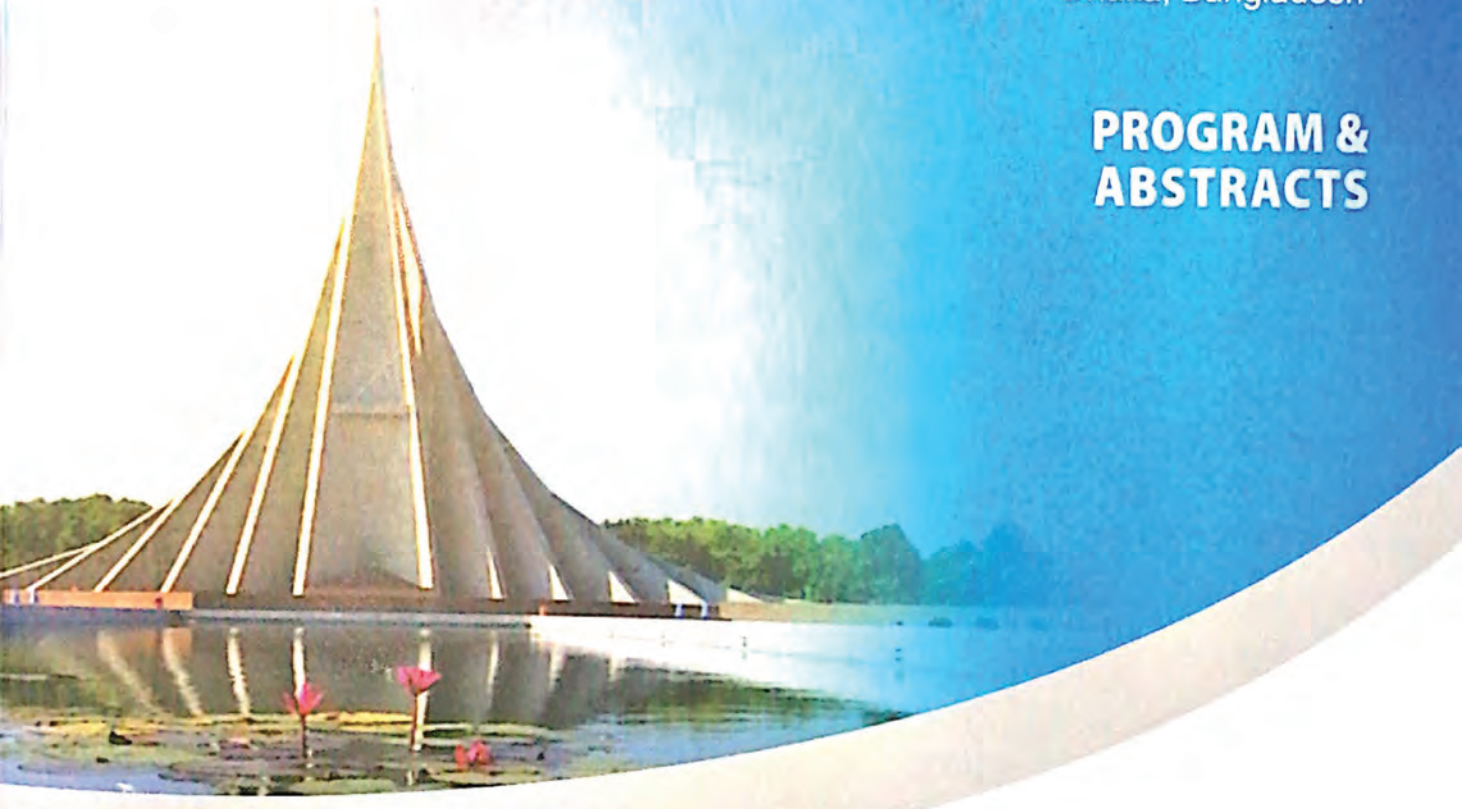

PROGRAM & ABSTRACTS

Organized by

Bangladesh Academy of Sciences (BAS)

Supported by

UNION BANK LTD
SHARIAH BASED BANK

Incepta Pharmaceuticals Ltd

National Museum of Science and Technology

OP 13

FUNCTIONALIZATION OF CARBON NANOTUBES USING OXYGEN PLASMA TO PREPARE JUTE NANOCOMPOSITES

Md Johurul Islam[1], Mohammad Jellur Rahman[1], Tetsu Mieno[2]

[1]Department of Physics, Bangladesh University of Engineering and Technology (BUET), Dhaka, Bangladesh; [2]Graduate School of Science and Technology, Shizuoka University, Shizuoka 422-8529, Japan

Search for conductive fibrous structures are in full growth because of their wide variety of potential applications in military sectors, sports, engineering, therapeutics, and the automotive or aerospace industries, etc. Synthetic fibers are still the most used type of fibers in industries. However, natural fibers such as jute, because of their low cost, abundance, biocompatibility and biodegradability, are very promising for replacing the syntheticones. But to make jute conductive it is required to incorporate conductive elements like carbon nanotubes (CNTs) onto it. However, owing to poor dispersibility in solvent it becomes very difficult to uniformly distribute CNTs onto the jute fibers. The most common method of improving their dispersibility is their strong acidic treatment, which requires a long processing time and produces a large amount of wastes. Therefore the objectives of this study is to functionalize the CNTs by an environment-friendly technique and incorporation of these CNTs onto the surfaces of the jute fibers to make them electrically and thermally conductive, thermally stable and mechanically strong. At first locally collected jute fiber is cleaned and treated with oxygen plasma. MWCNTs are sonicated in ethanol, dried in air and soaked in citric acid solution. Then the MWCNTs in the citric acid solution are treated in an RF (13.56 MHz) plasma reactor under oxygen environment. After the treatment, these functionalized MWCNTs is dispersed in distilled water to produced stable dispersed ink of MWCNTs, in which the treated jute fiber is repeatedly dipped and dried in air to obtain the jute nanocomposites. The MWCNTs is become stably dispersible owing to the citric-acid-assisted plasma processing. Due to the uniform distribution of MWCNTs onto the jute fibers it becomes conducting, thermally stable and mechanically strong. Due to enhanced electrical, mechanical, and thermal properties the jute nanocomposites hopefully will find applications in different electronic devices as well as in advanced technological products.